DOE/NASA 0227-1
NASA CR-165479
MTI 82-TR-4

NASA-CR-165479
19820003593

PRELIMINARY STUDY OF TEMPERATURE MEASUREMENT TECHNIQUES FOR STIRLING ENGINE RECIPROCATING SEALS

Donald F. Wilcock
Leo Hoogenboom
Mechanical Technology Incorporated

Maarten Meinders
Ward O. Winer
Georgia Institute of Technology

August 1981

Prepared for
NATIONAL AERONAUTICS AND SPACE ADMINISTRATION
Lewis Research Center
Cleveland, Ohio 44135
Under Contract DEN3-227

for
U.S. DEPARTMENT OF ENERGY
Office of Conservation and Solar Applications
Division of Transportation Energy Conservation
Washington, DC 20545

DOE/NASA 0227-1
NASA CR-165479
MTI 82-TR-4
DE-AIO1-77CS51040

PRELIMINARY STUDY OF TEMPERATURE MEASUREMENT TECHNIQUES FOR STIRLING ENGINE RECIPROCATING SEALS

Donald F. Wilcock
Leo Hoogenboom
Mechanical Technology Incorporated
Latham, New York 12110

Maarten Meinders
Ward O. Winer
Georgia Institute of Technology
Atlanta, Georgia 30332

August 1981

Prepared for
NATIONAL AERONAUTICS AND SPACE ADMINISTRATION
Lewis Research Center
Cleveland, Ohio 44135
Under Contract DEN3-227

for
U.S. DEPARTMENT OF ENERGY
Office of Conservation and Solar Applications
Division of Transportation Energy Conservation
Washington, DC 20545

FOREWORD

The infra-red scanning camera measurements of temperature were carried out under subcontract to Georgia Technology Research Institute under the direction of Professor Ward O. Winer. The measurements were made at the Mechanical Technology Inc. R&D Laboratories in Latham, New York.

ABSTRACT

Direct infra-red measurement of surface temperatures of a rod exiting a loaded cap seal or simulated seal are compared with surface thermocouple measurements. Significant cooling of the surface requires several milliseconds so that exit temperatures may be considered representative of internal contact temperatures.

TABLE OF CONTENTS

TABLE OF CONTENTS (Cont'd)

LIST OF FIGURES

LIST OF TABLES

1.0 SUMMARY

The seal materials used in sealing reciprocating piston rods in Stirling engines against the leakage of the high pressure working gas (usually H_2) are usually thermoplastic materials compounded with various inorganic fillers. Teflon resin is commonly used. The temperature reached at the surface is of concern because too high a temperature will soften the seal material and result either in failure or in excess leakage.

Two techniques were explored in this program: use of a sensitive surface thermocouple, and use of infra-red surface temperature measurement. In addition to preliminary low speed checkout of the instrumentation, two basic series of tests were conducted:

a) A pin of seal material reciprocating under load on either a Nitralloy plate (directly simulating the engine materials) or on an infra-red transparent sapphire plate, and

b) A rod cap seal reciprocating under controlled cap seal loading pressure.

Temperature rises above ambient as high as 40 to 50°C were observed under combinations of moderate reciprocating speed (1500 rpm), typical engine stroke (40 mm) and unit loadings up to 5×10^6 Pascals (NM^{-2}). Thermocouple measurements correlated directly with PV (the product of load and velocity) in pin-on-Nitralloy tests, the relationship being:

$$\Delta T\ (^{o}C) = 3.08 \times 10^{-6}\ PV \qquad (1)$$

Infra-red surface temperature measurements indicated a lesser degree of dependence on PV:

$$\Delta T\ (^{o}C) = 0.57 \times 10^{-6}\ PV \qquad (2)$$

above an ambient (metal) temperature that increased with speed.

Direct measurement through the sapphire of the maximum temperature in the pin contact indicated a trend line of:

$$\Delta T\ (^{\circ}C) = 1.0 \times 10^{-6}\ PV \qquad (3)$$

Measurement by infra-red of surface temperatures exiting a cap seal were more complex and did not show a consistent trend.

Infra-red surface temperature measurements were made at a repetition rate of 1500 cpm. At this frequency of observation, it was found that surface cooling of a significant magnitude ($>2^{\circ}C$) required more than 25 milli-seconds. Consequently, the use of this technique for estimating the surface temperature in a seal contact appears promising at speeds at and above engine idle (600 cpm) if the observation can be made close to the seal.

The high speed scanning IR technique appears promising as a tool for seal thermal studies. However, it is dependent upon simultaneous observation of a reference surface of known temperature and emissivity and a knowledge of the emissivity of the surface being studied. Further research appears very desirable and should include simultaneous observation of seal frictional force.

2.0 INTRODUCTION

Seals are widely used in reciprocating mechanisms, such as shock absorbers, hydraulic cylinders, and compressors. In these devices, they are frequently required to support large pressure differences ranging from one to ten megapascals. The velocities are frequently large also, so that even with friction coefficients of 0.1 to 0.3, significant quantities of energy are generated at the rubbing surface. As a result, one may expect large temperature rises above ambient at the local contact zones.

Elastomers and thermoplastic materials are frequently used in reciprocating seals because of their flexibility and low modulus. These properties permit intimate contact to be maintained between the seal and the reciprocating rod, thus providing good sealing. The contact temperatures that may develop, however, may deteriorate the elastomer or soften the thermoplastic. Thus, the ability to measure the surface temperature in a working seal will be of considerable utility in the engineering of long life seals.

This investigation was stimulated by the advent of serious development of the Stirling engine as a competitor for the power plant of efficient high mileage automobiles. Stirling engines of the type under development employ helium or hydrogen gas under pressures up to 20 megapascals. Seals must be employed around the piston rods to retain the working gas.

The sealing system currently being employed includes a "main" seal and a "cap" seal. The main seal is oil lubricated from below. A "scraper" seal is used to remove oil carried past the main seal and return it via an oil control valve to the crankcase. The cap seal is located on the rod above the main seal and scraper and separates a minimum cycle pressure volume above the main seal from the variable working pressure space of the engine. The cap seal must operate dry with pressure differences of the order of ten megapascals.

Elastomeric seals have not performed well under the high pressure high velocity conditions in the Stirling engine. The most successful seal materials to date have been formulations of PTFE (poly-tetra-fluoro-ethylene) with a variety of mineral fillers with or without solid lubricants such as graphite or

molybdenum-disulfide. This type of material softens rapidly as temperature is raised, increasing both wear rate and deformation.

Because of these factors, this investigation was undertaken to explore methods of determining the contact surface temperature in reciprocating seals. Two methods were selected for exploration. One was the use of infra-red radiometry using a scanning infra-red camera. The other was the use of a sensitive surface thermocouple having a low mass in order to obtain high speed response (for a stroke of 40 mm at 1500 rpm, a 3 mm wide loaded seal is over a thermocouple in the rod surface for only one milli-second).

3.0 TEST APPARATUS

The test apparatus used for these experiments on the measurement of reciprocating seal surface temperatures consisted of two reciprocating test rigs and two temperature measurement means. Each is described and defined in this section. In addition, simple crude means were used to create reciprocation under load for preliminary check-out of the fast-response thermocouple and the infra-red camera. These means are not described in detail.

3.1 Pin-on-Plate Reciprocating Rig

The pin-on-plate reciprocating rig was built for conducting screening tests on the relative wear rates of seal materials for use in Stirling engine seals. It has been described in detail by Bhushan and Wilcock [1]. In this apparatus, a pin of 3/16" diameter seal material is loaded by a dead-weight compound lever system against a Nitralloy steel plate, matching the engine piston rod in material and surface finish. The plates are carried in a moving carriage and are replaced with new plates for each test.

The carriage is supported on linear ball bushings and is reciprocated by a crank and connecting rod mechanism. The crank is driven by a variable frequency AC motor with speed control and a digital frequency meter. The screening rig is shown in a general view in Figure 3.1.

The screening rig carries six test plates and has six dead-weight loading devices. For the tests in this program, it was modified in several ways:

(1) A single test pin and test plate were used.

(2) A bracket was bolted to the carriage to hold the test plate in a vertical position (see Figure 3.2).

(3) A new lever loading system was positioned to hold a 3/16" pin against the test plate.

(4) The test plate was increased in thickness to permit solid flush mounting of the fast response thermocouple.

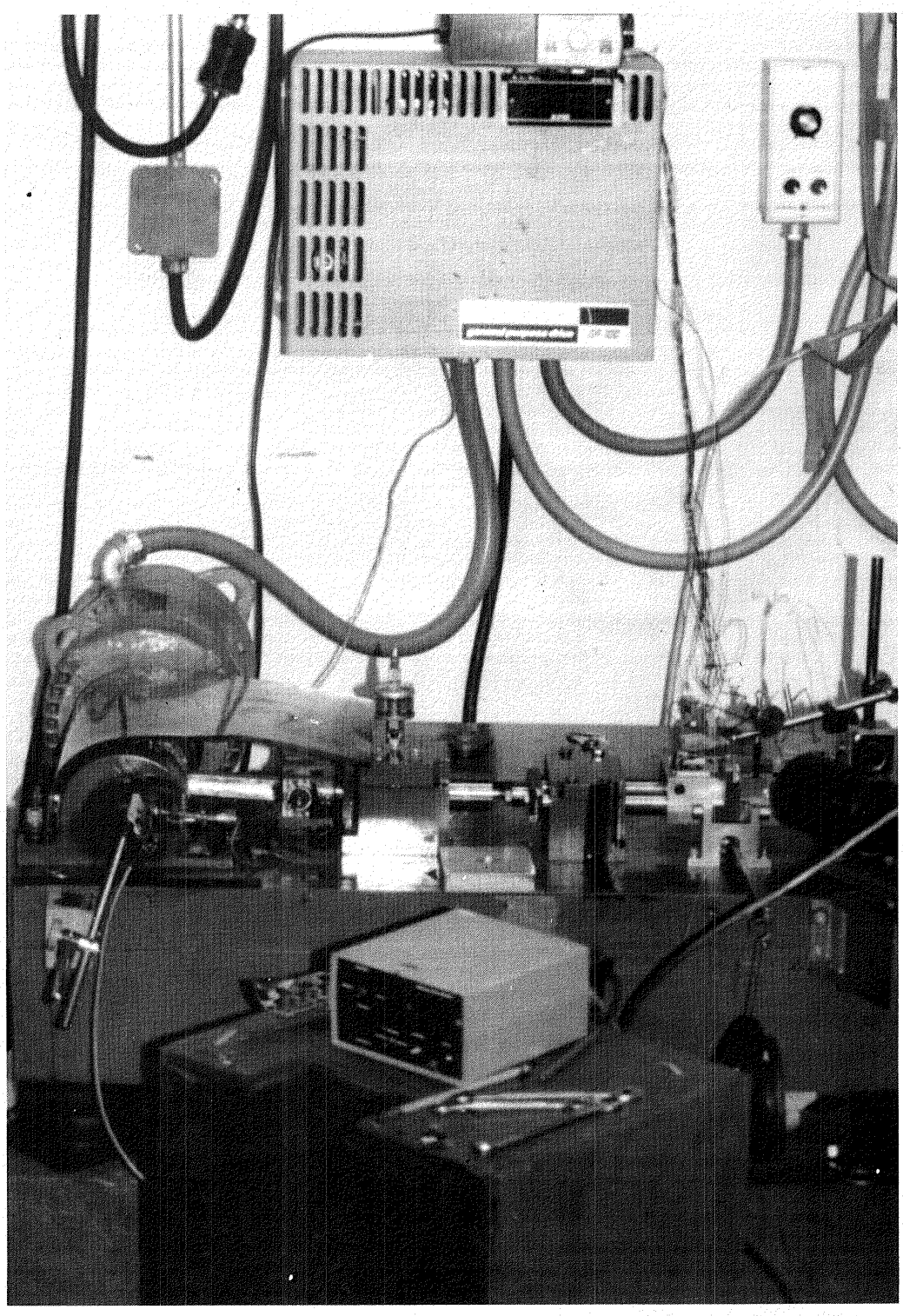

Figure 3.1 General View of Screening Rig

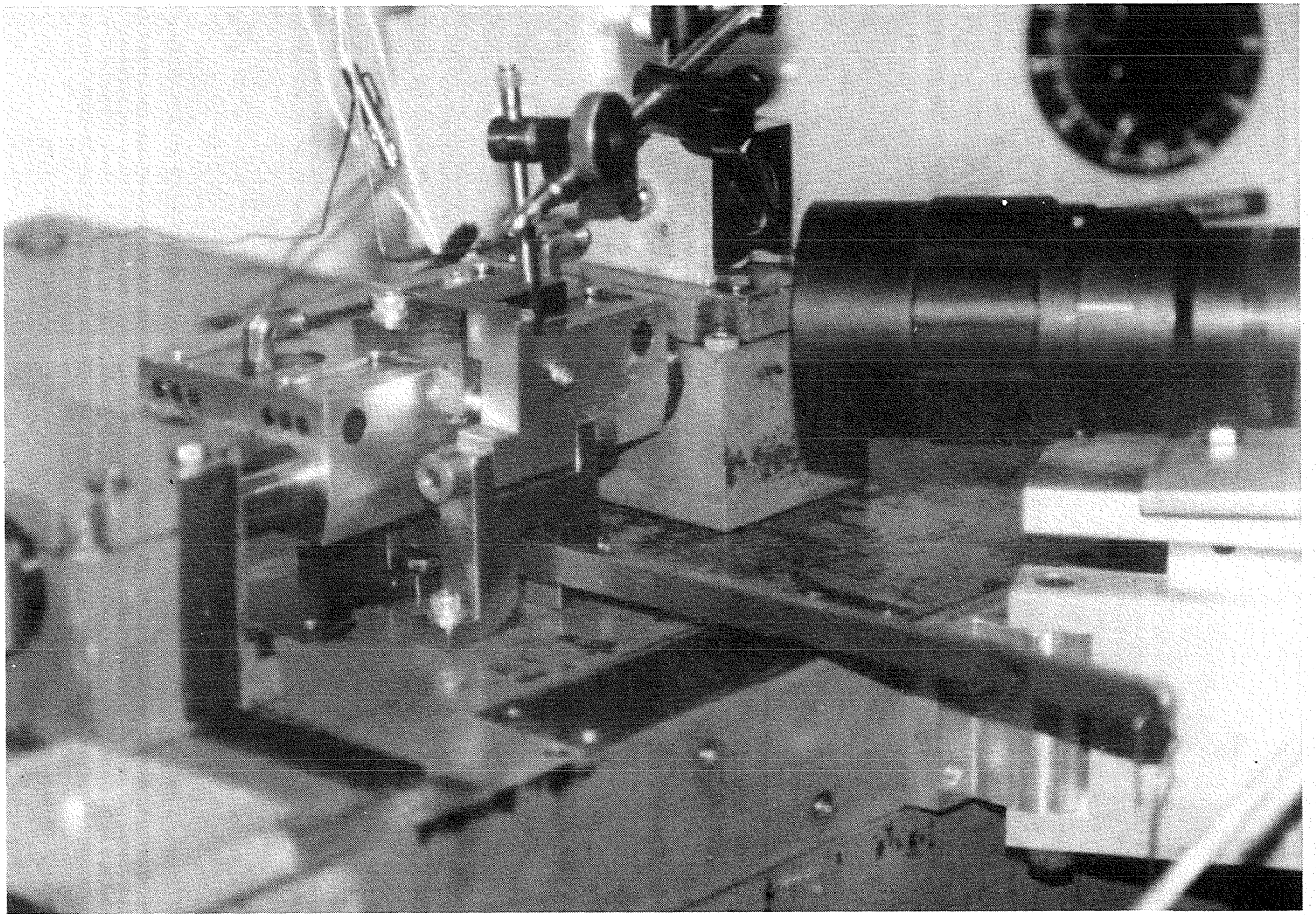

Figure 3.2 Close-up of Carriage and Bracket, Screening Rig

(5) A heavy camera mounting bracket of a double-arm design was built for the infra-red camera. The bracket was solidly mounted to the 4" thick steel bed plate of the screening rig in order to minimize camera vibration due to vibration of the shock-mounted bed plate.

The vertical orientation of the test plate was necessary because the camera sight angle must be approximately horizontal. This is necessary in order to retain the LN_2 coolant in the camera trap.

The test assembly is shown in Figure 3.3.

A second version of the pin-on-plate reciprocating rig was fabricated for experiments in which a sapphire plate was substituted for the Nitralloy plate. In this case, the thermocouple could not be used, but the camera could look through the plate at the rubbing contact zone at the end of the pin.

In order to keep the contact zone in view, the pin was placed in a fixed mounting bracket on the carriage, and the infra-red transparent sapphire plate, mounted in a steel bracket, was loaded against the pin by the dead weight compound lever system. This assembly is shown in Figure 3.4.

The sapphire plate was cut with a diamond saw from a single crystal of Al_2O_3, 3-mm thick, with optically flat polished surfaces.

For both types of test, the carriage could be operated at speeds up to 2500 rpm. However, data was taken only up to 1500 rpm because of excessive vibration in the camera system above that speed. The stroke was 40 mm.

The loading arm carried a hanging pan for kg weights. The lever system multiplier was 2.12. The tare weight of pan and arm was 0.28 kg.

The pin area for a 3/16" pin is:

$$17.8 \times 10^{-6} \quad (m^2)$$

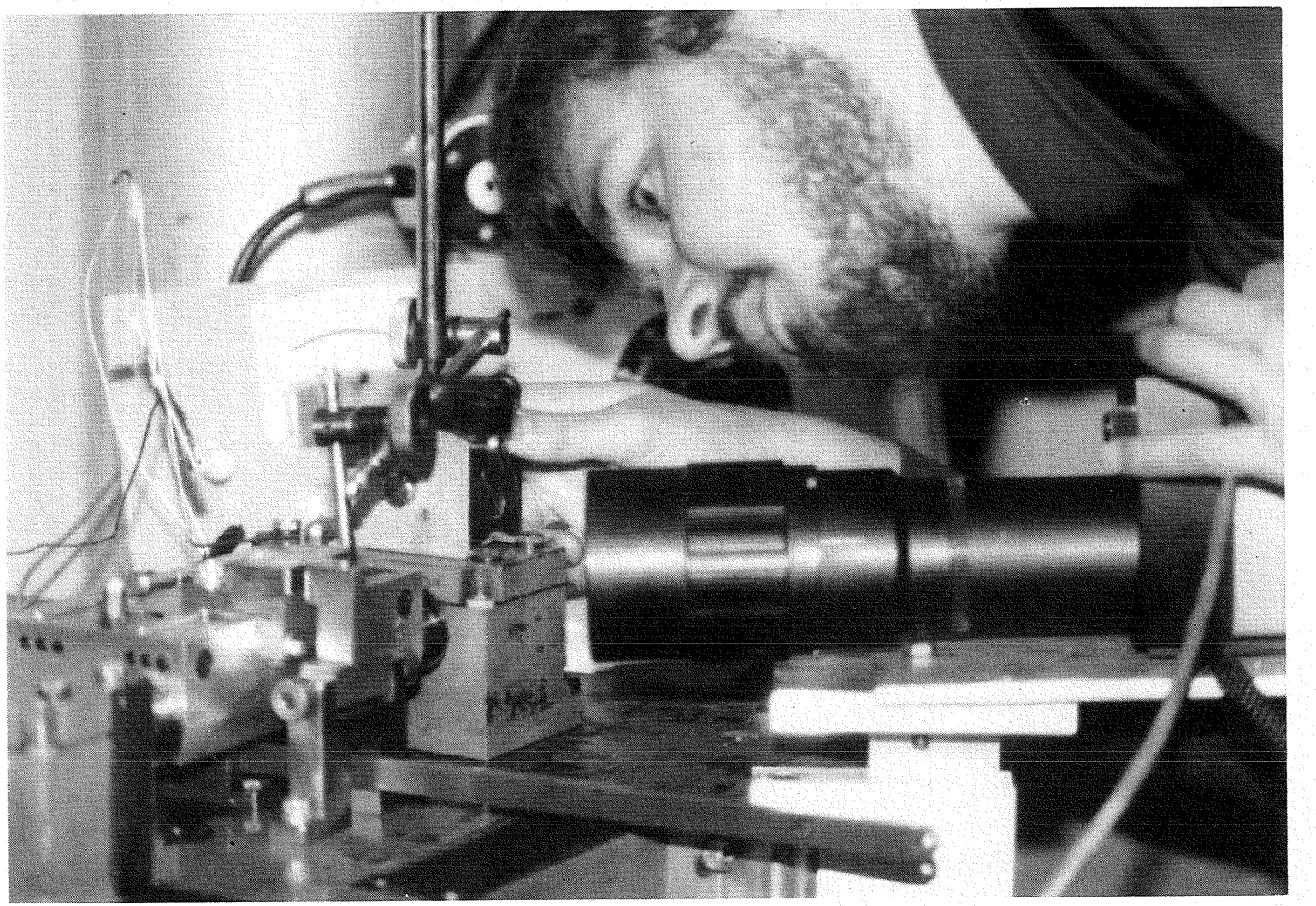

Figure 3.3 Test Assembly, Pin-on-Plate Reciprocating Rig

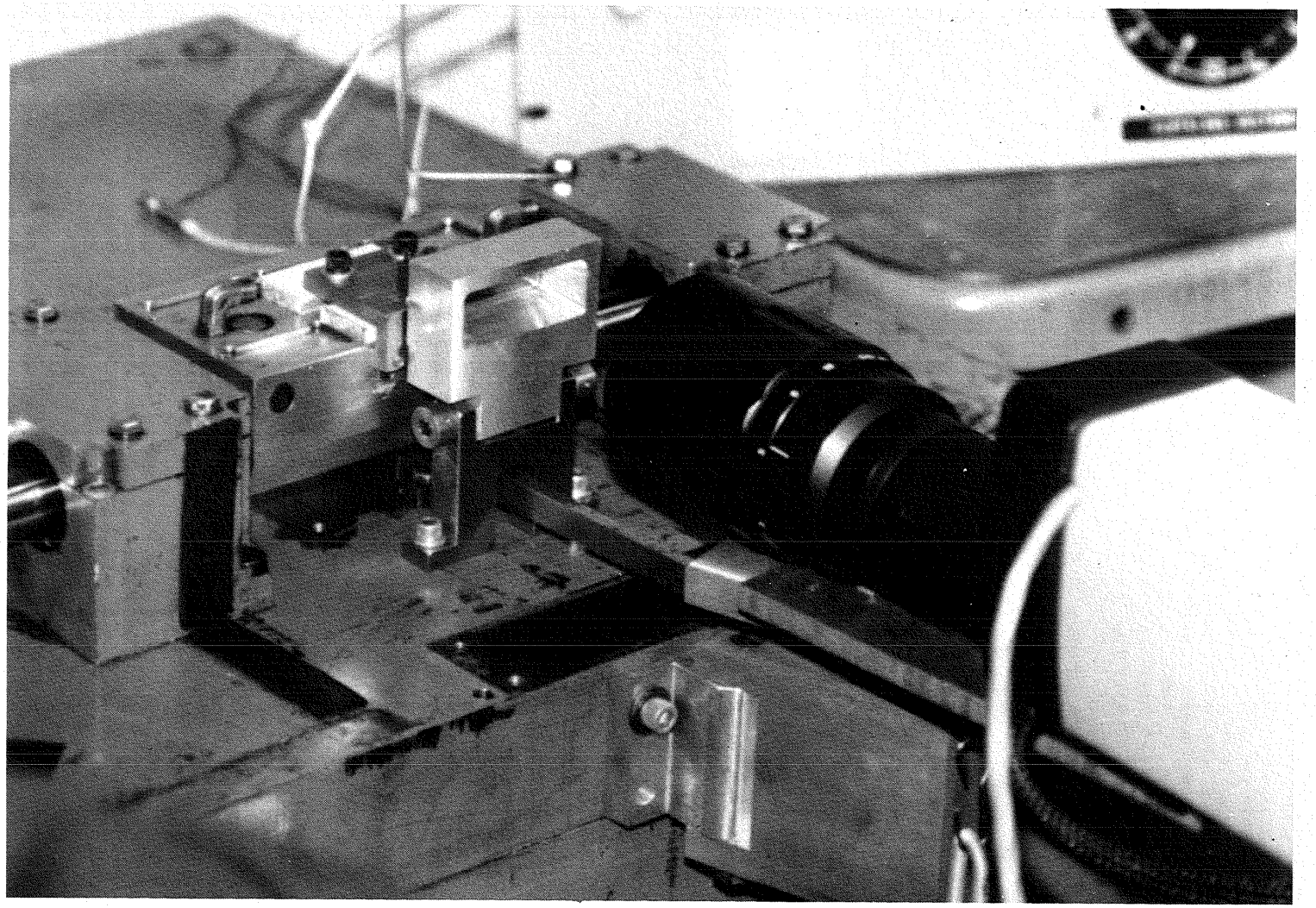

Figure 3.4 Assembly of Pin-on-Plate Reciprocating Rig

MTI- 20671

The unit load for a weight of W kg on the pin is:

$$P = 1.17 \times 10^{6} \ (W + 0.28) \quad (Pa) \tag{3.1}$$

If N is the drive rpm, the velocity at mid-stroke (maximum) is:

$$V_m = 2.09 \times 10^{-3} \ N \quad (m/s) \tag{3.2}$$

The PV factor in SI units is then:

$$PV_m = 2440 \ N \ (W + 0.28) \ (Pa \times m/s) \tag{3.3}$$

3.2 Reciprocating Seal Test Rig

The Reciprocating Seal Test Rig (RSTR) was built for measuring the performance of pumping ring seals. It is described in detail in NASA Report No. CR-165271.

The test piston rod in the RSTR is oriented vertically. The rod is mounted in a crosshead driven by a heavy-duty crank mechanism. This in turn is driven by a variable frequency AC motor with speed control. Lubrication is provided by an external lubrication system. Three cranks of 1", 1-1/2", and 2" (25, 38, and 51 mm) stroke can be inserted.

The test rod is replaceable. The rod is guided in hydrostatic bearings, one above and one below the test section. The oil feed to the hydrostatic pockets is individually controlled to each pocket in order to provide precision control of the rod position in the test seals. Two seals pumping against each other are used in each test.

For this program, the upper test housing including the upper hydrostatic bearing was removed. A shorter rod was fabricated, and a modified test cartridge was designed and fabricated to hold a cap seal.

A section through the test assembly is shown in Figure 3.5. The cap seal is held in place by a thin upper plate so that the surface of the rod immediately above the seal can be viewed directly by the infra-red camera. Nitrogen

REVISIONS		SIZE D	SK-D-7012	REV A
SYM	DESCRIPTION	DATE	APPROVED	
A	MACHINING DIMENSIONS ADDED	12/15/80		

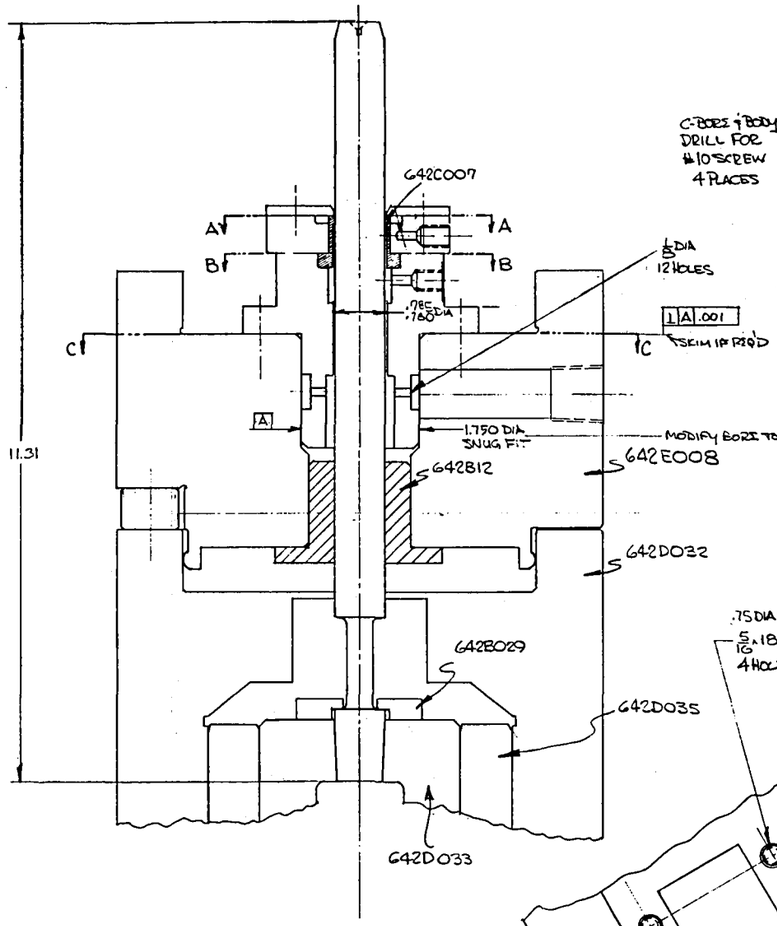

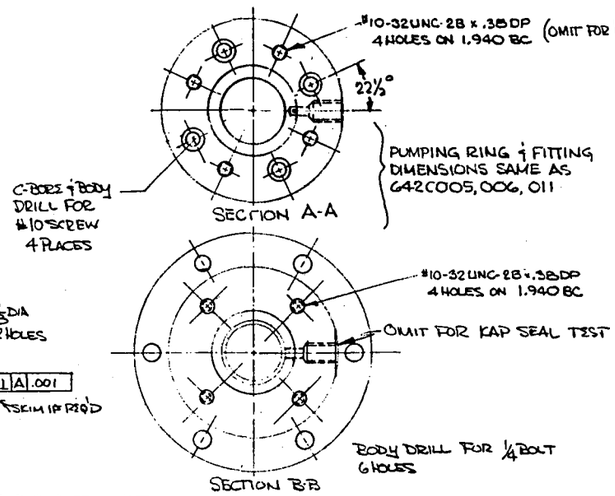

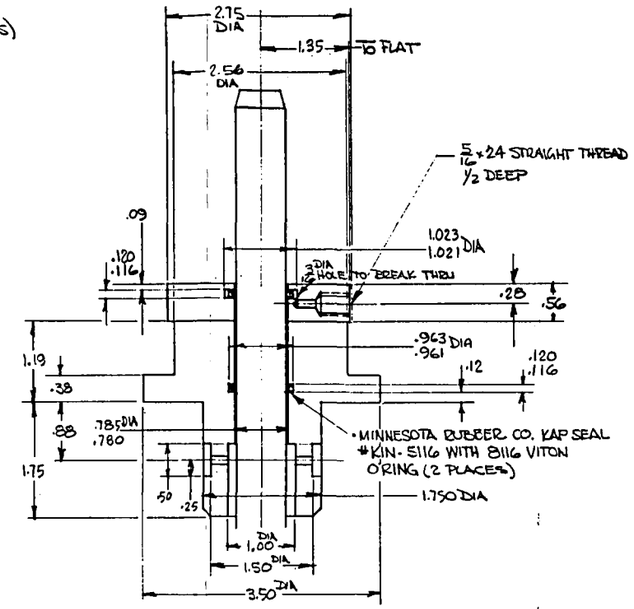

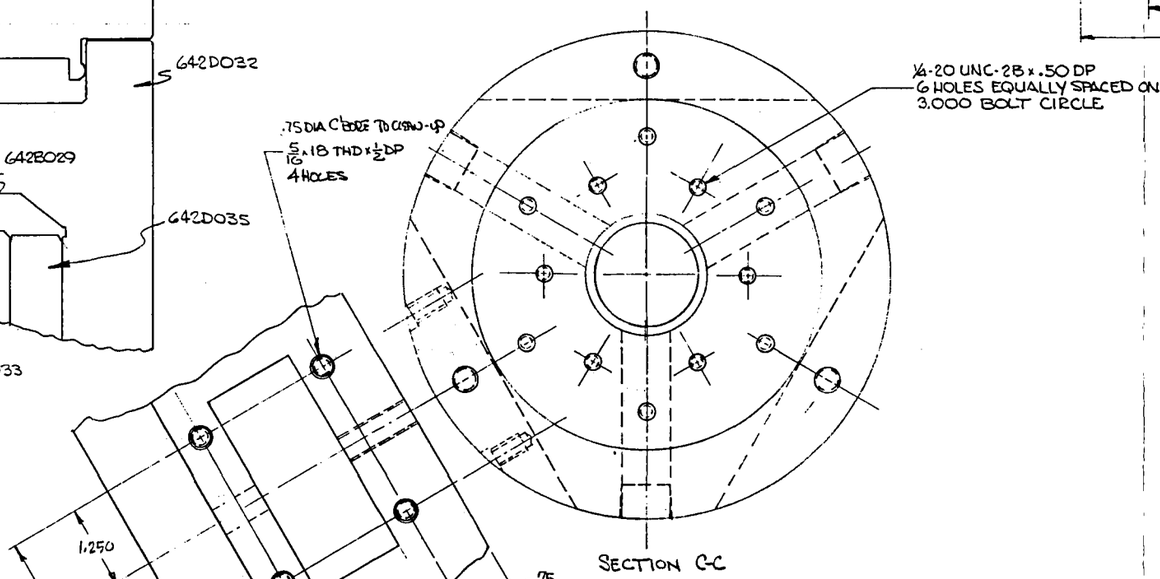

Figure 3.5 Section of Rig as Re-Designed

UNLESS OTHERWISE SPECIFIED DIMENSIONS ARE IN INCHES TOLERANCES ON: DECIMALS FRACTIONS ANGLES .XXX ± ± ± .XX ± ALL SURFACES ✓ BREAK SHARP CORNERS AND REMOVE BURRS	DRAWN 12/5/80	Mechanical Technology Incorporated Latham, New York
MATERIAL STN STL AISI 416	CHECK	TITLE CONVERSION OF G42E001 FOR RUB TESTING
TREATMENT HEAT TREAT TO R_c 28-32	DESIGN	
	ANALYTICAL	
	MATERIALS	
	MFG. ENGR.	
	PROJ. ENGR.	
	QUALITY CONTROL	CODE IDENT NO. 26741 · SIZE D · SK-D-7012
		ISSUED · SCALE · SHT. OF

BRUNING 40-105 2214S-1

under pressure can be admitted behind the O-ring of the cap seal in order to load the seal. Figure 3.6 shows the upper test assembly with the camera in position.

Lubricating oil could not be completely prevented from reaching the rod beneath the test cap seal so that the tests reported in the following section were of a lubricated seal.

The stroke used in the tests in this program was 50.8 mm (2.00"). The rig can be operated up to 2500 rpm since the crank shaft is counter-balanced. However, a resonance was encountered in this program at 1200 rpm which vibrated the camera excessively. (This resonance is normally transited rapidly in pumping rig test series.) Consequently, thermal seal test data was taken up to 1100 rpm only.

The maximum velocity in the cycle is $V_m = 2.92\ N$ (m/s)

3.3 High Response Thermocouple

The thermocouple used was a NANMAC Model E6-1, Type T, Copper-Constantin with a sensitivity of 4.27 mV/100°C. The couple construction is shown in cross-section in Figure 3.7. In it are shown:

a) Thermocouple wires that have been flattened to 0.001 inch thick ribbons at the end.

b) An insulating layer of 0.0002 inch of mica between the two ribbons, and additional mica sheets on the outside of the ribbons.

c) A tapered holder for the wires and the mica sheets.

d) A housing with an internal taper that supports the tapered holder. The taper is used to generate the compression necessary to obtain a sealed assembly.

The thermocouple junction is obtained in a unique way - by abrasion of the tip of the assembly described above. When the tip is abraded, the two metals smear across the thin mica barrier that separates them. Wherever they contact, a junction is formed. These junctions have virtually no thermal mass,

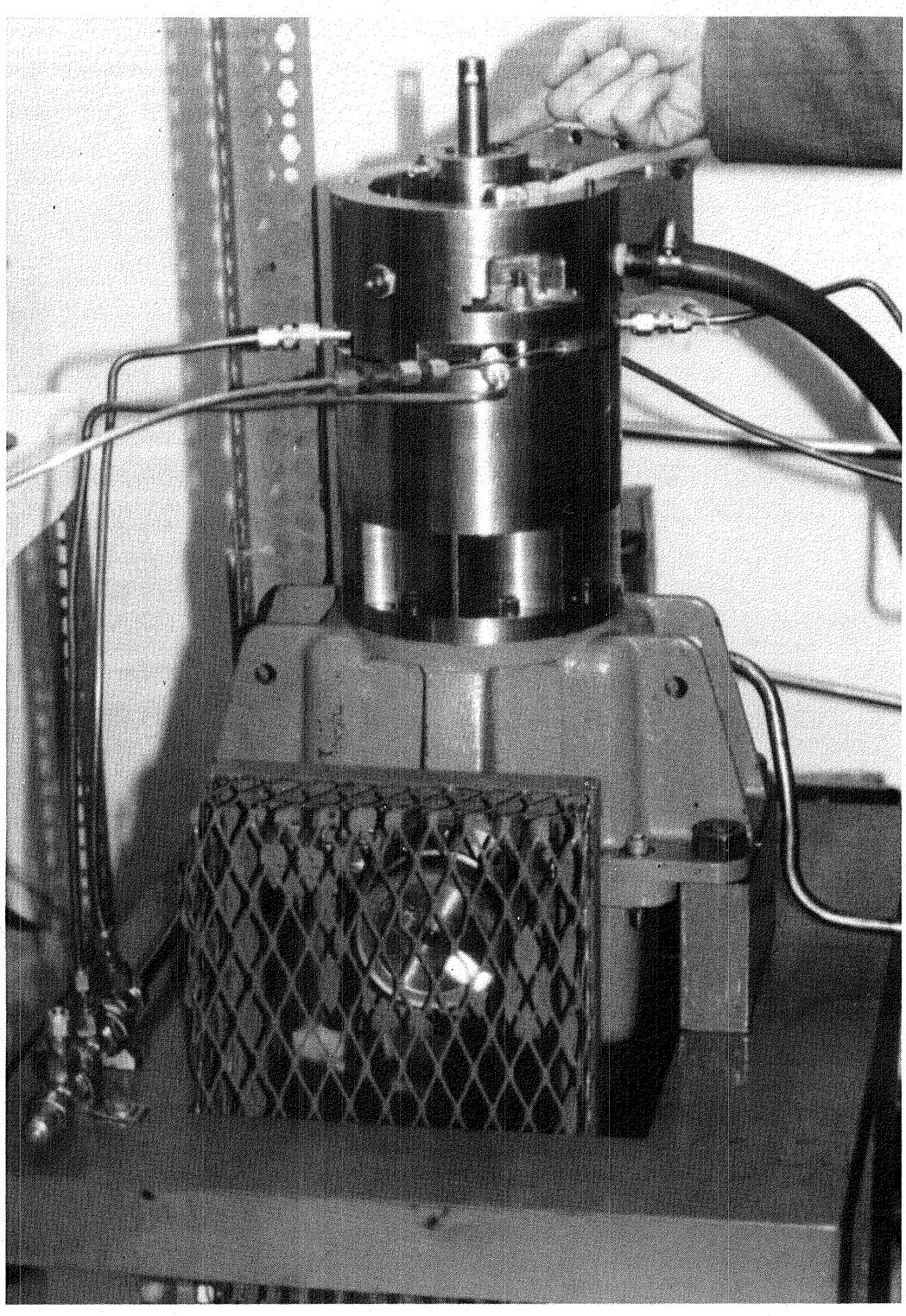

Figure 3.6 Upper Test Assembly Reciprocating Seal Test Rig

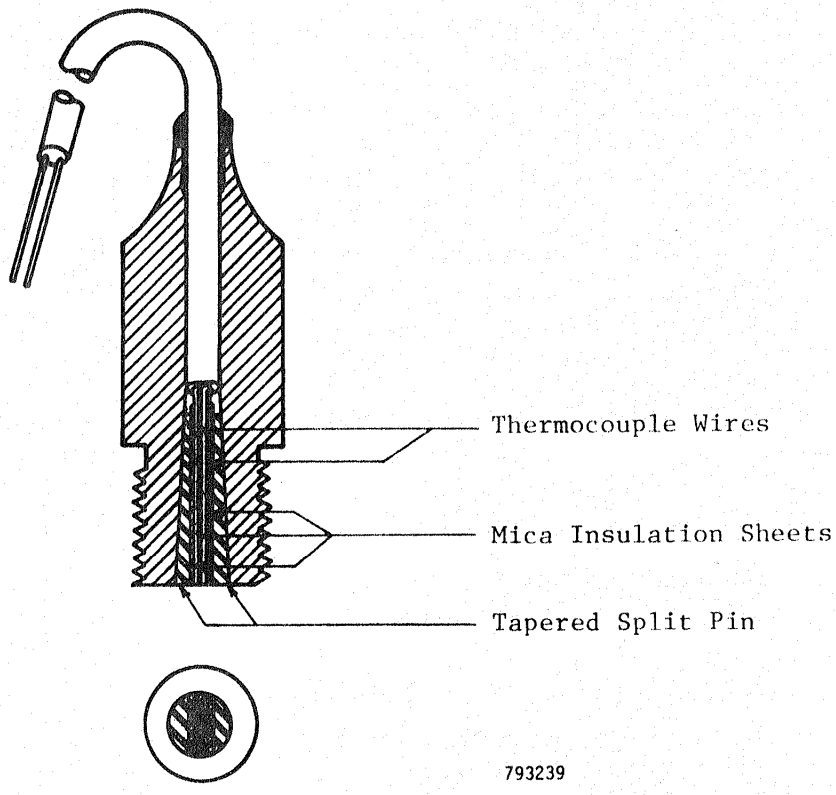

Figure 3.7 Cross-Sectional View of NANMAC Thermocouple

so that as a result an extremely short response time to thermal transients is obtained. The performance of this couple is well established, and it is used for transient temperature measurements of a wide variety. It has a response time of approximately 10 micro-seconds. The seal temperature measurements contemplated fall well within its area of application.

The thermocouple potential is read directly on an oscilloscope or through an amplifier on a chart recorder or tape recorder.

As packaged for this program, the couple is contained in a 3-mm diameter sheath threaded on the outside for mounting.

3.4 Infra-Red Camera

Obtaining accurate rapid thermal readings with the infra-red camera is much more than a "point and shoot" operation. The total system required is shown in Figure 3.8, and involves analog storage, A/D conversion, and computerized data handling in addition to the camera. This system, including details of calibration and scaling, is described in detail in Appendix A. The system was developed and calibrated at GTRI and used for the experimental observations at MTI. Data reduction was then done at GTRI.

The computerized infra-red analysis system as illustrated in Figure 3.8 requires a variety of instruments, each of which needs to meet very specific specifications in order to contribute to the total system. In addition, it is of vital importance that a proper communication link be established between the various components. This section describes the relevant capabilities and limitations of each instrument as well as the procedures used to determine these limitations.

3.4.1 The AGA 750 Thermovision Camera

The AGA 750 is the eye of the total system and the first link in the chain of four operations. It is an optical scanning device which converts electromagnetic thermal energy radiated from an object into electronic video signals. Electromagnetic energy radiated by an object is focused by a lens into an eight-sided prism that rotates around a horizontal axis and thus causes a vertical scanning motion (see Figure 3.9). This prism is rotated at 3.125 rps

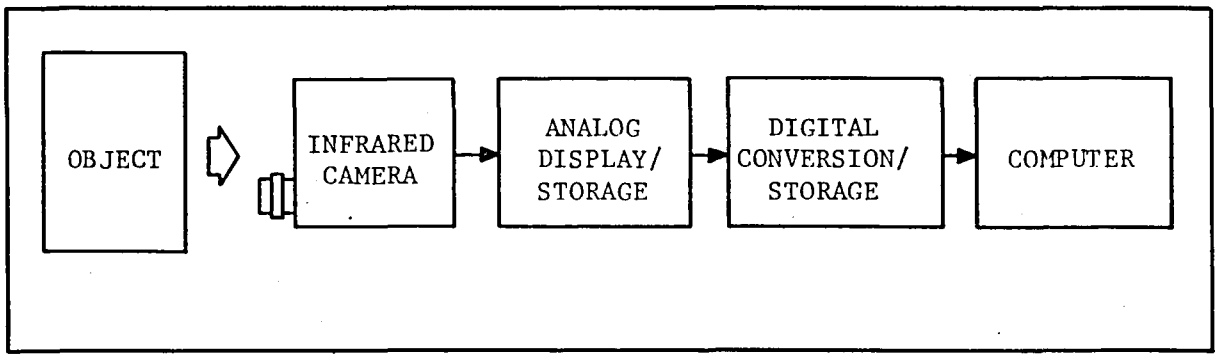

Figure 3.8 The Total Infra-Red Camera System

812276

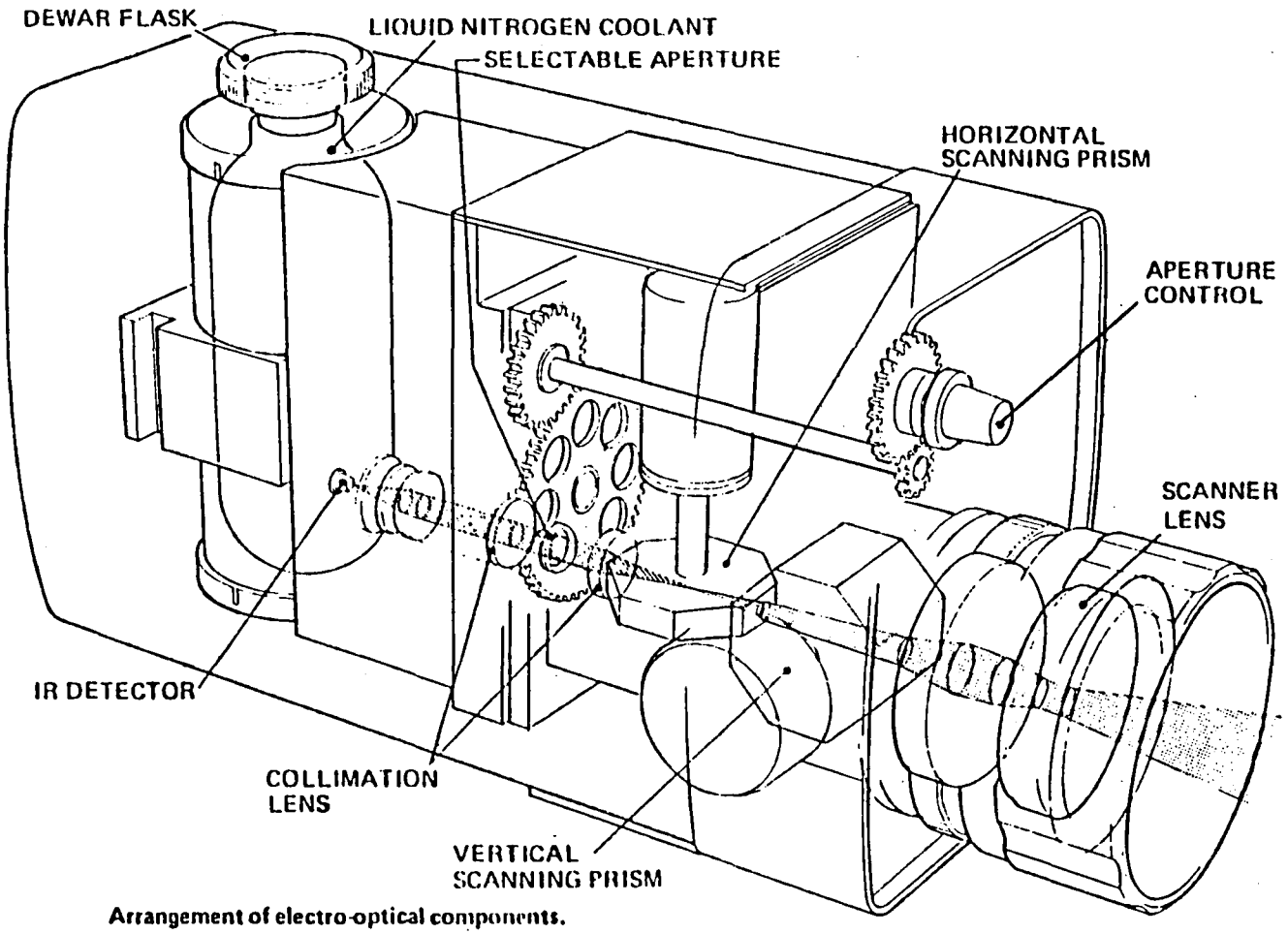

Figure 3.9 The AGA 750

by a D.C. motor. The optical output from the vertical prism is passed through a second prism which rotates around a vertical axis at 312.5 rps and thus causes a horizontal scanning motion. The rotation of both prisms is controlled by two slotted discs which rotate on the same shafts as the respective prisms. The rotating slotted discs are electronically connected to the horizontal and vertical triggering circuits, to provide horizontal and vertical trigger pulses (HTP and VTP) to the monitor. These pulses also control the speed of the vertical and horizontal prism motors to synchronize their rotation.

Output from the horizontal prism is passed through a set of relay optics containing a selectable aperture unit and a filter cassette unit and finally focused onto a single element point detector located in the wall of a dewar chamber. Liquid nitrogen coolant (LN_2) maintains the chamber at a temperature of -196°C thus causing the detector to be sensitive to the two 5.6 μm infra-red wavelengths. The detector produces an electronic signal output which varies in proportion to the radiation from the object. This signal is amplified within the scanner unit.

Two infra-red lenses can be used with the camera, one with a 7° field of view and the other with a 20° field of view. For close-up work, three extension rings of the following lengths were used:

ring 1: 12 mm
ring 2: 21 mm

These rings can be mounted between the lens and the camera body to permit a significant reduction of the working distance of the camera.

In addition to the features described above, a special "remote control" unit was built which allows the vertical scanning prism to be stopped and single-stepped through any angle at a step size of approximately 800 steps per complete revolution. This allows the operator to fix any horizontal line within the field of view and scan it at a rate of 2500 lines per second (the scanning rate of the horizontal prism). A digital counter indicates which line in the picture is being scanned.

Rather than having each VTP occur at every hundred horizontal scans, the remote control unit also allows for external triggering. This is accomplished by a small infra-red transmitter-receiver device that causes a trigger pulse to occur each time the infra-red beam between the transmitter and receiver is interrupted by a chopper linked to the moving mechanism to be observed. This feature is particularly useful when observing reciprocating machinery since VTP's synchronized with the mechanical cycle provide information concerning the absolute location of the reciprocating mechanism.

3.4.2 Selection of Lens Combination

Several combinations of lens and spacer ring were evaluated for their capability in spatial resolution. The results of the tests are summarized in Table 3.1. The conclusion was that for our purpose all combinations but one (the 7° lens with extension ring no. 3) were unsatisfactory, mainly because of the amount of distortion caused by the lens. Of all choices, the 7° lens with extension no. 3 offered the maximum resolution possible (nine spots per line) with an acceptable amount of distortion.

3.4.3 Calibration Procedure for Camera Voltage Levels

In order to use computer analysis for temperature measurements, a relationship must be established between the radiation seen by the camera and the voltage level outputs of the video pre-amp.

A Barnes blackbody infra-red radiator was used as a calibrated temperature source and varied in temperature from 60°C to 230°C at 15°C intervals. The corresponding voltage output from the pre-amp was monitored on an oscilloscope. This procedure was repeated for all camera apertures.

The temperature values were converted into isotherm units using the AGA supplied HP-65 programs for temperature to isotherm conversions (see Figure 2-8 and 2-9 in Appendix A). This resulted in a direct relationship between voltage and isotherm units (radiation level) independent of aperture. These data were plotted and correlated by means of a linear regression. The following equation resulted:

$$I = 165.46V + 8.4513 \qquad (3.4)$$

TABLE 3.1

CAMERA RESOLUTION USING DIFFERENT EXTENSION RINGS

Lens	Extension Rings	Object to Tip of Lens (mm)	Field of View (mm)	Spotsize Diameter at 50% (mm)	At 100%	Number of Resoluble Spots per Scanned Line per 100%	Lens Distortion	Comments w.r.t. our Application
20°	1 + 2	89	17	0.43	0.98	17	very much	unacceptable*
	2	70	12	0.33	1.40	9	much	not recommended
	(1 + 2 + 3)	46	4	0.57	2.40	2	very little	unacceptable
7°	3	161	16	0.56	1.80	9	little	most useful
	(1 + 2 + 3)	118	11	0.46	1.70	6	very little	useful but limited resolution
	(1 + 2)						much	

*Of limited use if object can be centered exactly

with a correlation coefficient of $r^2 = 0.976$, where

I = radiation in isotherm units

V = voltage in volts.

The conversion of isotherm units to temperature used by the HP-65 programs is of the following form:

$$T = \frac{B}{\ell n(I) - \ell n(A)} - 273°C \qquad (3.5)$$

3.4.4 The Honeywell 101 Tape Recorder

The Honeywell 101 is the second link and can be called the primary memory of the system. Its function is to store temporarily the continuous stream of video data coming from the AGA 750 so that it can be analyzed at a later time and at a slower rate suitable for computer analysis. The Honeywell 101 is a high quality magnetic tape recorder with built-in microcomputer control. It has eight tape speeds and up to 14 record and reproduce channels. In addition, it also has both direct as well as FM record and reproduce capabilities. We chose to use FM because it was able to cover a signal frequency range of zero to 80 kHz at a signal to noise (S/N) ratio of 50 dB. These specifications are sufficient to record the AGA 750 video signal adequately which requires a frequency response of DC to 80 kHz at a minimum S/N ratio of 46 dB.

The multichannel and multispeed capabilities allowed us to record the signal as well as the HTP's and VTP's on different channels at 120 ips while reproducing them later at 7.5 ips, thus reducing the maximum signal frequency by a factor 16, suitable for A/D conversion.

3.4.5 The AR-11 A/D Converter

The AR-11 is the third link in the system and its function is to translate the continuous signal played back from the Honeywell 101 into a form which can be understood and analyzed by a digital computer.

The AR-11 has a ten bit conversion accuracy which means it can distinguish one part in $(2)^{10}$. The conversion time is approximately 43 micro-seconds. Its

primary advantage is that it is built into the PDP-11 minicomputer and can be operated by means of a program written in PDP-11 assembly language as well as BASIC. (See also Chapter III, Section A, Appendix A.)

3.4.6 The PDP-11/10 Minicomputer

The PDP-11 is the fourth and final link and forms the brain of the system. It takes the information translated by the A/D converter and reduces it to useful information in the form of graphs, tables or single numbers.

The PDP-11/10 minicomputer is a 16 bit word machine with 28K word magnetic core memory. 24K words of memory are available to the user. The machine is equipped with a CAPS-11 magnetic cassette tape mass storage system and an operating system that supports a BASIC computer language. A built-in AR-11 module allows the user to perform software controlled A/D conversions either in BASIC or assembly language. Interactive graphics in BASIC are possible by means of a GT-40 random scan graphics terminal.

These last two features especially made the use of the PDP-11 attractive since digitized data could easily be displayed and manipulated on the graphics screen.

3.4.7 The EXPLORER III Digital Oscilloscope

In addition to the instruments mentioned before, we also made use of a digital oscilloscope manufactured by Nicolet Instrument Corporation. The Explorer III oscilloscope is a versatile instrument that allows us to look at a signal, store it in digitized form in a 4K memory and plot it on an x-y plotter. The Explorer III has a built-in 32K floppy disk unit which allows it to store eight 4K signals or 32 1K signals. The maximum digitizing rate is 2 MHz and the resolution is 0.025 percent. Once data have been "frozen" on the screen, they may be inverted, moved, added, subtracted, expanded, erased, or transferred to a pen recorder.

The main advantage of this instrument to this project is its capability to freeze signals and output them to a pen recorder, which allows preview of a signal before analyzing it with the computer.

3.4.8 Data System Operation

The operation of the system described in handling data from the experiments is discussed in depth in Appendix A.

4.0 TEST RESULTS

Temperature observations were made under a number of test arrangements. These were as follows:

1) Preliminary tests under simple non-controlled rubbing conditions: a) at MTI on the NANMAC thermocouples, and b) at GTRI on the infra-red camera.

2) Rulon on Nitralloy in the pin-on-plate reciprocating test rig, using both thermocouple and infra-red camera (at MTI).

3) Rulon on sapphire in the pin-on-plate reciprocating test rig using the infra-red camera (at MTI).

4) Rulon cap seal on Nitralloy rod in the RSTR using the infra-red camera (at MTI).

4.1 Preliminary Tests

A reciprocating saw was used to drive a small steel plate against which a Rulon pin could be pressed. The pin was made of Rulon S. One of the NANMAC thermocouples was mounted through a hole in the steel plate and lapped flush. The thermocouple was connected to a sensitive C.R. oscilloscope.

Difficulty was experienced in establishing the thermocouple junction by rubbing with the Rulon. Rubbing with a steel pin or with abrasive paper would establish junction.

When such a junction was rubbed by the Rulon pin with pressure applied by hand, a small voltage output was obtained corresponding to about 2°C. The life of the junction was short, and it often had to be reestablished by the technique outlined above. As a result, it was questionable whether the thermocouple would work in the reciprocating pin-on-plate rig.

At GTRI, preliminary tests were run by looking at the end of a Rulon pin rubbing on a sapphire surface. The infra-red camera was used in the normal two dimensional mode. The data was tape recorded and analyzed by the method described in Section 3.4 and in Appendix A. Details are contained in Appendix A.

Data from one preliminary run was analyzed by computer to provide the isotherm diagram shown in Figure 4.1 (also see Appendix A, Figure 3.3). Note that the end of the pin is not uniformly heated. With the camera in the display screen mode, hot spots were observed to shift location or move about with time.

4.2 Rulon on Nitralloy, Pin-on-Plate Rig

These tests were intended to provide simultaneous information from the thermocouple and from the infra-red camera. However, a reliable thermocouple junction could not be established during the infra-red test series. At a later date, further experimentation made possible establishment of a junction by removing the plate from the apparatus and abrading the surface with a fine grinding wheel. While this technique would not be suitable for seal tests because of the surface roughening, it did make possible a series of tests with good results at the same load and speed conditions used for the camera tests.

4.2.1 Infra-Red Data

The infra-red camera was used in the repetitive single line scan mode. Details of the tests are given in Appendix A including the reference temperature surface used and the estimation of the surface emissivity.

A typical thermogram for a single scan, as produced by the data reduction process is shown in Figure 4.2. The peak over the thermocouple position is partly due to the difference in emissivity of the mineral insulation around the thermocouple and partly due to the lower heat conductivity in this area.

The maximum temperature observed on the plate under a variety of load and speed conditions is listed in Table 4.1 for two assumed values of plate emissivity. Surface temperatures were observed to reach equilibrium rapidly, in about twenty seconds, at each test condition.

Additional information is given in Appendix A.

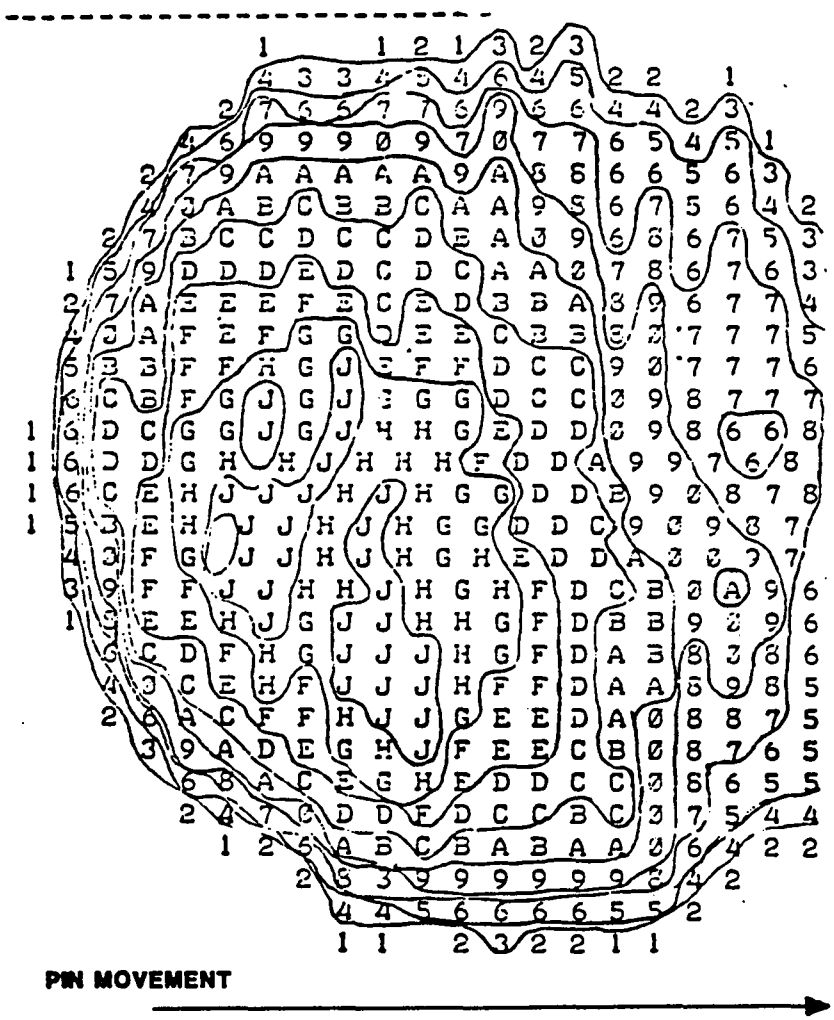

Figure 4.1 Isothermal Map of Rulon on Sapphire Contact Area

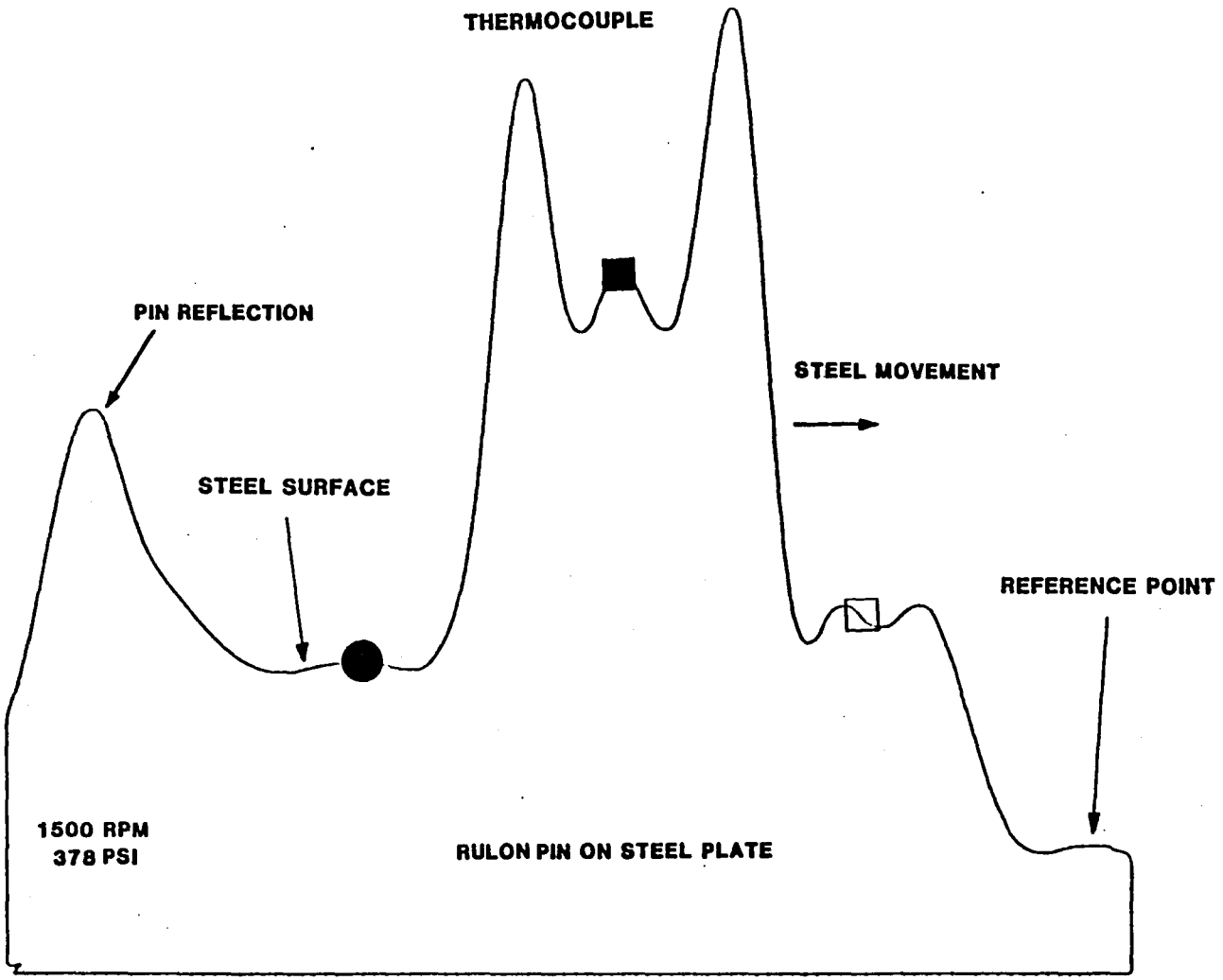

Figure 4.2 Rulon Pin on Steel Plate Center Line Scan

TABLE 4.1

Maximum Plate Temperatures, Rulon Pin on Nitralloy

Speed, RPM	Load, Kg*	PV x 10^{-6} (N/m · s)	Maximum Temperature E = 0.1	Maximum Temperature E = 0.3
500	1.0	1.56	53	36
	2.0	2.78	53	35
	4.0	5.22	56	38
1000	1.0	3.12	59	38
	2.0	5.57	62	40
	4.0	10.45	68	43
1500	1.0	4.69	78	48
	2.0	8.35	79	48
	4.0	15.7	84	52

*Does not include 0.28 Kg tare load

4.2.2 Thermocouple Data

Measurements were made using the fast-response thermocouple under the same load and speed conditions as for the camera observations. These were made, however, at a later date after the TC junction was established by grinding the surface with a fine wheel.

A typical observation is shown in Figure 4.3. Here the temperature increases in the vertically downward direction. The broad band shows the trend with time, the temperature levelling out after some 20 seconds. The horizontal jagged curve shows the individual readings on a more open time scale. The "W" section of this curve indicates the passage of the pin, followed by a gradual cooling temperature decay. The double peak is the result of using a pin with a V notch cut in the end.

The data obtained are listed in Table 4.2. The base equilibrium temperature is the lowest temperature at the beginning of the pulse. The pulse ΔT is the highest of the pulse above the base temperature. Both measurements were scaled from Polaroid pictures of the scope, taken after equilibrium had been reached.

4.3 Rulon on Sapphire, Pin-on-Plate Rig

In these experiments, data could be taken only with the infra-red camera, since the fast response thermocouple could not be inserted in the sapphire plate. The camera viewed the rubbing pin contact zone through the sapphire plate.

The data from this experiment were examined for contact temperatures at the point of maximum velocity during the stroke as well as at the reciprocating point as the pin was in its rightmost position. The field of view of the camera was limited to the right half of the stroke and the temperature values at the very leftmost part of the screen are less reliable because of lens edge distortion. Therefore, the temperatures for maximum velocity (being on the left hand side of the screen) were recorded as the pin was moving to the left as well as when it reappeared on the screen going to the right. These temperatures are based on a measured emissivity value for Rulon J of E = 0.9.

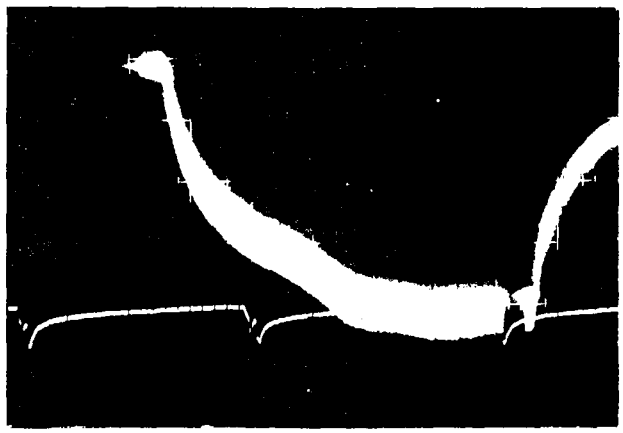

Figure 4.3 Variation of Temperature with Time

TABLE 4.2

Thermocouple Temperature Measurements of Rulon Pin on Nitralloy

Speed, RPM	Load*, Kg	PV x 10^{-6} (N/ms)	Equilibrium Temperature, °C	
			Base**	Pulse ΔT
311	2.0	1.73	28.1	0.6
612	2.0	3.41	34.5	0.6
927	2.0	5.16	41.7	0.8
1523	2.0	8.48	56.7	1.8
2020	2.0	11.24	61.1	2.1
312	3.95	3.22	33.5	2.6
623	3.95	6.43	45.4	5.1
912	3.95	9.42	53.9	5.7
1512	3.95	15.61	71.8	5.7

*Does not include tare of 0.28 Kg

**Room temperature (cold junction), 25°C

The difference between the minimum and maximum temperatures during one stroke never exceeded 10°C as can be seen in Table 4.3, and the maximum temperature observed was 66°C at 1500 rpm and 4.18 kg. The low-temperature point in the cycle was always found during the point of zero velocity at the right-hand side of the screen.

Table 4.3 lists the reciprocating speed, the load, and the calculated PV at the point of maximum velocity. The maximum temperature listed is the average of the maximum observed moving left and moving right. Additional information is provided in Appendix A.

A temperature profile of the pin, derived from the line scan data, is shown in Figure 4.4. This figure presents the pin as it is moving to the left at 1500 rpm, at 4.18 Kg loading. Similar plots have been made at different speeds and it was found consistently that at high loads the left side of the pin was hotter than the right side, regardless of the direction in which the pin was moving. We believe this was due to uneven loading during the movement of the pin.

Additional information is given in Appendix A.

4.4 Rulon on Nitralloy, Cap Seal Test Rig

Data taken on the Stirling Engine Seal Simulator are listed in Table 4.4. The PV factor is calculated at the maximum rod velocity. The temperatures listed were measured at the high and low temperature points in the cycle.

In the Seal Simulator Rig, the camera line scan was horizontal, looking across the rod just above the seal end plate. A typical scan is shown in Figure 4.5. This shows the rod temperature peak and the hex nut area where temperature was measured by thermocouple.

The data taken from the experiment were analyzed to find the highest and lowest temperatures during one cycle of steady state operation at each speed and seal pressure. These temperatures were based on an emissivity for the steel of 0.05, the value measured with the camera at MTI. However, these

TABLE 4.3

Pin Temperatures for Rulon J Sliding on Sapphire (E = 0.9)

Speed, RPM	Load*, Kg	$PV_{max} \times 10^{-6}$ (N/ms)	Temperatures, °C Max(AV)‡	Min	ΔT(AV)
500	1	1.56	55.5	47	8.5
	2	2.78	55	47	8
	4	5.22	59	48	11
1000	1	3.12	50	43	7
	2	5.57	53	46	7
	4	10.45	60.5	49	11.5
1500	1	4.69	51.5	47	4.5
	2	8.35	57.5	52	5.5
	4	15.7	65.5	58	7.5

*Does not include tare of 0.28 Kg

‡Average of maximum temperatures, moving left and moving right

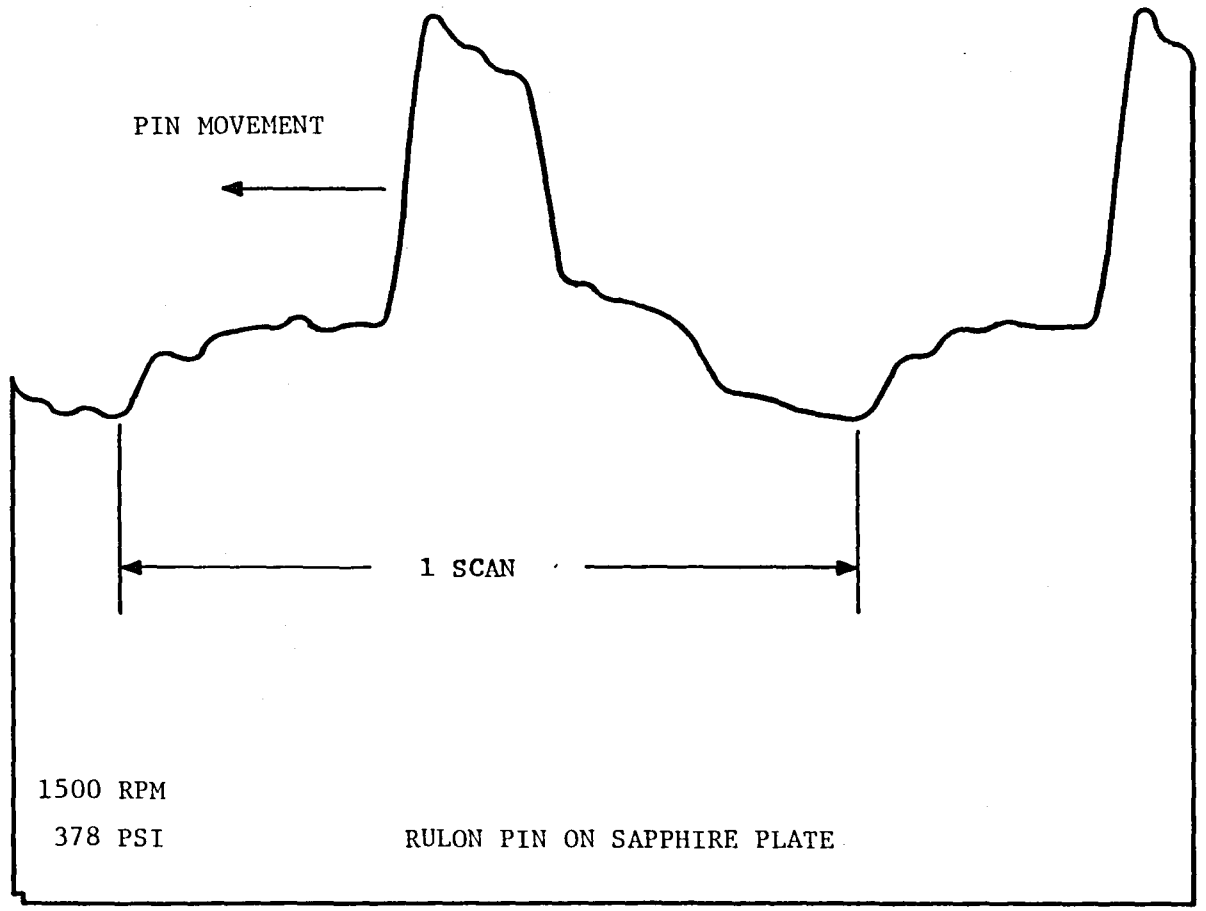

Figure 4.4 Rulon on Sapphire Single Line Scan

812280

TABLE 4.4

Rod Temperatures Near Cap Seal on Stirling Engine

Seal Simulator Test Rig (E = 0.05)

Speed, RPM	Cap Seal Back Pressure, Pa x 10^{-6}	PV x 10^{-6} (N/ms)	Temperatures, °C		
			Max.	Min.	ΔT
300	-0-	-0-	110	94	16
	1.55	1.23	115	104	11
	3.10	2.47	113	104	9
	4.65	3.70	111	104	7
	6.21	4.93	110	101	9
600	-0-	-0-	114	106	8
	1.55	2.47	116	105	11
	3.10	4.93	124	106	18
	4.65	7.40	136	112	24
	6.21	9.87	142	119	23
1100	-0-	-0-	123	104	19
	1.55	4.52	136	115	21
	3.10	9.04	159	123	36
	4.65	13.6	180	141	39
	6.21	18.1	195	153	42
900	-0-	-0-	123	108	15
	1.55	3.70	115	105	10
	3.10	7.40	120	114	6
	4.65	11.1	122	109	13
	6.21	14.8	122	108	14

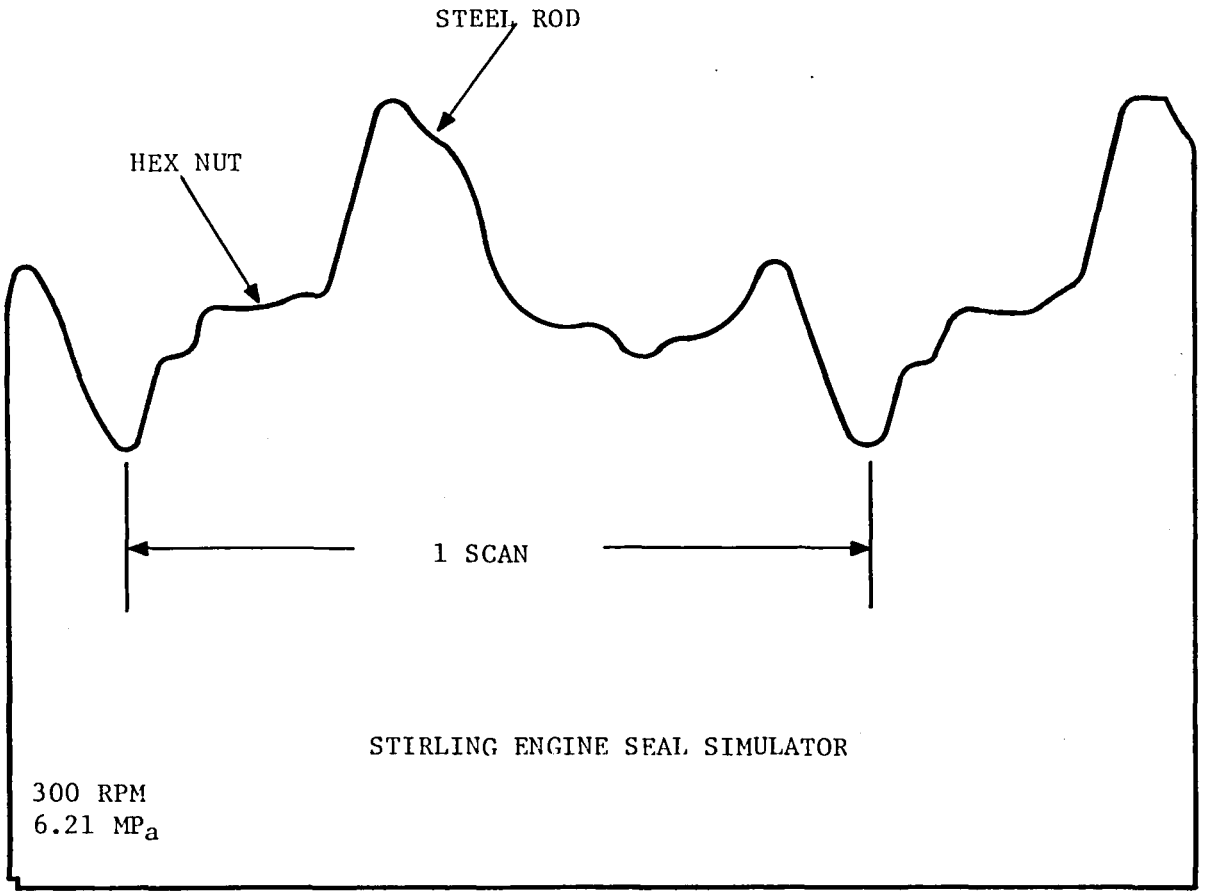

Figure 4.5 Stirling Engine Seal Simulator Single Line Scan

812329

temperatures may represent an upper limit because the surface of the rod was not as smooth as the sample used for emissivity calibration and because a slight oil film was present on the rod. This may have changed the emissivity to a value as high as 0.3, which would lower the maximum observed temperature at 1100 rpm and 900 psi from 195°C to 97°C.

The temperature at the center of the rod is plotted in Figure 4.6 as a function of time, using data from a number of line scans through a full cycle. This is for the 600 rpm, 6.21 MPa (900 psi) experiment. One would expect that the rod would cool off during its excursion above the seal, re-entering the seal at a lower temperature. In Figure 4.6, the rod is emerging in the right-hand temperature cycle, and re-entering the seal in the left-hand temperature cycle. The temperature profile is essentially symmetrical with respect to the lower reciprocating point in the stroke, i.e., the rod's temperature profile is nearly identical for the downward part of the stroke and the upward part. This indicates that during steady state operation the cooling rate of the rod is slow compared to the mechanical cycle time which controls the heating, due to the thermal mass. Since the bottom and top of the rod always enter the seal at low velocities the temperature remains low at these points while the middle of the rod remains hottest because it always enters and leaves the seal at highest velocity.

Additional information is given in Appendix A.

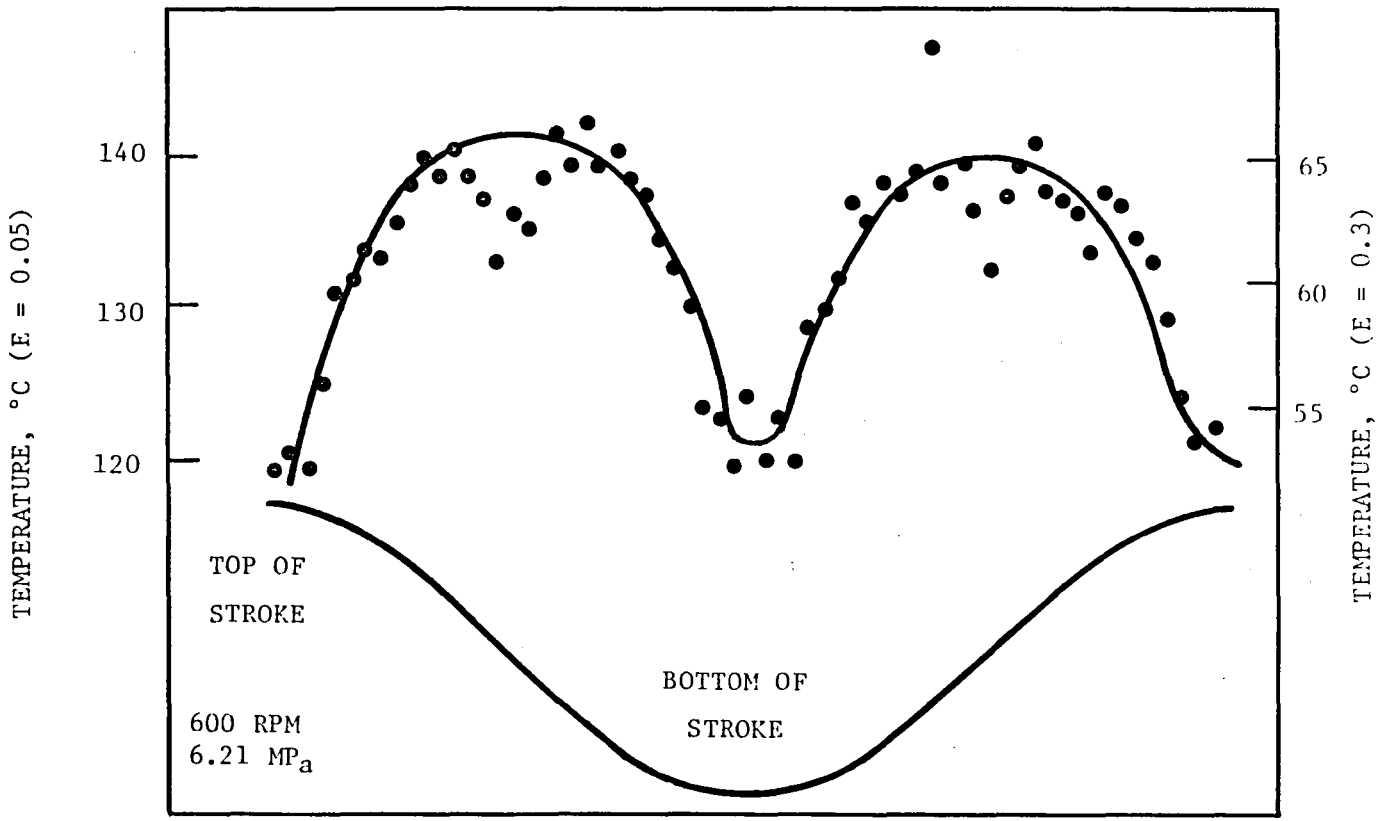

Figure 4.6 Stirling Engine Seal Simulator Rod Temperature During One Cycle

5.0 DATA ANALYSIS

The temperature rise that occurs in a rubbing seal is the result of frictional heating. The total rate of energy input from frictional heating is the product of the load, the rubbing velocity and the coefficient of friction. This is balanced against the rate of heat dissipation from the surface which is a function of temperature level, conductivity and geometry of the part. The temperature attained is then a balance between input and output energy rates.

A general understanding of these factors is essential in assessing techniques for measuring surface temperatures. In this section, each of the experiments will be analyzed and discussed individually, followed by a general review of the findings.

5.1 Rulon J on Nitralloy Plate

The equilibrium base temperatures measured by thermocouple, as given in Table 4.2, are plotted in Figure 5.1 as a function of PV. (Here P is calculated as the total load divided by the cross-sectional area of the pin). The results for loads of 2 and 4 Kg fall on a single line, and it is apparent that the base equilibrium temperature is a function of PV.

The temperature rise measured by thermocouple, the "Pulse ΔT" in Table 4.2, is plotted in Figure 5.2 as a function of PV. Two distinct curves are seen, one for each load condition. The pulse response at the higher load is three times that at the lower load at equivalent PV factors. One possible explanation for this behavior is that due to the surface preparation method, the thermocouple surface may be slightly below the plate surface, so that the true load on the thermocouple was much lighter than expected at the 2 Kg load condition. The effective load ratio was therefore much higher than 2.

The infra-red measurements of plate temperature were made at the edge of the pin and are listed in Table 4.1. Temperatures calculated for E = 0.3 appear to correlate better with the thermocouple data. Using these, the curves for 500, 1,000 and 1,500 rpm are plotted in Figure 5.3 versus PV, superimposed on the thermocouple base equilibrium temperature curve. The observed temperatures increase with speed as well as with PV. If each curve is extrapolated back to

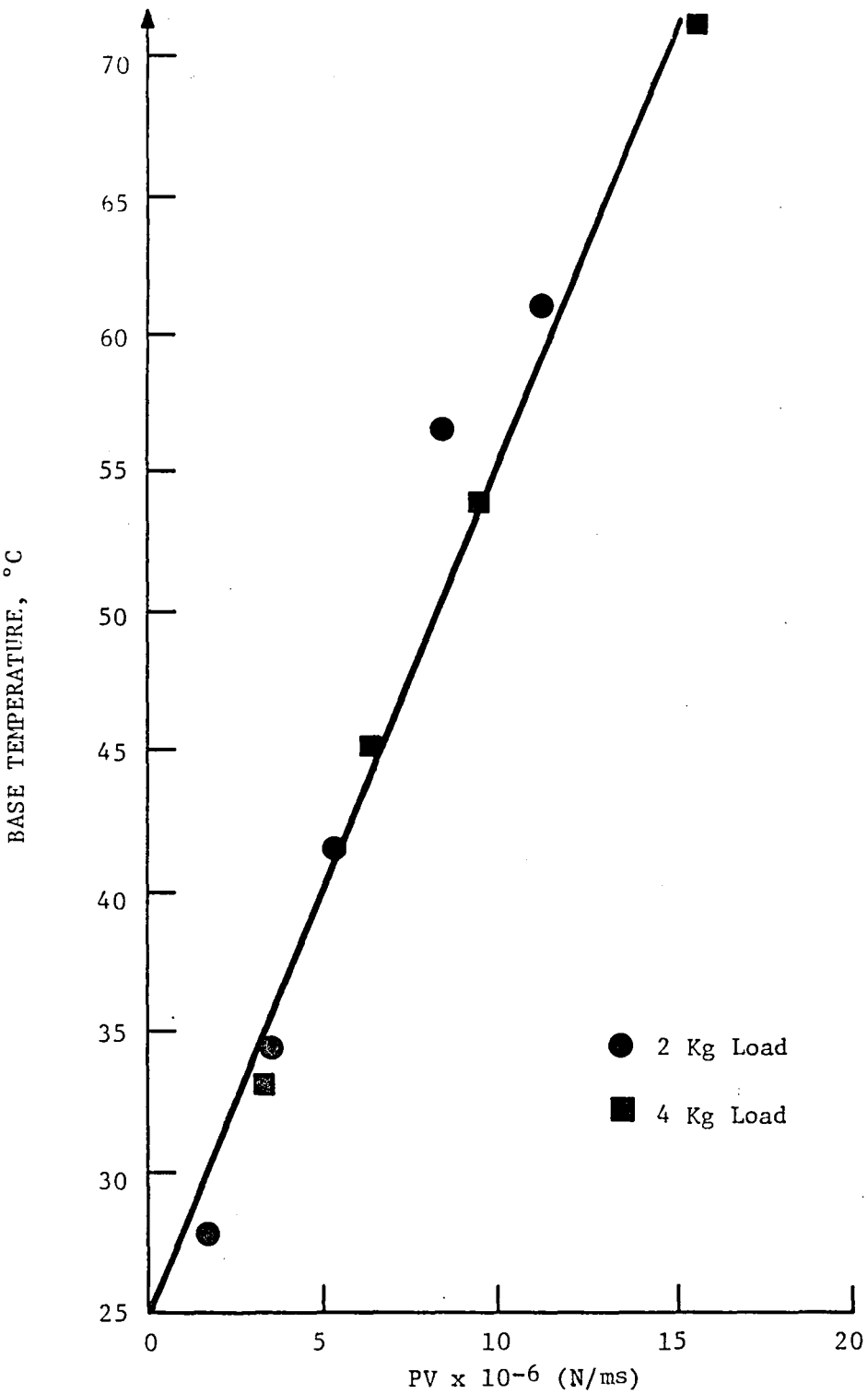

Figure 5.1 Thermocouple Base Temperature as Function of PV, Rulon J on Nitralloy

812273

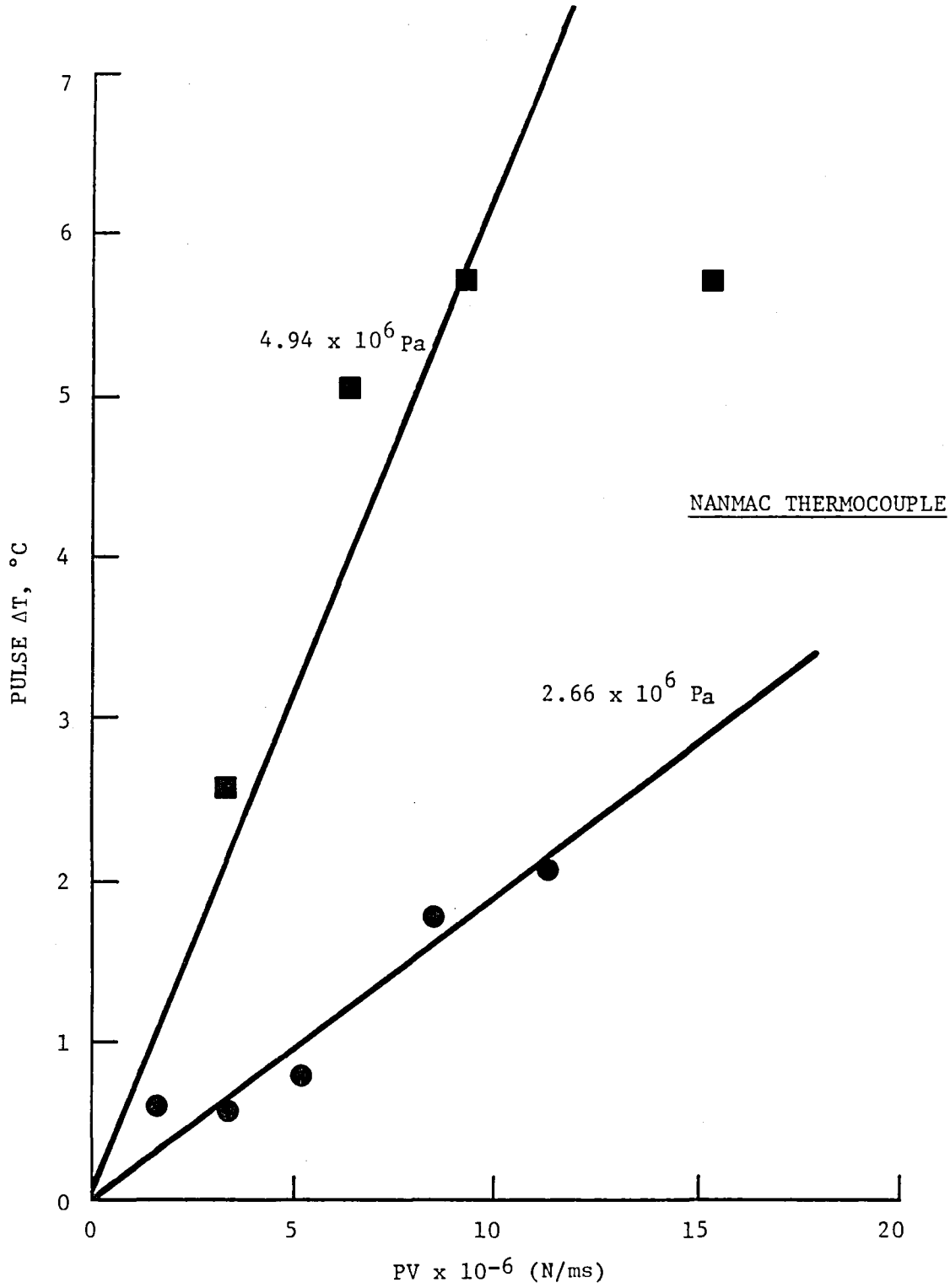

Figure 5.2 Thermocouple Pulse Temperature Rise as Function of PV and P

812272

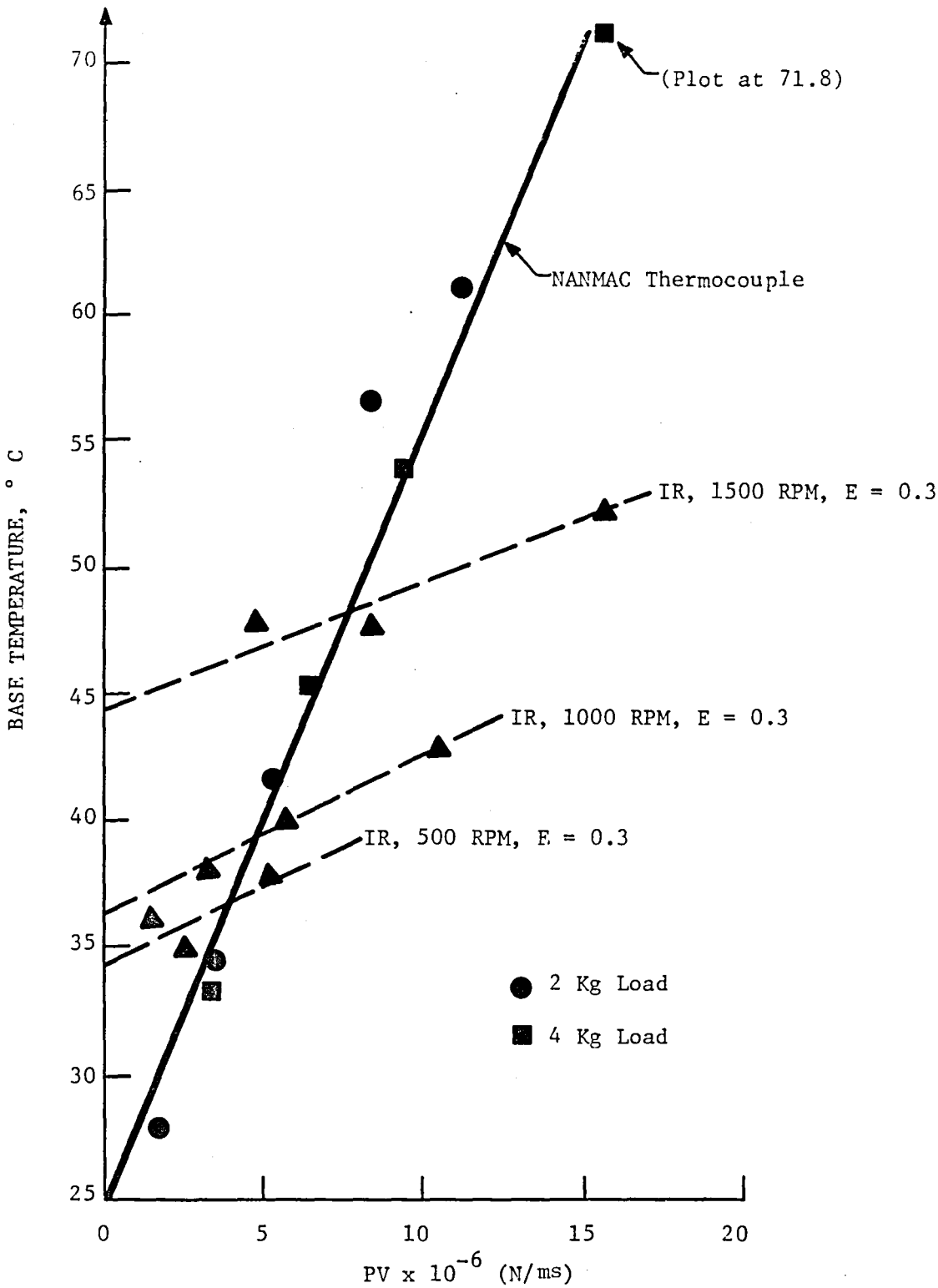

Figure 5.3 Infra-Red Max. Temperature as Function of PV and RPM, Rulon J on Nitralloy

812274

zero PV to obtain a base temperature for that speed, the results can be plotted as temperature rise versus PV as shown in Figure 5.4. Here the deviation from the mean curve is a maximum of 1°C, within the experimental error.

5.2 Rulon J on Sapphire

In these experiments, direct observation by single line scan was made of the rubbing end of the pin. From the temperatures listed in Table 4.3, Figure 5.5 shows the maximum pin temperature (averaged for both directions of sliding) as a function of PV. The 500 rpm points lie above those for 1,000 and 1,500 rpm, but the deviations are only about 2°C, about the maximum that should be expected from this technique. More significant is the absence of a trend toward ambient temperature as PV approaches zero. This may be ascribed to thermal inertia and the lower conductivity of sapphire.

This point may be explored further by plotting the temperature difference observed along the track between maximum and minimum, as shown in Figure 5.6 as a function of PV. Temperature differences decrease with speed, but non-linear curves would be required to pass through zero ΔT at zero PV. It seems apparent that some 3-dimensional thermal analysis would be required to fully explain this phenomenon.

5.3 Cap Seal Measurements

The cap seal is a more complex mechanical element than the simple pin used in the preceding experiments. As tested here, it consisted of an inner sleeve which had a small clearance between its I.D. and the rod, outside of which was an elastomeric O-ring. The assembly was held between metal side plates. Gas pressure could be admitted to the space outside of the O-ring, deforming it so that it would compress the inner sleeve onto the rod. The pressure between the sleeve and the rod could not be measured directly.

From the test results summarized in Table 4.4, the maximum observed temperature is plotted in Figure 5.7. Distinct curves for each speed are seen, indicating a lack of correlation by PV alone. In this case, since the "P" used in PV is the external gas pressure, it is evident that some contact and frictional heating

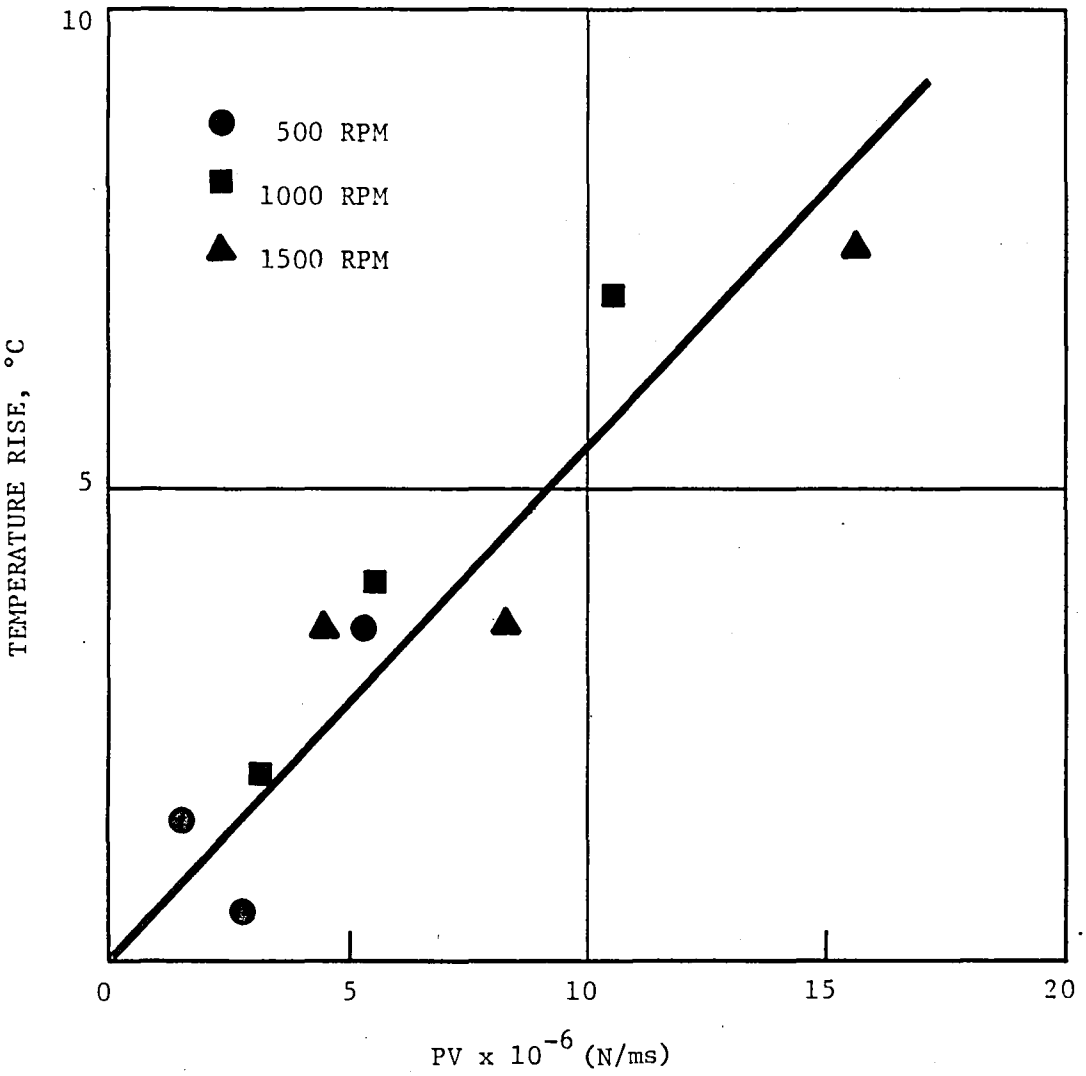

Figure 5.4 Emerging Plate Temperature Rise at V_{max} as Function of PV, Rulon J on Nitralloy

812277

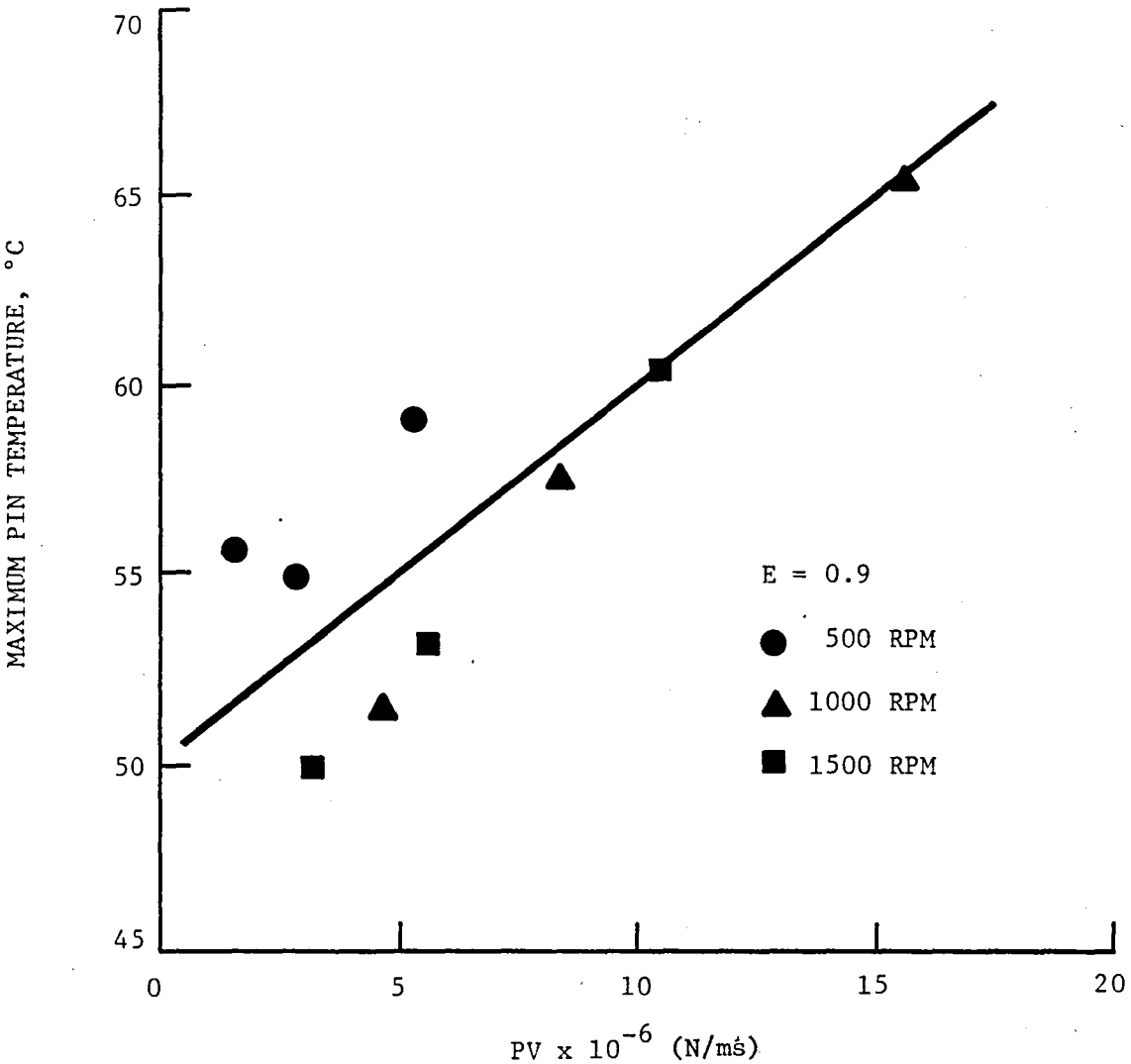

Figure 5.5 Maximum Pin Temperature, °C (E = 0.9), Rulon J on Sapphire

812275

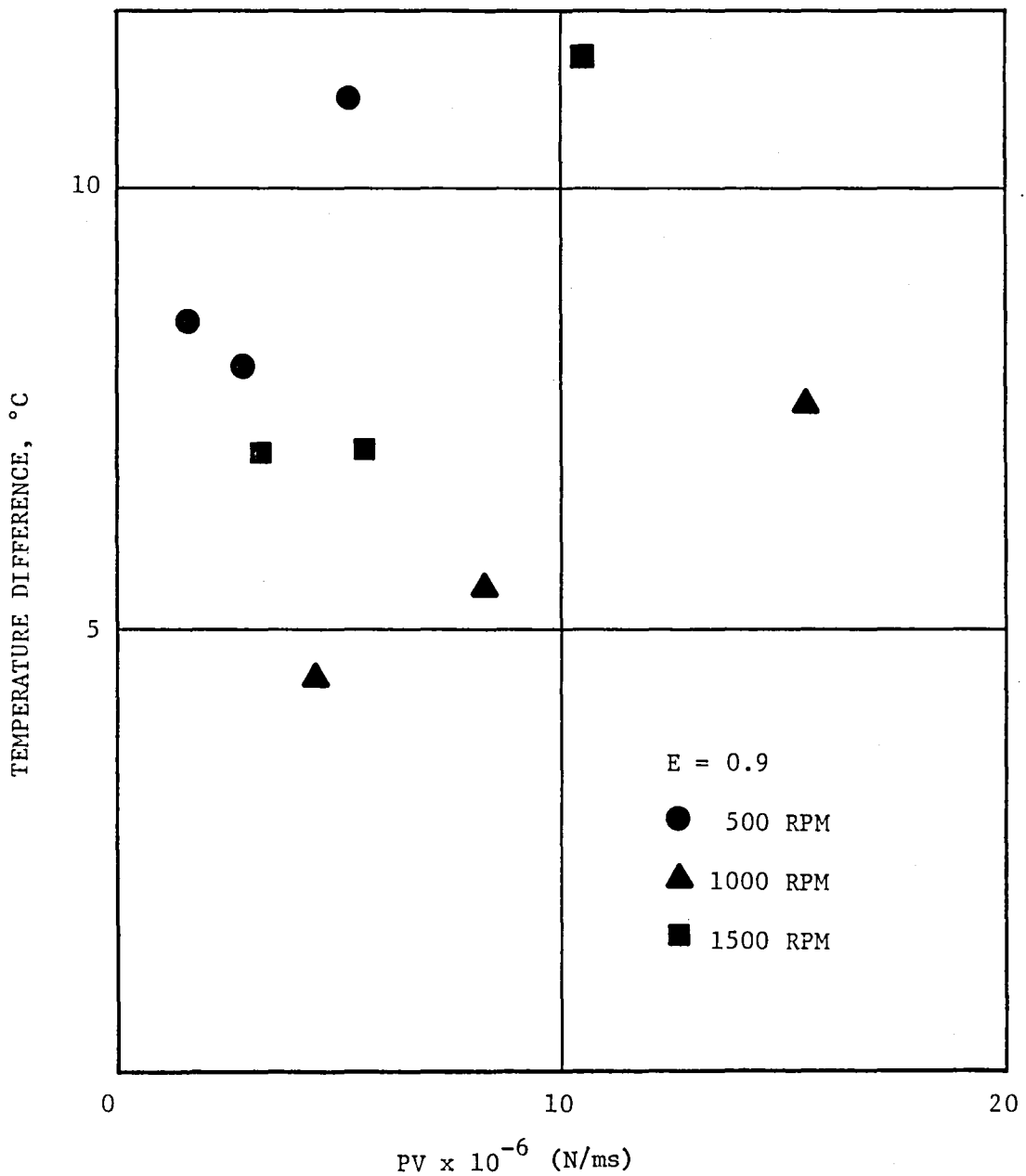

Figure 5.6 Difference Between Maximum and Minimum Pin Temperature in Cycle, Rulon J on Sapphire

812278

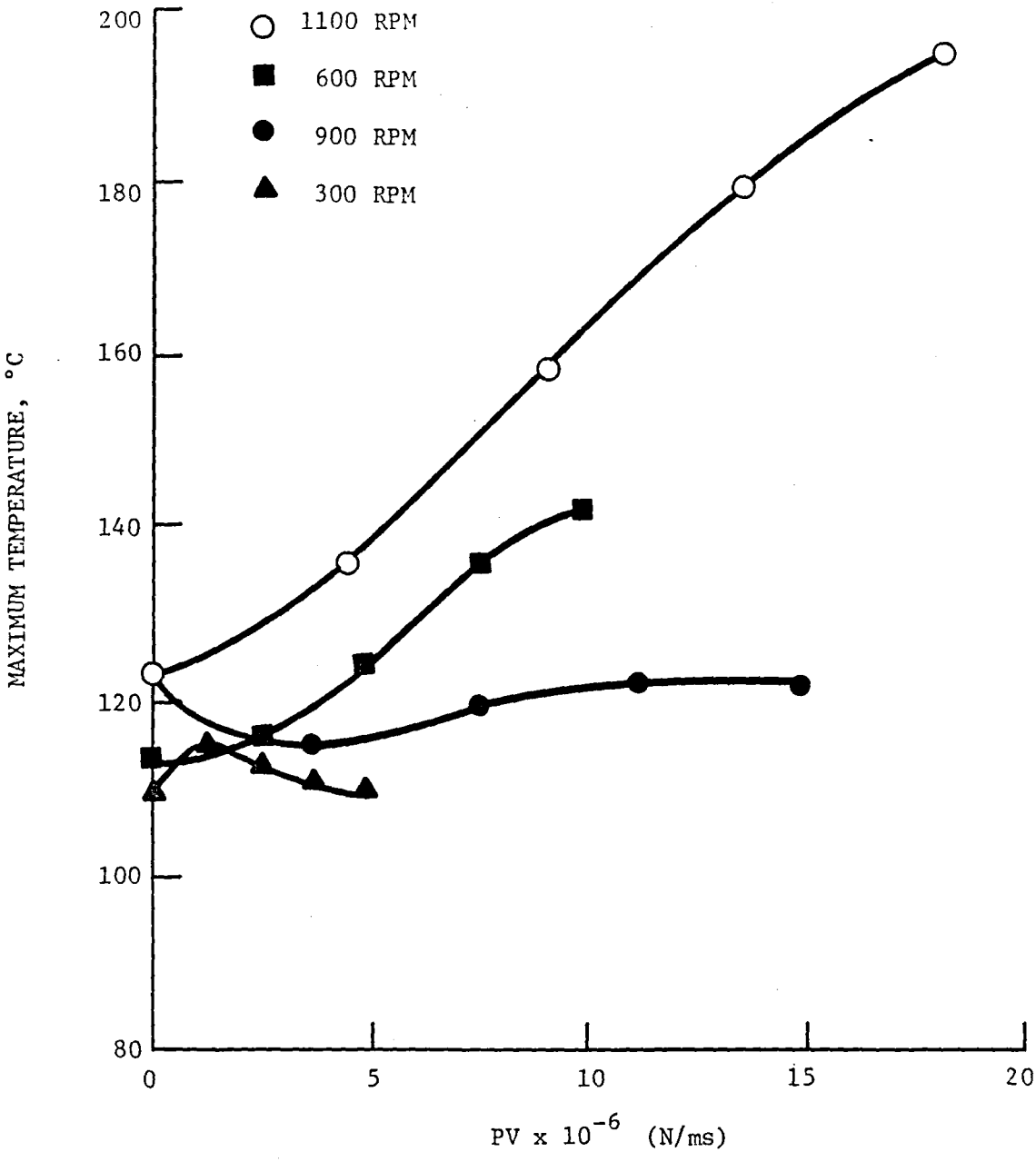

Figure 5.7 Maximum Temperatures Observed in Cap Seal Tests as Function of PV (E = 0.05)

812257

are occurring at zero gas pressure. This is evident also in the increase in maximum temperature at zero PV as speed increases from 300 to 600 to 1100 rpm.

The 900 rpm curve appears to be out of sequence, and shows almost no influence of PV. The 900 rpm runs were made after the other runs had been done, the previous one being the 1100 rpm run. Since the measurements at 900 rpm were made in order of increasing pressure, it is conceivable that the rod did not have a chance to cool off adequately after the 1100 rpm run and thus caused the low pressure temperature readings at 900 rpm to be too high. This explanation seems particularly likely since the cooling rate of the rod was observed to be considerably longer than its heating rate.

The maximum-minimum temperature differences are shown in Figure 5.8 as a function of PV. Here, the general trend appears to be correct, but large deviations of the order of 10°C are observed.

In examining temperature rise data as a function of PV, the expectation of a linear proportional relationship implies that the coefficient of friction is constant over the range of variables studied. This is not unreasonable, but one can expect that temperature itself may influence the coefficient. There are limits of this effect in the data reviewed here, where the Rulon J base material, PTFE, softens as temperature rises.

Another interesting effect is seen in Figure 4.6. Here the temperature *decreases* slightly at the point of highest velocity in the stroke and thus causes a "dip" in the graph at both peaks. This may be the result of an oil film being developed at the high velocities. (A thin layer of oil was present on the rod.) Frictional energy is a product of friction coefficient, velocity and load. As the velocity increases the friction coefficient may decrease if an oil film forms between the two rubbing surfaces. If the decrease in friction coefficient more than offsets the increase in velocity, the temperature will decrease locally.

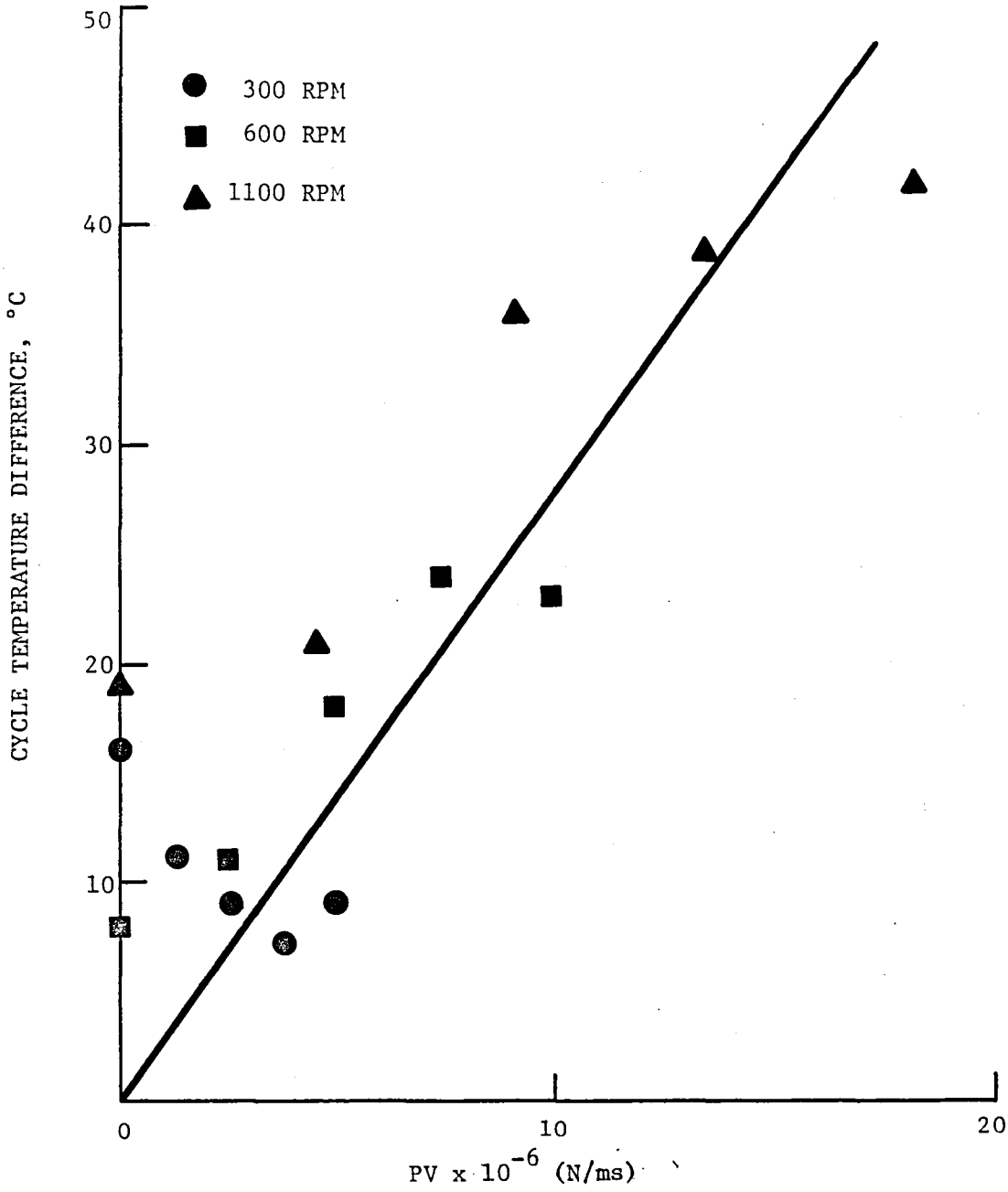

Figure 5.8 Cycle Temperature Differences in Cap Seal Tests as Function of PV (E = 0.05)

812271

6.0 DISCUSSION

The objective of this program was to explore the feasibility of methods of directly measuring the surface temperatures in reciprocating seals. Two methods were to be explored: one, a fast response surface thermocouple; and two, a high sensitivity scanning infra-red camera. If one method could be used to verify the results of the other, greater confidence would be gained in both.

6.1 Fast Response Thermocouple

The NANMAC fast response thermocouple proved difficult to use because of the delicate measuring junction that has to be formed in place by a rubbing or abrasive action. Rubbing with a plastic material could be made to form a junction, but continued test rubbing opened the junction most of the time so that reliable data could not be obtained. For this reason, no direct comparison of the thermocouple and infra-red methods in the same experiment were obtained.

When the junction was formed by a heavier abrasive action prior to the rubbing experiments, a strong reliable junction was formed. However, a roughened metal surface surrounding the thermocouple was created simultaneously. For this reason, it seems unlikely that this method will be practical for direct application to seals.

The results from the rubbing experiments on the NANMAC junction were nevertheless valuable. They showed that the "base" temperature, which can be assumed to be the temperature in the insulation surrounding the thermocouple, is directly proportional to PV.

The temperature rise or "pulse" data was clearly separable into two curves, one for each load. Each load showed ΔT proportional to PV. The possibility of the thermocouple being slightly recessed so that at light loads full equivalent pressure was not placed on the junction may explain the phenomenon.

With proper surface preparation, the rather delicate NANMAC type thermocouple can be made to work. Its response capability has been demonstrated - the time of passage of the 4.8 mm pin over the couple at 1500 rpm is 1.6 milli-seconds.

During this time temperature rises of about the same magnitude as those recorded by the infra-red camera were observed.

The rough surface preparation required, and the difficulty of introducing the thermocouple into a working counter-seal surface, make it unlikely that the thermocouple can be used easily to provide direct surface temperature data.

6.2 Infra-Red Camera

The infra-red scanning camera can read surface temperatures directly. The experiments conducted in this program have shown the level of temperatures indicated to be roughly the same as those measured by thermocouple. The rate of surface temperature decay as the counter-surface leaves the contact is slow enough that excellent indications of contact temperature can be obtained by observing the surface outside of the immediate seal contact zone.

By modifying the normal 2-dimensional scanning mechanism to provide a repetitive single line scan, detailed data at a repetition rate of 2500 cps is available to the experimenter.

The primary problem with use of the infra-red scanning camera is the determination of emissivities so as to obtain absolute rather than relative temperatures. This is evident in two areas. The first area has to do with establishing a reference point during each measurement. In these experiments, care was taken to have in the field of view at all times a surface of known emissivity and known temperature. The temperature was measured with a thermocouple. The emissivity was measured via a separate calibration.

The second and more difficult area is the emissivity of the test surface. The emissivity of a rod surface, for example, can be determined in a separate calibration. However, it may become coated with oil, changing its value. The surface finish may change during the test; and the seal material may deposit on the surface - both factors which may influence emissivity. Thus accurate work will require careful attention to these factors in calibration. (NOTE: Further discussion of this point may be found in Appendix A.)

Despite these problems, the infra-red technique is viewed as having great potential for studying the thermal behavior of seals. Some careful research should elucidate the effects of the factors that have appeared to influence the behavior patterns.

7.0 CONCLUSIONS AND RECOMMENDATIONS

The general conclusions that can be drawn from this program are as follows:

1. That the fast response NANMAC thermocouple can be made to work with aggressive surface preparation, but it does not promise to be a useful tool for seal research;
2. That the scanning infra-red camera has high promise of being a useful and valuable research tool for seals, particularly in the single-line-scan mode;
3. That careful attention must be paid to the calibration of emissivity of the surface being examined in order to obtain accurate data; and
4. That the thermal phenomena related to rubbing seals are complex.

It is recommended that the thermal behavior of rubbing seals be investigated in further research, using the infra-red camera as a principal instrument. The simple pin-on-plate experimental approach can be used to advantage in exploring the fundamental behavior of seals using both steel and sapphire coupons. It is recommended that such research should include the direct measurement of friction force as part of the work. The research should then be extended to rubbing rod seals of both the dry and lubricated type.

APPENDIX A

FINAL REPORT

MTI P.O.# 102-04197

THERMAL BEHAVIOR OF STIRLING ENGINE SEALS

Principal Investigator:
Ward O. Winer, Professor

Graduate Research Assistant:
Maarten A. Meinders

Prepared for:
Mechanical Technology, Incorporated
968 Albany-Shaker Road
Latham, New York 12109

June, 1981

GEORGIA INSTITUTE OF TECHNOLOGY
School of Mechanical Engineering
Atlanta, Georgia 30332

ABSTRACT

A system has been developed to perform a computer analysis on surface temperature data in tribological systems, taken by an infrared radiation scanning device. The infrared scanner which normally scans 25 fields per second at 100 lines per field has been modified to scan any single line at 2500 lines per second. The system was used to analyze four friction experiments as part of of a thermal behavior study of stirling engine seals in cooperation with Mechanical Technology Inc. (MTI), Latham, New York. The friction experiments involved two tribo-pairs: Rulon on steel and Rulon on sapphire.

TABLE OF CONTENTS

LIST OF TABLES

LIST OF ILLUSTRATIONS

LIST OF ILLUSTRATIONS (Continuation)

NOMENCLATURE

A	first calibration curve constant
B	second calibration curve constant
B	octal number designator
C	correction factor
C_2	correction factor
f_1	closest standard f-stop less than f_2
f_2	non-standard f-stop
f_3	closest standard f-stop greater than f_2
HTP	horizontal trigger pulse
I	intensity level
I	isotherm level
ΔI	difference in isotherm levels
sp	starting pulse
S_1	input parameter for determining S_3 in program MAP
S_2	input parameter for determining S_3 in program MAP
S_3	cutoff level for intensity I
T	temperature (degrees centigrade)

Subscripts

o	object
oa	object - absolute
r	reference
ra	reference - absolute

CHAPTER I

INTRODUCTION

This report describes the development and utilization of a scanning infrared temperature measurement system as part of a thermal behavior study of stirling engine seals in cooperation with Mechanical Technology, Inc. (MTI), Latham, New York under Purchase Order Number 102-04197.

The development included:

1. Development of software for data analysis on a digital computer.
2. Modifying the infrared scanner to scan any desired line within one field repetitively at a rate of 2500 lines per second.
3. Checking out the data system on a simple low speed reciprocating contact apparatus.
4. Assisting MTI at Latham, New York in using the infrared scanner and data reduction system to make thermal profile measurements in the rub exit zone for a) Rulon on nitralloy (a low alloy steel), and b) Rulon on sapphire.
5. Assisting MTI at Latham, New York in using the infrared scanner and data reduction system to measrue exit temperature profiles on a pumping ring seal operating in the MTI pumping ring test apparatus.

Previous infrared radiation measurements have been made by Nagaraj [1] who used a Barnes Rm 2A single spot microscope detector. This instrument however has no automatic scanning feature and is of limited use in moving contacts. Kool [2] later studied the applicability

of an AGA 750 scanning device to tribological systems and found it to be useful. However, area resolution and interpretation of the thermogram produced by the camera was a problem. The temperature measurement techniques described in this report is a continuation of Kool's work in that a digital computer is used to reduce the data rather than visual interpretation of the thermogram. A diagram of the system can be found in Figure 1-1.

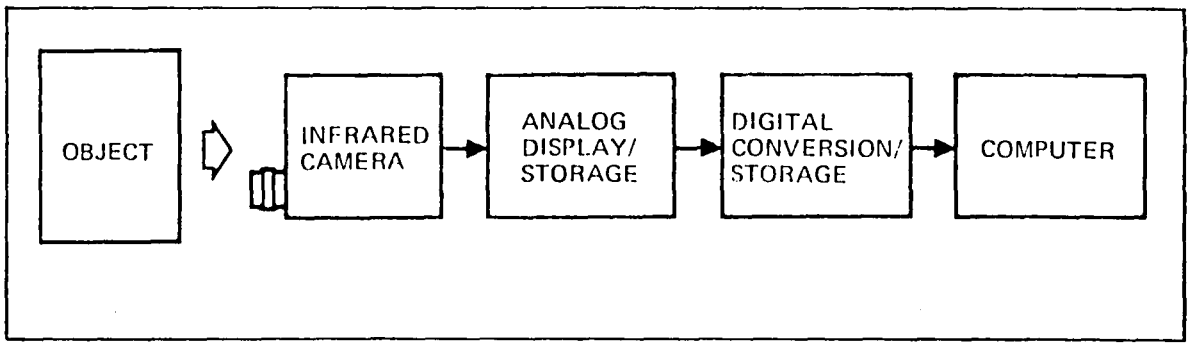

Figure 1-1. The Total System

CHAPTER II

INSTRUMENTATION

The computerized infrared analysis system as illustrated in Figure 1-1 requires a variety of instruments each of which needs to meet very specific specifications in order to contribute to the total system. In addition it is of vital importance that a proper communication link is established between the various components. This chapter describes the relevant capabilities and limitations of each instrument as well as the procedures used to determine these limitations.

A. The AGA 750 Thermovision Camera

The AGA 750 is the *eye* of the total system and the first link in a chain of four instruments (See Figure 1-1). It is an optical scanning device which converts electromagnetic thermal energy radiated from an object into electronic video signals. Electromagnetic energy radiated by an object is focussed by lens into an eight-sided prism that rotates around a horizontal axis and thus causes a vertical scanning motion (see Figure 2-1). This prism is rotated at 3.125 rps by a d.c. motor. The optical output from the vertical prism is passed through a second prism which rotates around a vertical axis at 312.5 rps and thus causes a horizontal scanning motion. The rotation of both prisms is controlled by two slotted discs which rotate on the same shafts as the respective prisms. The rotating slotted discs are

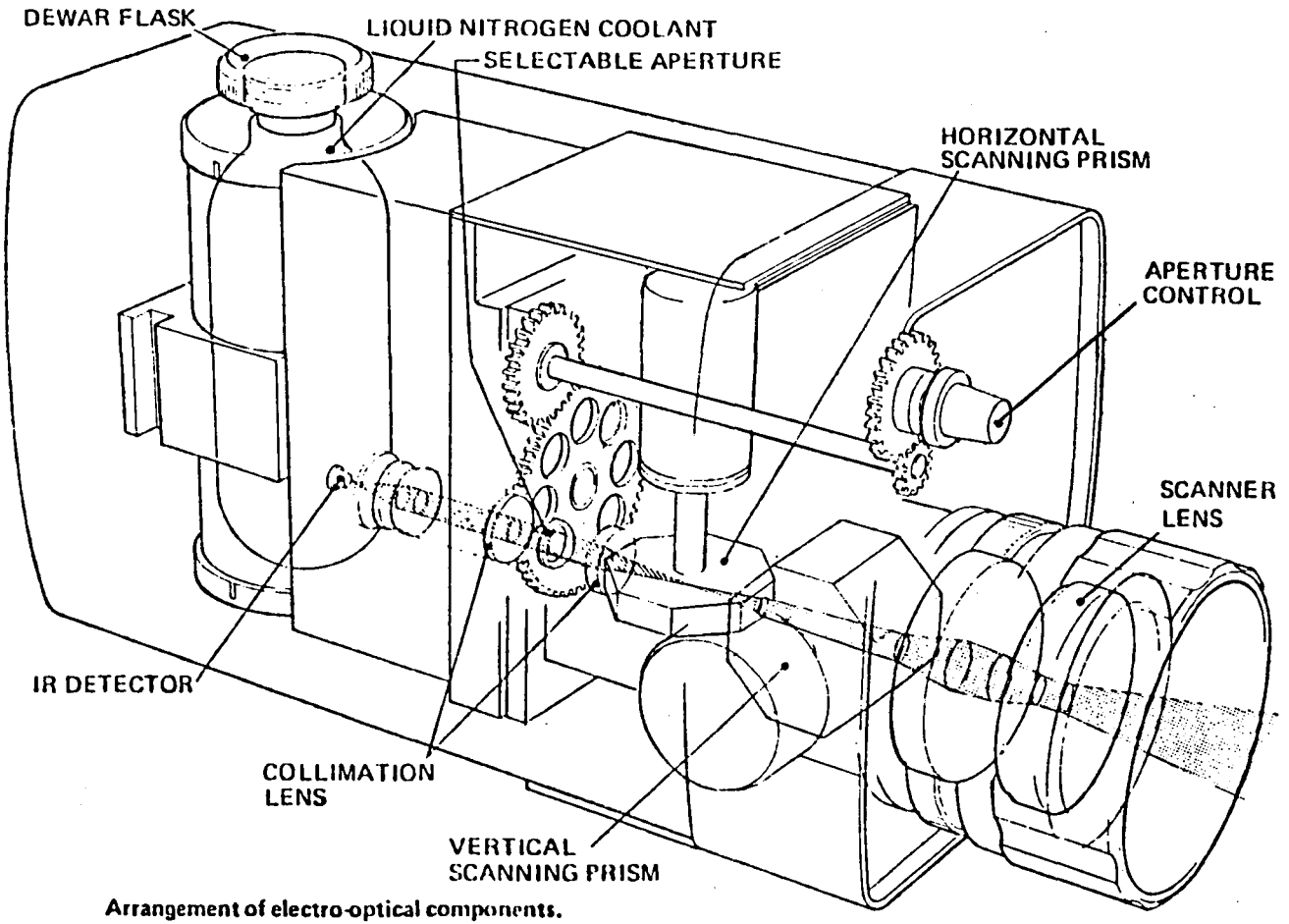

Figure 2-1. The AGA 750

electronically connected to the horizontal and vertical triggering circuits, to provide horizontal and vertical trigger pulses to the monitor. These pulses also control the speed of the vertical and horizontal prism motors to synchronize their rotation.

Output from the horizontal prism is passed through a set of relay optics containing a selectable aperture unit and a filter cassette unit and finally focused onto a single element point detector located in the wall of a dewar chamber. Liquid nitrogen coolant (LN_2) maintains the chamber at a temperature of -196°C thus causing the detector to be sensitive to the 2 - 5.6 μm infrared wavelengths. The detector produces an electronic signal output which varies in proportion to the radiation from the object. This signal is amplified within the scanner unit and produces a video signal which is applied via an interconnecting cable to the black and white monitor chassis [3].

Two infrared lenses can be used with the camera, one with a seven degree field of view and the other with a 20° field of view. For close-up work three extension rings of the following lengths were used:

ring 1: 12 mm

ring 2: 21 mm

ring 3: 66 mm

These rings can be mounted between the lens and the camera body and permit a significant reduction of the working distance of the camera. An evaluation of their usefulness can be found in Section C of Chapter II.

In addition to the features described above a special "remote control" unit was built which allows the vertical scanning prism to be stopped and single-stepped through any angle at a step size of approximately 800 steps per complete revolution. This allows the operator to fix any horizontal line within the field of view and scan it at a rate of 2500 lines per second (the scanning rate of the horizontal prism). A digital counter indicates which line in the picture is being scanned. When operated in this single line scanning mode the monitor display will display each consecutive line scan right below the previous one, until 100 lines are displayed after which a V T P occurs and the next line is again started at the top of the screen.

Rather than having each VTP occur at every hundred horizontal scans the remote control unit also allows for external triggering. This is accomplished by a small infrared transmitter-receiver device that causes a trigger pulse to occur each time the infrared beam between the transmitter and receiver is interrupted by a chopper linked to the moving mechanism to be observed. (See Figure 2-2). This feature is particularly useful when observing reciprocating machinery since VTP's synchronized with the mechanical cycle provide information concerning the absolute location of the reciprocating mechanism.

B. The AGA 750 Scanning Pattern

The scanned field as produced by the monitor is controlled by horizontal and vertical trigger pulses. The beam starts at the left

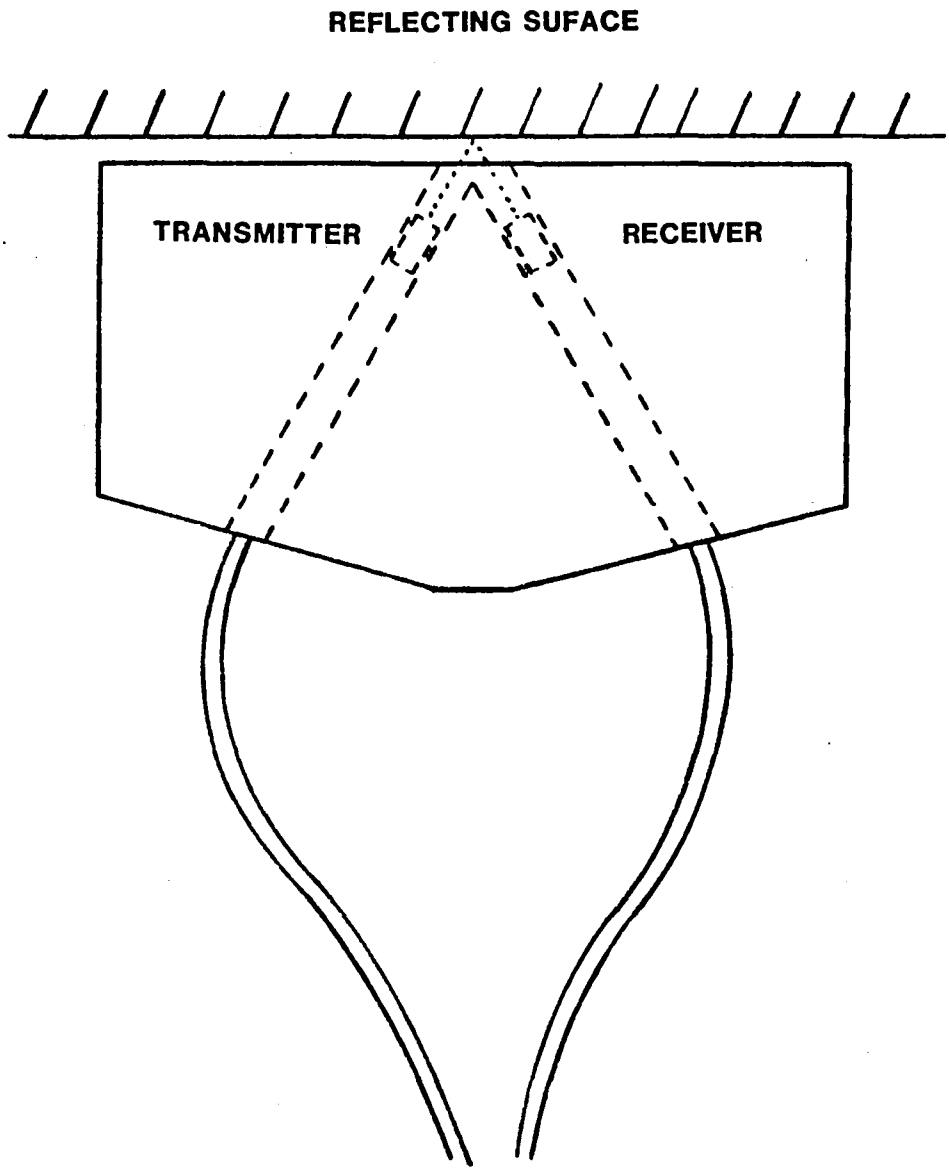

Figure 2-2. The External Triggering Device

upper corner of the video screen triggered by the coincidence of a vertical and horizontal trigger pulse (VTP and HTP). The beam sweeps to the right and downward until it reaches the right hand edge of the field. While its downward motion continues as a result of the continuous motion of the vertical prism a new HTP instantaneously forces the beam back to the left hand side of the field from where its motion downward and to the right continues.

After 100 HTP's the beam will cross the lower edge of the field and is drawn back to the top of the field by a VTP. This however occurs at an x-position shifted to the right by one quarter of a field width as compared to its x-position at the occurrence of the previous trigger pulse. This is caused by the fact that the horizontal prism rotates at 100-1/4 times the rotational speed of the vertical prism.

This phase difference results in the so-called interlacing effect. Rather than the beam tracing its exact original path *each* time a VTP occurs it does so at every fourth VTP. Each *consecutive* VTP starts the beam off at a point where it will trace a path shifted downward one fourth the original distance between two lines. This causes the next three fields to fill in the space between the lines scanned during the scanning of the first field (See Figure 2-3). Four interlaced fields are called a "FRAME".

C. Determination of Spatial Resolution

1. Procedure

In order to obtain a relative measure of the spatial resolution of the camera at maximum magnification (using three extension rings

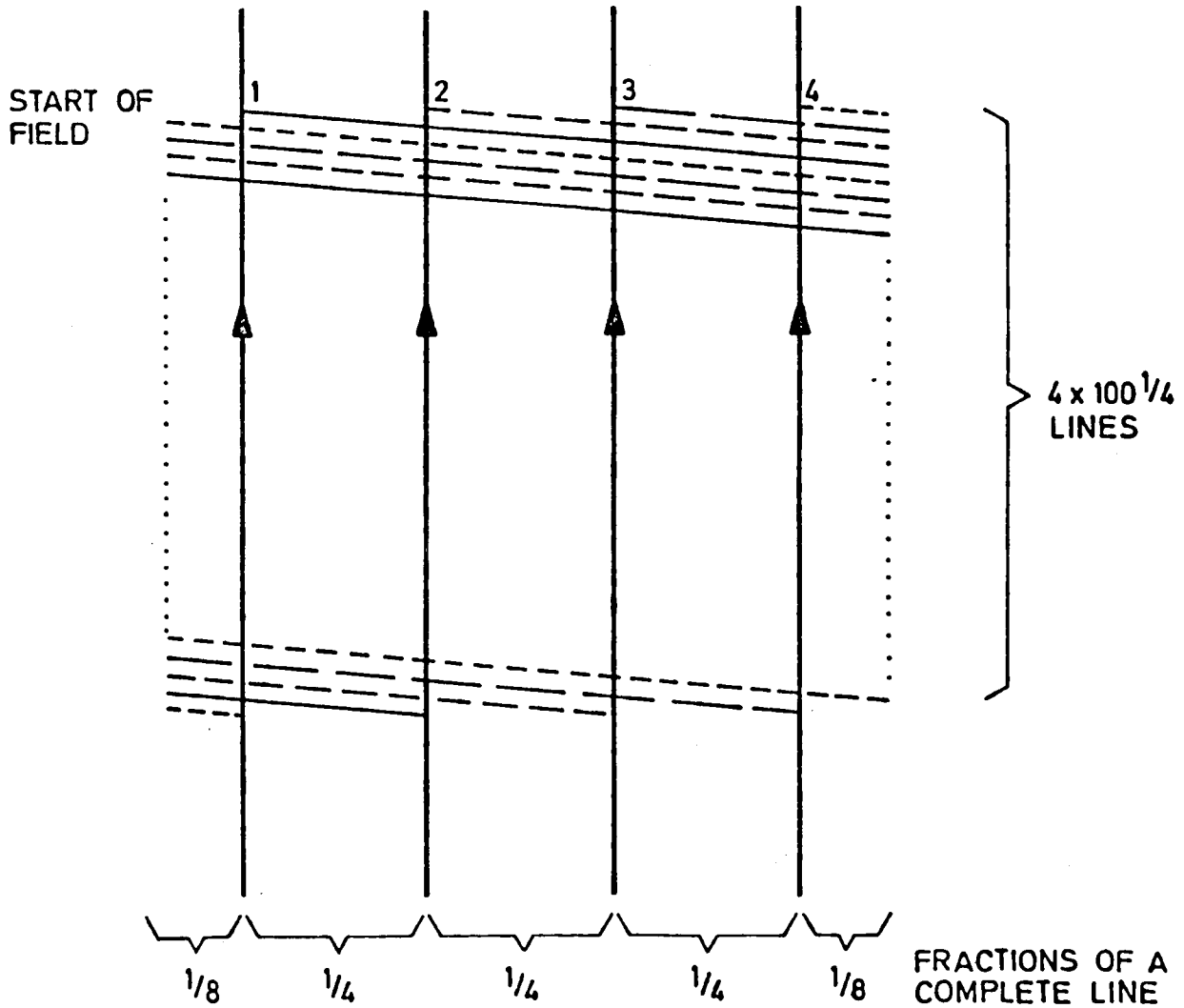

Figure 2-3. Scanning Pattern of the Thermovision 750

mounted between the lens and the camera) the following test was devised:

A sheet of carbon steel 0.014 cm thick with a series of 25 holes drilled in it varying from 0.343 mm to 1.18 mm was mounted in front of a flat walled container whose sides were painted flat black. The container was filled with water and heated to approximately 90°C by means of an immersible electrical heater. The camera was placed in front of the steel sheet and focussed such that the radiation measured through each hole was maximized. This was verified by means of an oscilloscope.

The test pattern of holes was drilled in such a way that the camera could always see at least one test hole next to a reference hole. (See Figure 2-4).

The camera was aimed at the top of the test pattern and lowered vertically, maintaining the front of the lens parallel to the surface of the metal sheet. The respective levels of infrared radiation passing through the holes were then recorded with the Honeywell 101 recorder. This procedure was repeated using several combinations of extension rings in combination with the 20° lens as well as the 7° lens. The object of this test was to find the smallest test hole that would appear to transmit the same amount of radiation as the large reference hole located next to it. This would be indicative of the smallest spotsize the camera could resolve. Any apparent attenuation of the radiation passing through the test hole would indicate that the camera was integrating some of the colder area surrounding the hole.

2. Results

It was found that the resolution of the camera varied with the

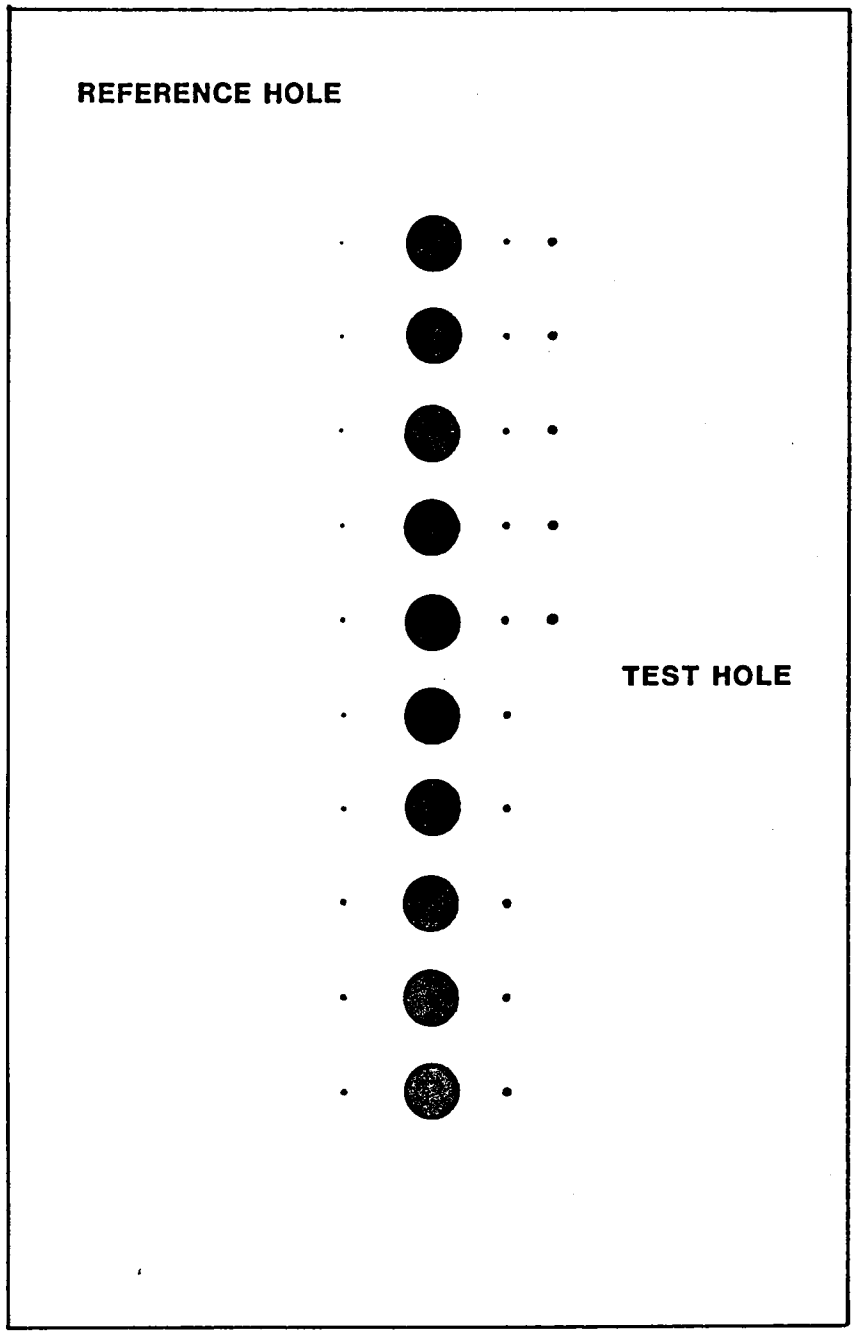

Figure 2-4. The Spatial Resolution Test Pattern

lenses and extension rings used. The results can be found in Figures 2-5 and 2-6 where the percentage of radiation measured relative to the reference hole is plotted against the test hole diameter for several combinations of extension rings and lenses. From these curves it can be seen that the optimum resolution was attained using the 20° lens in combination with extension rings no. 1 and no. 2, resulting in a minimum spot diameter of approximately 1 mm at 100 percent radiation measured.

However, by aiming the camera directly at the black side of the container at a uniform temperature of 90°C, it was also found that using this combination of lens and extension rings the signal was seriously attenuated at the edges of the lens. Instead of seeing a flat voltage profile on the oscilloscope the signal resembled a triangle with the peak in the center of the screen. This phenomenon must be attributed to distortion caused by the lens.

This discovery prompted us to record the signal attenuation for all the different lens-extension ring combinations. The resulting attenuated signals can be found in Figure 2-7. From Figure 2-7 it can be seen that the combination of the 20° lens with extension ring 1 as well as (1 + 2) creates an unacceptable amount of distortion as well as the 7° lens combined with rings nos. 1 and 2.

It was also found that the slope of the distorted signal was not constant, but varied according to the temperature of the observed surface. Therefore in trying to find the absolute temperature of an object in the field of view it becomes very difficult to correct

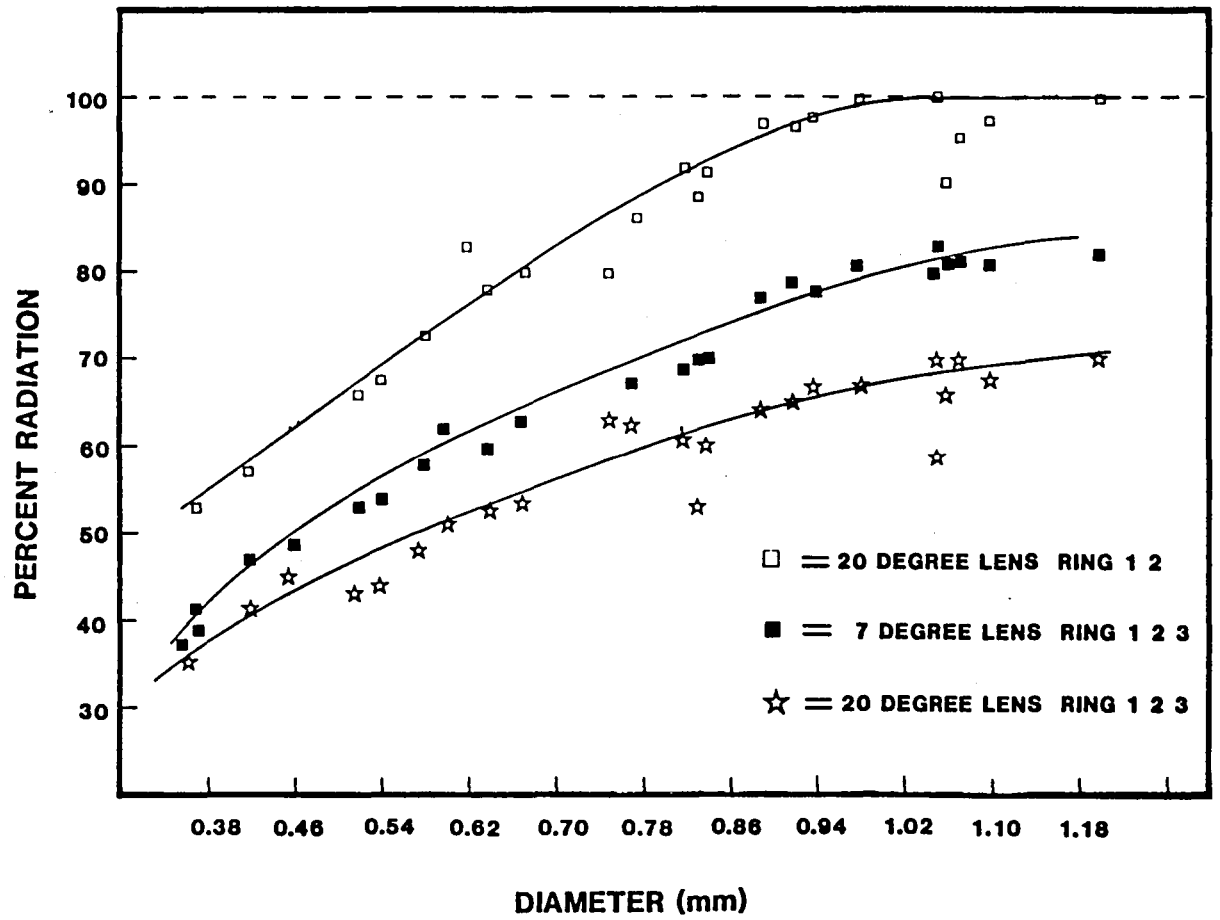

Figure 2-5. Spatial Resolution of the AGA 750

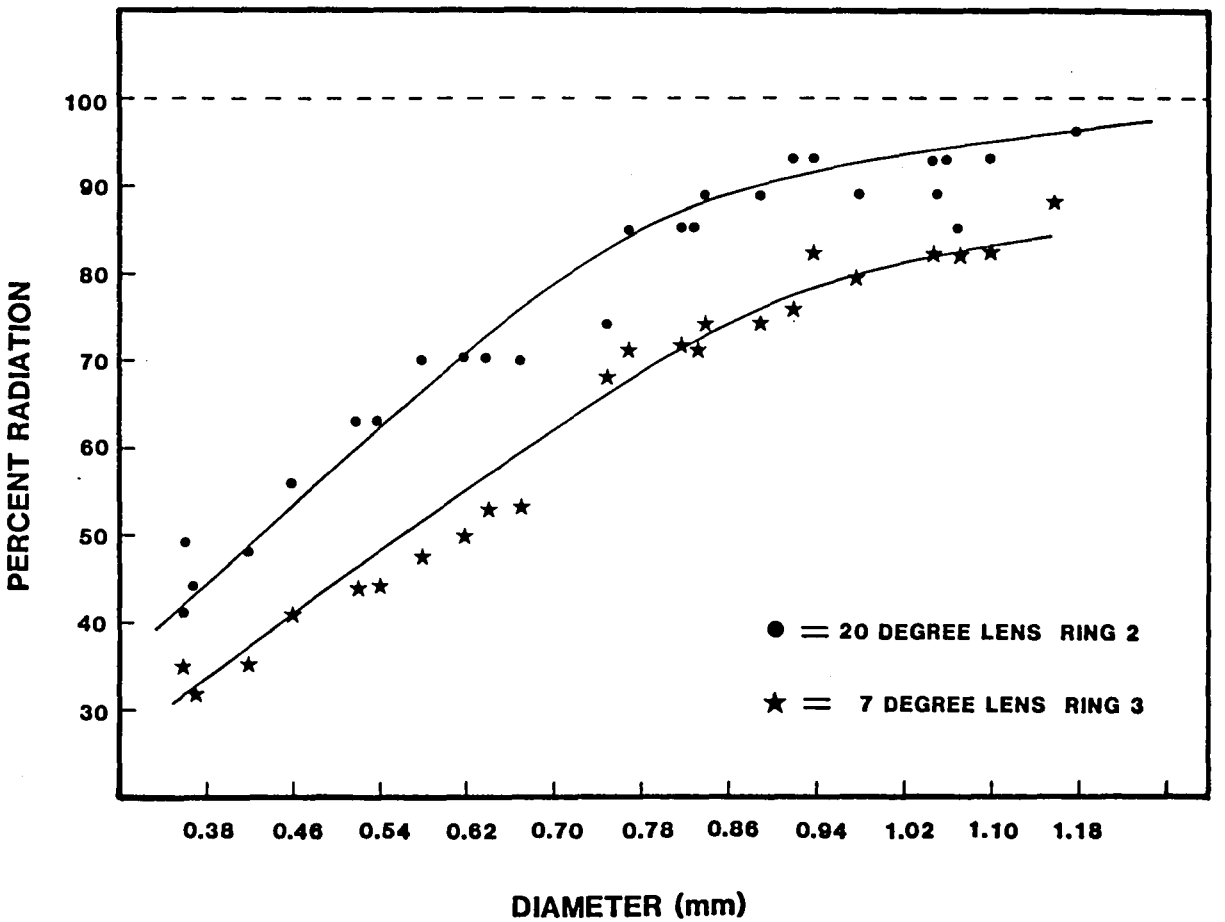

Figure 2-6. Spatial Resolution of the AGA 750

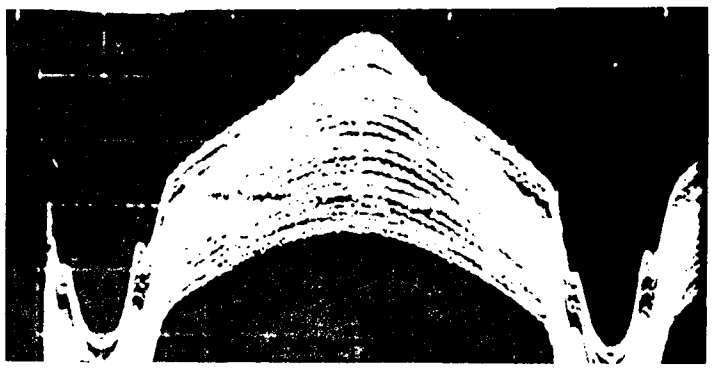

20° lens rings 1 + 2

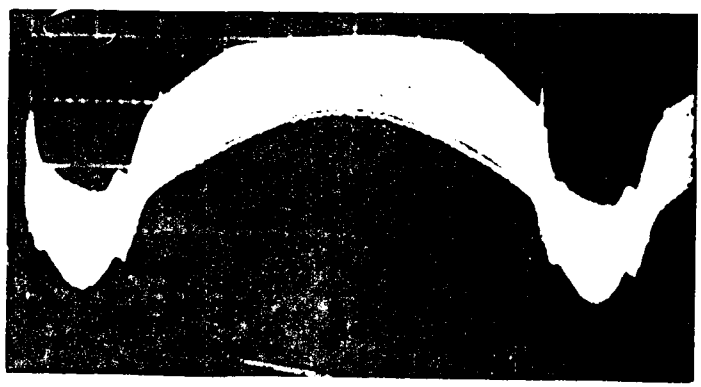

20° lens ring 2

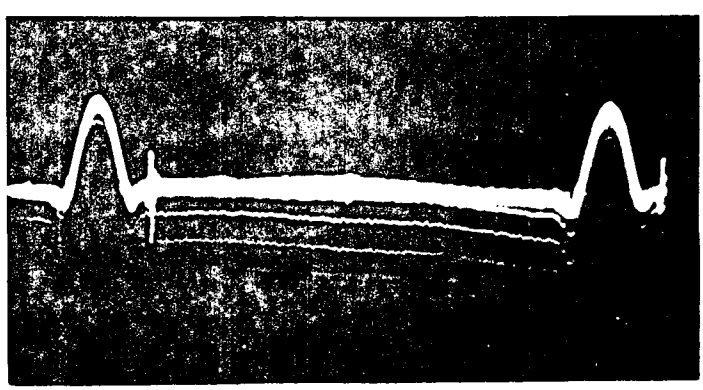

20° lens ring 1 + 2 + 3

Figure 2-7. Lens Distortion using Different Extension Rings

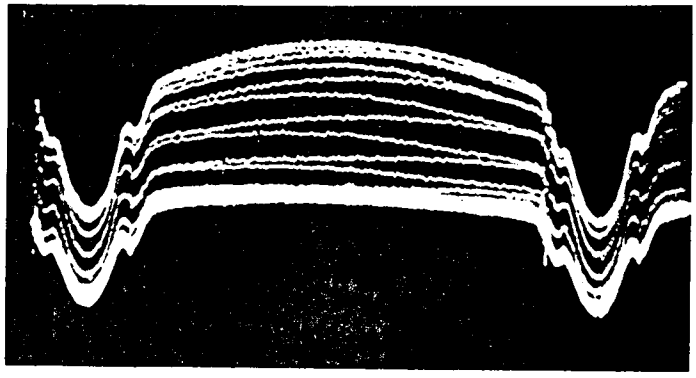

7° lens ring 3

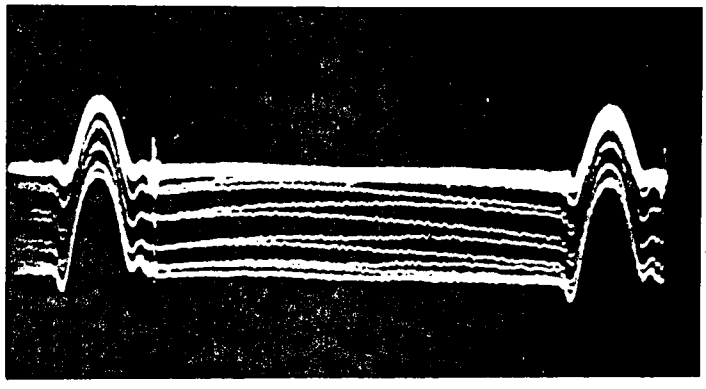

7° lens ring 1 + 2 + 3

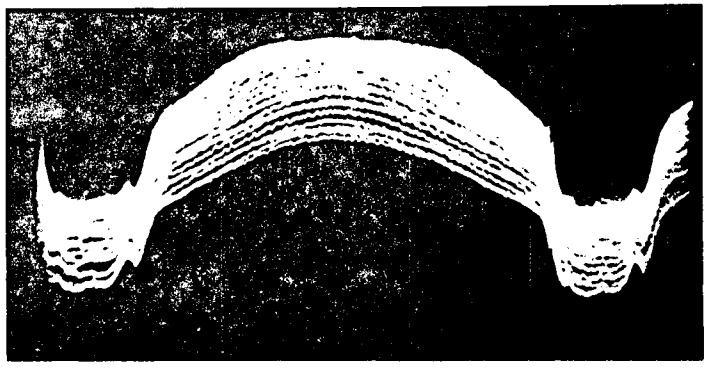

7° lens ring 1 + 2

Figure 2-7. Lens Distortion using Different Extension Rings (Continuation)

mathematically for the attenuation of the signal at the edges of the screen since the temperature must be known to know the amount of attenuation. The findings of the resolution test are summarized in Table 2-1.

The conclusion was that for our purpose all combinations but one (the 7° lens with extension ring no. 3) were unsatisfactory, mainly because of the amount of distortion caused by the lens. Of all choices the 7° lens with extension no. 3 offered the maximum resolution possible (nine spots per line) with an acceptable amount of distortion. This is not to say that all other combinations of lenses and rings may not be valid in different applications. Especially the 20° lens and rings nos. 1 and 2 combination could be very useful for observing small objects when they can be positioned in the exact center of the screen.

D. Calibration Procedure for Camera Voltage Levels

In order to use computer analysis for temperature measurements a relationship had to be established between radiation seen by the camera and voltage level outputs by the video pre-amp.

A Barnes blackbody infrared radiator was used as a calibrated temperature source and varied in temperature from 60C to 230C at 15C intervals. The corresponding voltage output from the pre-amp was monitored on an oscilloscope. This procedure was repeated for all camera apertures.

The temperature values were converted into isotherm units using the AGA supplied HP-65 programs for temperature to isotherm conversions.

Table 2.1 Camera Resolution using Different Extension Rings

Lens	Extension Rings	Object to tip of Lens (mm)	Field of View (mm)	Spotsize Diameter at 50% (mm)	At 100%	Number of Resoluble Spots per Scanned Line per 100%	Lens Distortion (See Figure 2.7)	Comments w.r.t. our Application
20°	1 + 2	89	17	0.43	0.98	17	very much	unacceptable*
	2	70	12	0.33	1.4	9	much	not recommended
	(1 + 2 + 3)	46	4	0.57	2.4	2	very little	unacceptable
7°	3	161	16	0.56	1.8	9	little	most useful
	(1 + 2 + 3)	118	11	0.46	1.7	6	very little	useful but limited resolution
	(1 + 2)						much	

*of limited use if object can be centered exactly

(See Figures 2-8 and 2-9). This resulted in a direct relationship between voltage and isotherm units (radiation level) independent of aperture. These data were plotted and correlated, by means of a linear regression the following equation resulted.

$$I = 165.46V + 8.4513$$

with a correlation coefficient of $r^2 = 0.976$, where

I = radiation in isotherm units

V = voltage in volts .

The conversion of isotherm units to temperature as supported by the HP-65 programs is of the following form

$$T = \frac{B}{\ell n(I) - \ell n(A)} - 273C$$

where A and B are empirical constants dependent on the aperture of the camera. These constants and their corresponding calibration curves can be found in Figures 2-8 and 2-9).

These curves correspond to the standard f-stop settings on the camera. However, whenever extension rings are mounted between the lens and the camera, the f-stop is changed to one for which no standard curves are available. In that case, the closest standard curve with a smaller f-stop is used to calculate temperatures and the answer is corrected by means of a correction factor. The exact procedure can be found on page 42 and 86.

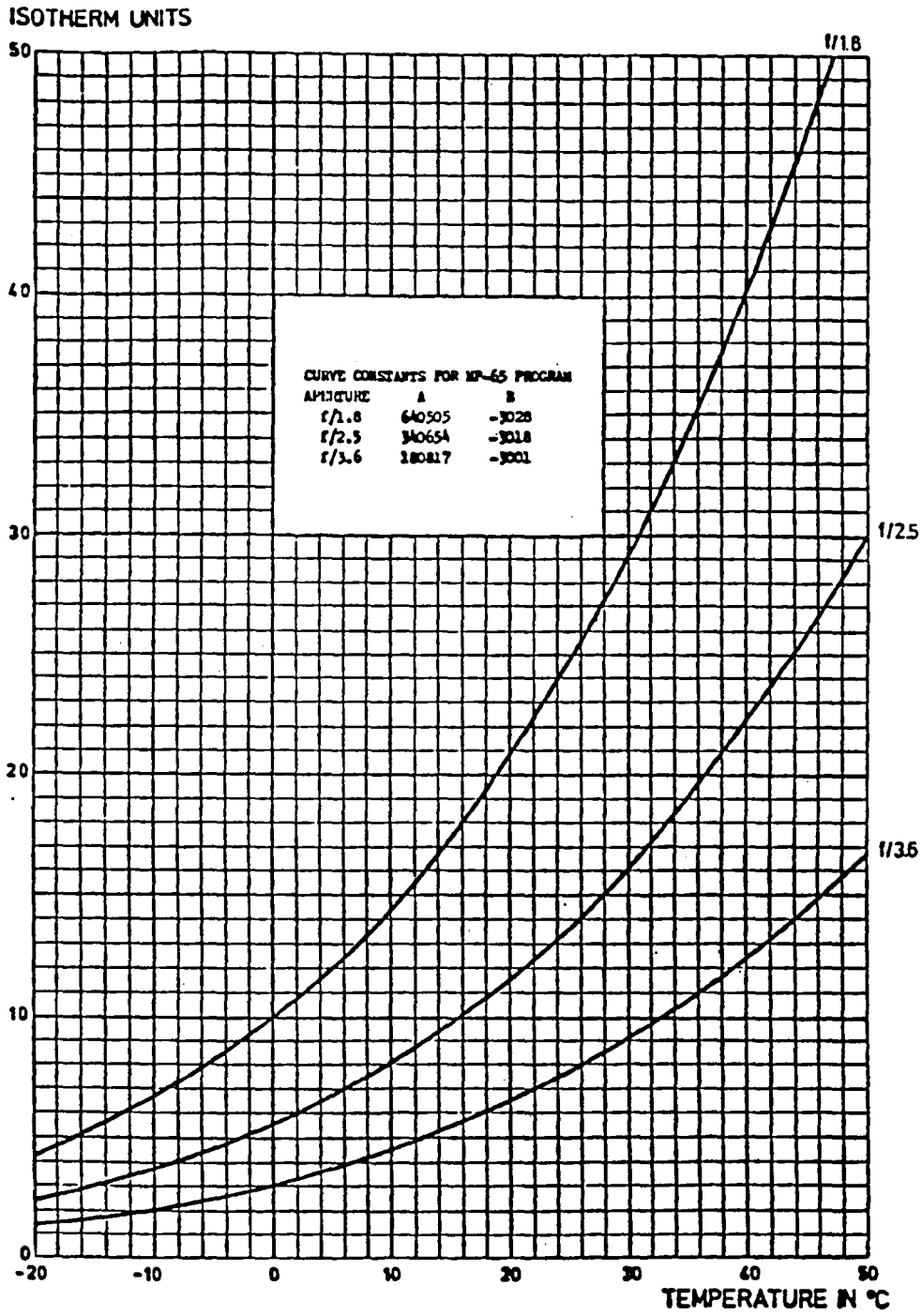

Figure 2-8. AGA Standard Calibration Curves

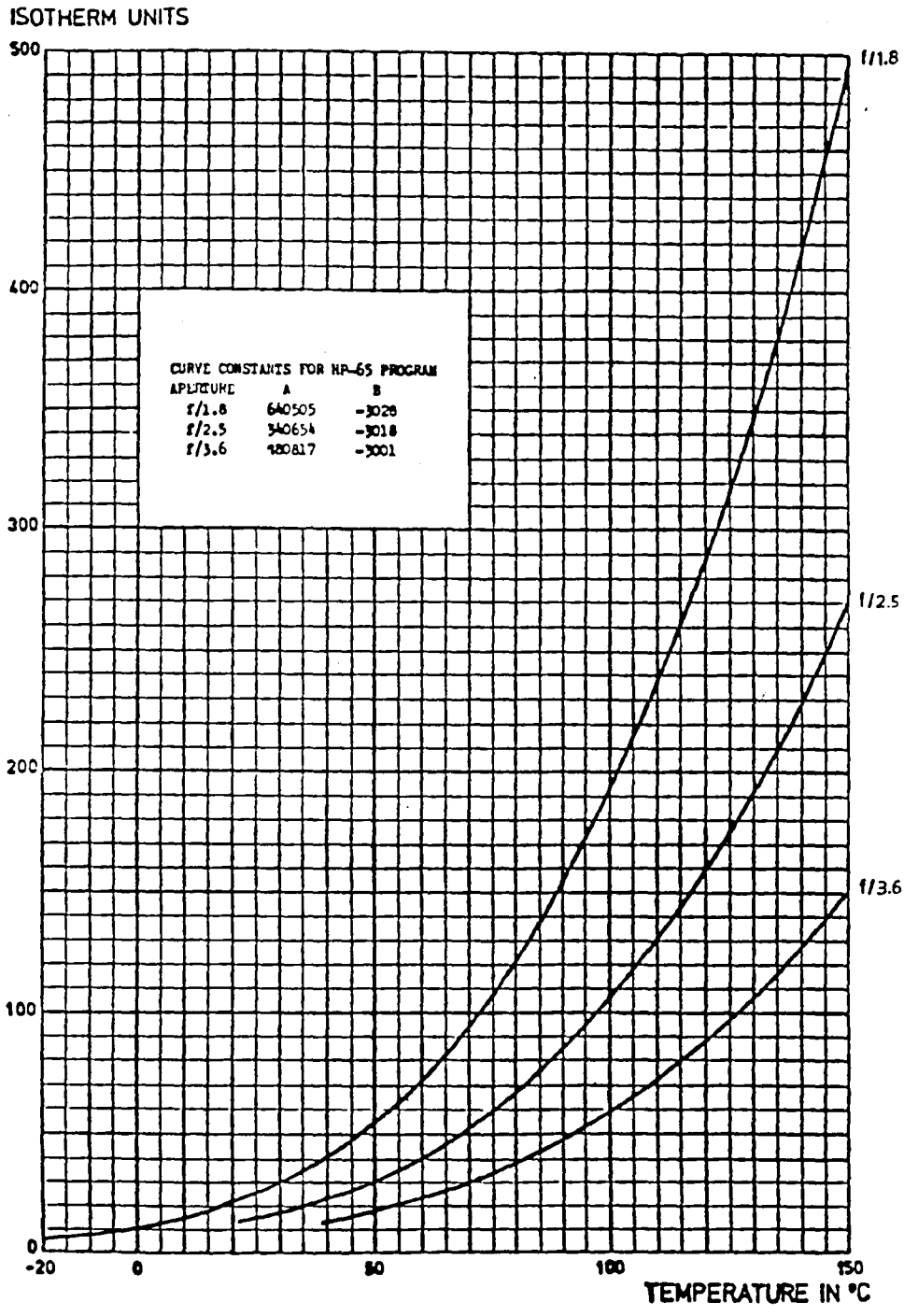

Figure 2-9. AGA Standard Calibration Curves

E. The Honeywell 101 Tape Recorder

The Honeywell 101 is the second link and can be called the primary *memory* of the system. It's function is to temporarily store the continuous stream of video data coming from the AGA 750 so that it can be analyzed at a later time and at a slower rate suitable for computer analysis. The Honeywell 101 is a high quality magnetic tape recorder with built-in microcomputer control. It has eight tape speeds and up to 14 record and reproduce channels. In addition it also has both *direct* as well as *FM* record and reproduce capabilities. We chose to use FM because it was able to cover a signal frequency range of zero to 80 kHz at a signal to noise (S/N) ratio of 50 dB. These specifications are sufficient to adequately record the AGA 750 video signal which requires a frequency response of DC to 80 kHz at a minimum S/N ratio of 46 dB.

The multichannel and multispeed capabilities allow us to record the signal as well as the HTP's and VTP's on different channels at 120 ips while reproducing them later at 7.5 ips, thus reducing the maximum signal frequency by a factor 16, suitable for A/D conversion.

F. The AR-11 A/D Converter

The AR-11 is the third link in the system and its function is to *translate* the continuous signal played back from the Honeywell 101 into a form which can be understood and analyzed by a digital computer. This process is called analog to digital conversion (A/D conversion). For a more detailed description of this process, see Chapter III, section A.

The AR-11 has a ten bit conversion accuracy which means it can distinguish one part in $(2)^{10}$. The conversion time is approximately 43μ seconds. It's primary advantage is that it is built into the PDP-11 minicomputer and can be operated by means of a program written in PDP-11 assembly language as well as BASIC. (See also Chapter III, section A.)

G. The PDP-11/10 Minicomputer

The PDP-11 is the fourth and final link and forms the *brain* of the system. It takes the information, translated by the A/D converter, and reduces it to useful information in the form of graphs, tables or single numbers.

The PDP-11/10 minicomputer is a 16 bit word machine with 28K word magnetic core memory. 24K words of memory are available to the user. The machine is equipped with a CAPS-11 magnetic cassette tape mass storage system and an operating system that supports BASIC computer language. A built-in AR-11 module allows the user to perform software controlled A/D conversions either in BASIC or assembly language. Interactive graphics in BASIC is possible by means of a GT-40 random scan graphics terminal.

These last two features especially made the use of the PDP-11 attractive since digitized data could easily be displayed and manipulated on the graphics screen.

H. The EXPLORER III Digital Oscilloscope

In addition to the instruments mentioned before we also made use of a digital oscilloscope manufactured by Nicolet Instrument Corporation.

The Explorer III oscilloscope is a versatile instrument that allows us to look at a signal, store it in digitized form in a 4K memory and plot it on an x-y plotter. The Explorer III has a built-in 32K floppy disk unit which allows it to store eight 4K signals or 32 1K signals. The maximum digitizing rate is 2 MHz and the resolution is 0.025 percent. Once data have been "frozen" on the screen they may be inverted, moved, added, subtracted, expanded, erased or output to a pen recorder.

The main advantage of this instruments to this project is its capability to freeze signals and output them to a pen recorder, which allows preview of a signal before analyzing it with the computer.

CHAPTER III

SOFTWARE

Programs (software) were written to instruct the A/D converter and the computer how to go about collecting and analyzing the stream of data coming from the Honeywell 101. This chapter describes the various considerations that had to be taken into account to accomplish accurate data transfer and interpretation and how they were implemented in the respective computer program algorithms.

A. Computer Analysis Considerations

Because of the nature of a digital computer any analog (continuous) signal to be analyzed must first be converted to a digital form (discrete points). This is accomplished by feeding the signal through an analog to digital (A/D) converter. The critical parameters in A/D conversion are speed and accuracy. Typical values for high speed and high accuracy (resolution) are 20 μsec/conversion or less and 16 bit accuracy (1 part in 65536).

The PDP-11 minicomputer that was used for data analysis contains an A/D conversion module (AR-11) that is software controlled. The accuracy is 10 bits (one part in 1023) and the conversion speed was found to be approximately 43 μsec which classifies it as a medium-fast, medium-accurate converter.

Because of its complex nature the data analysis would have to be done in a high level computer language which also suggested the use of a high level language to drive the software controlled A/D converter. Since the PDP-11 supports BASIC some extensive tests were taken to determine the applicability of pre-written BASIC subroutines for A/D conversion. It was found that the use of BASIC decreased the speed of the A/D converter by a factor ten and only 2300 conversions per second could be made. Since it takes a minimum of ten points per period to reasonably describe a sine wave this suggested that the maximum frequency of any signal to be digitized would be limited to 200 Hz! This was clearly inadequate in the light of the fact that the maximum video frequency as recorded on an FM recorder even after having been reduced by a factor 16 could still be as high as 2500 Hz.

A second problem was that in order for the convertor not to limit the spatial resolution of the camera, at least 100 points per horizontal scanning line would have to be converted. This would require a minimum of 10,000 words of computer memory per field digitized, just for data storage. Because the PDP-11 contains only 24K (24 x 1023) available words of memory 16K of which is taken up by the BASIC interpreter in addition to the memory space required to store a program, there would not have been enough core memory space available to store half of a field.

This justified the decision to separate the A/D conversion process from the analysis stage so that a low level language could be used to digitize the data at greater speed and less memory.

It was found that a program could be written in PDP-11 assembly language capable of driving the AR-11 converer at 23,000 conversions per second while leaving approximately 20K words of memory for data storage. This was clearly sufficient for our purpose. The program that resulted is capable of selecting any specified field as recorded on analog tape to be digitized. It will then proceed to fill up about 9,700 words of core memory with digitized data points after which it writes all data on cassette tape in the appropriate format so that the data can later be analyzed by a program written in BASIC.

B. A/D Conversion Considerations

The AR-11 A/D converter resident in the PDP-11 can be programmed to operate in the range of -2.5V to 2.5V as well as 0V to 5V. For our purpose we chose the 0 to 5 volt range, meaning that the AR-11 can distinguish any signal between 0 and 5 volt at intervals of 4.888×10^{-3} volt. (5/1023). This implies that in order to benefit most from this fixed resolution, the signal being fed into the AR-11 should always be amplified or attenuated such that its total amplitude range spans 5V. Any range less than 5V would decrease the accuracy of the A/D converter while any range greater than 5 volt would cause saturation.

In the case of our specific application there is the added complication that the signal output by the interface between the AGA 750 and the Honeywell 101 is *inverted* and thus spans a range from 0 to -1 volt.

This problem was solved by using a Tektronix 502A dual beam oscilloscope to invert and amplify the signal until it satisfies the

requirements for optimal A/D conversion. The Tektronics scope proved particularly useful for this purpose because of its following features:

a) large amplification range,
b) large DC offset capability,
c) standard input channel which always causes the signal to be inverted (180° out of phase),
d) ability to monitor two signals simultaneously on the screen.

C. Description of Trigger Pulse Timing

In order for the computer to be able to reconstruct the data in intelligible form it is important that the assembly program keeps accurate track of all vertical trigger pulses (VTP's) and horizontal trigger pulses (HTP's) since they are the only reference points in a continuous stream of data.

In order to accomplish this order the VTP's and HTP's are recorded separately from the video signal on independent channels and fed into the computer on separate channels. When displayed on an oscilloscope where the two pulses are superimposed on each other with the VTP inverted, the picture looks like Figure 3-1. This picture illustrates that the VTP and HTP are out of phase and that each consecutive VTP is shifted over to the right one quarter, thus causing the interlacing effect.

The camera generates 2500 lines/sec. Therefore one line is scanned in 400 μsec. Since the data are recorded at 120 ips and played back at 7.5 ips, Table 3-1 can be generated.

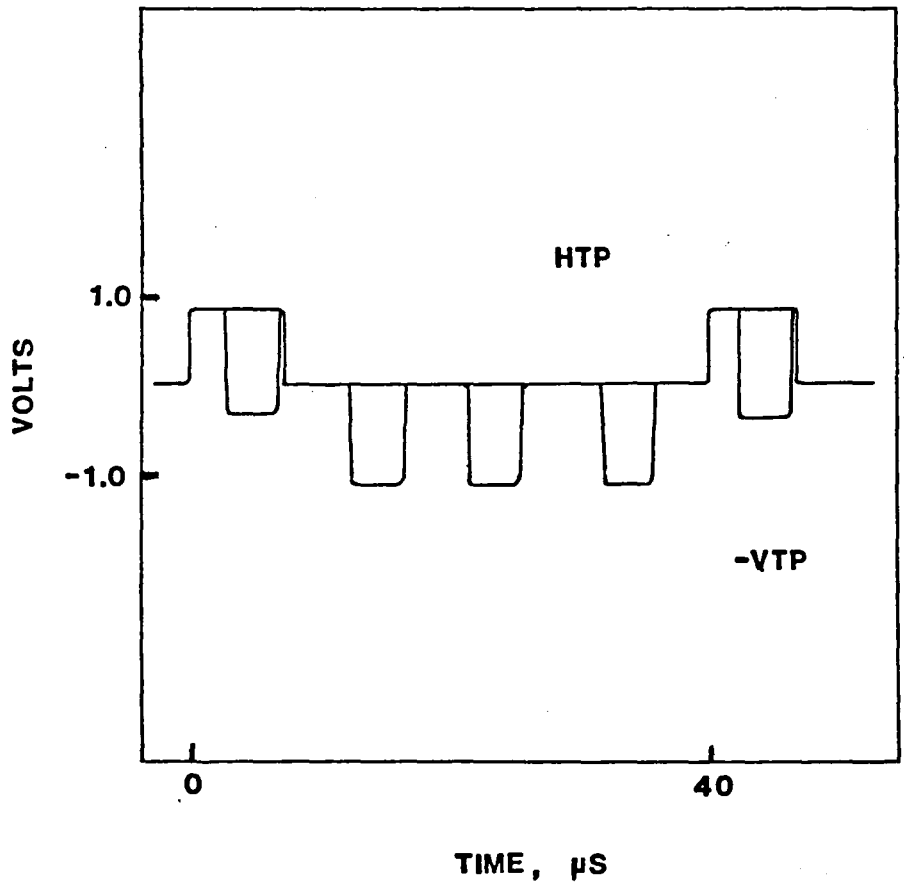

Figure 3-1. Trigger Pulse Timing Diagram

Table 3-1. A/D Timing Chart

TAPE SPEED	120 ips	7.5 ips
line frequency	2500 lines/sec	156.3 lines/sec
line scanning time	400 μsec	6400 μsec
V.T. duration	35 μsec	560 μsec
H.T. duration	80 μsec	1280 μsec
maximum conversions per line (at 43 μsec/conv)	10	149
maximum conversions per V.T. (at 43 μsec/conv)	1	13
maximum conversions per H.T. (at 43 μsec/conv)	2	30

D. The A/D Conversion of Data Collecting Algorithm

The PDP-11 has a core memory of 28K words or 56K bytes. 4K words at the top of the memory are not available for general use. When the assembly program is loaded, the following memory allocation is established. (See Figure 3-2)

After all variables are initialized the program requests six input parameters:

1. # of fields to skip before digitizing the first field
2. total # of fields to digitize
3. # of fields to skip in between each digitized field
4. # of lines to skip in each field before digitizing the first line
5. total # of lines to digitize in each field
6. # of lines to skip between each digitized line.

All these parameters should be entered as decimal integers. As soon as the last parameter has been entered the program starts to make a series of A/D conversions on channel three of the A/D converter until a starting pulse of at least 0.8 volt is found. This starting pulse has been pre-recorded on a separate channel on the Honeywell 101 and is a reference point for the computer.

As soon as the starting pulse is found the program abandons channel 3 and shifts to channel 2 to look for a vertical trigger pulse which would indicate the start of a field. As soon as a VTP is found the program checks how many fields (and thus VTP's) it was supposed to skip and compares this with the number of times it has already

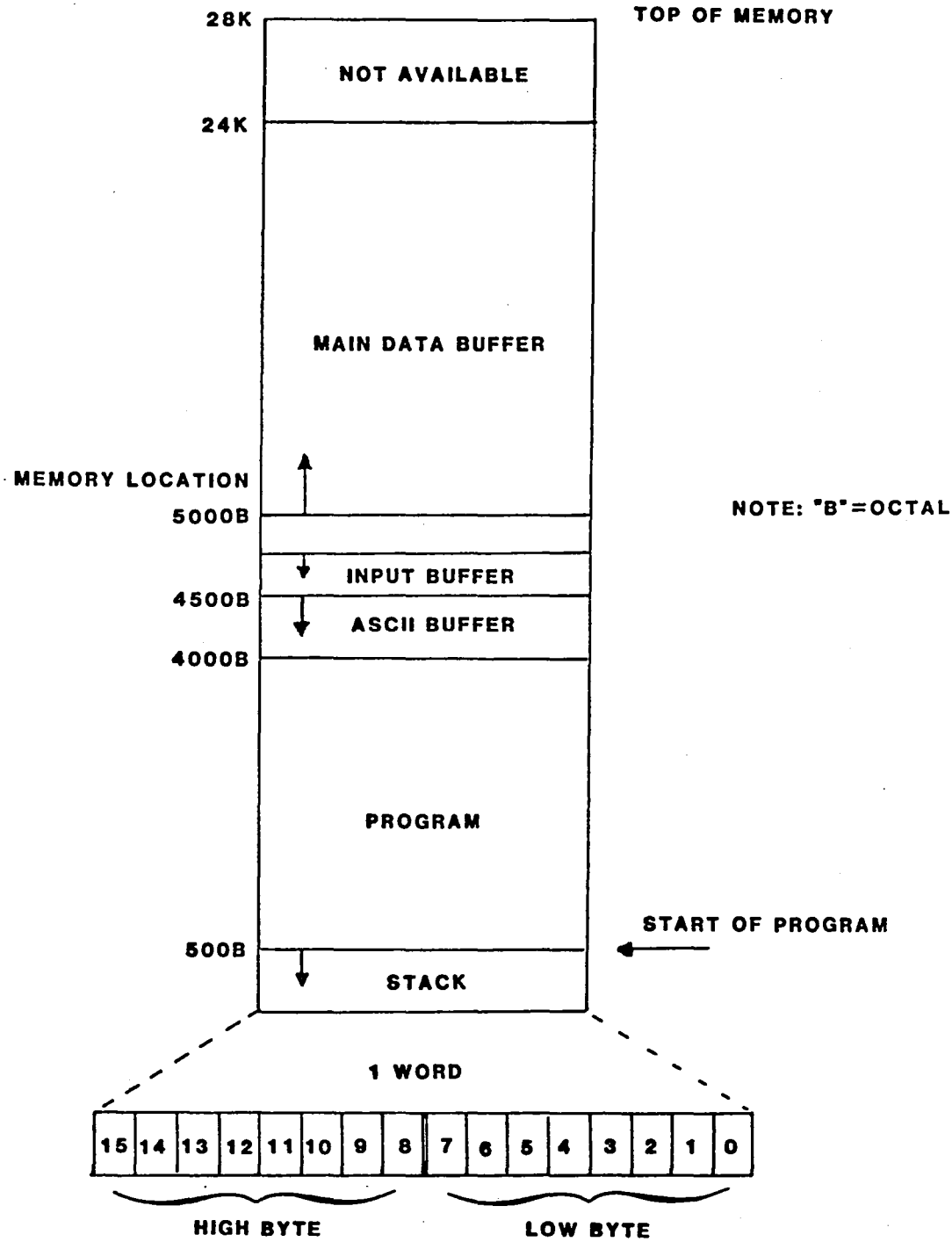

Figure 3-2. PDP-11 Memory Allocation

found a VTP. If not enough have been skipped it proceeds with checking channel 2 for new VTP's, discarding the next 16 checks in order to allow the previous VTP to vanish. Every time a VTP is found a special mark (#4000B) is stored in the data buffer. As soon as the appropriate amount of fields has been skipped the program assumes it has found the top line of a new field and shifts to channel zero to start converting the video signal. The first 160B (one hundred sixty *octal*) conversion are discarded since the program has no way of telling where on the top line it found the vertical trigger pulse. (Only one in every four trigger pulses starts at the beginning of a line.) It then shifts to channel one to look for a HTP. As soon as a HTP is found the program now knows for certain that it has found the beginning of the third line from the top. It then checks how many lines it was to skip and discard a corresponding number of HTPs. When the first line to be converted is reached a HTP mark (#3000B) is written in the data buffer and the program switches to channel zero to convert the signal. One hundred sixty-five octal data points per line are being converted and immediately stored in the data buffer. After 165B conversions, the program knows it has almost reached the end of the line and switches back to channel one to look for a horizontal trigger pulse. When found, another HTP mark is written in the data buffer and the procedure repeats itself. Whenever a certain amount of lines is to be skipped between lines the program simply discards those digitized data during the specified amount of HTPs. The program will then repeat the search procedure for VTPs while discarding as many VTPs as needed between the last digitized field

and the next one. Since the maximum number of lines that will fit on a 150 foot cassette is approximately 80, it is vital that the number of lines to digitize times the number of fields to be digitized does not exceed 80.

The program finishes by placing 41B End-Of-File (EOF) marks in the data buffer and stores the memory location of the last EOF mark. Finally the program terminates the A/D conversion cycle and proceeds to rewind the cassette and writes a header record to get the cassette ready to accept the data.

Before the data can be written on tape they first need to be converted from binary to decimal according to the standards of the AMERICAN STANDARD CODE for INFORMATION INTERCHANGE (ASCII). The ASCII code for number zero through nine is 60B through 71B.

Each data word is retrieved sequentially from the beginning of the main buffer and converted to eight bytes of ASCII code. These bytes are stored in an intermediate Buffer (ASCII Buffer) that can hold 128 bytes. As soon as the ASCII Buffer is full it is "emptied" on cassette tape after which the next block of data is read from the main buffer into the ASCII Buffer. This procedure continues until the end of the main buffer is reached. The program then terminates the tape write by writing a so-called *"sentinel file"* which marks the logical end of the tape. The tape then rewinds and the program is automatically restarted, ready to accept a new cassette.

E. The Data Analysis Programs

The software to analyze the digitized data is written in BASIC and consists of five programs each capable of performing different functions. The division into five different programs was necessary because of limited core memory space which did not allow for one large program capable of performing all desired functions. This section describes the different programs and their capabilities.

Program MAIN

The purpose of this program is to allow the user to display the signal of one individual horizontal scan as a function of voltage versus position along the scan on the GT-40 graphics screen. Because of the detailed information that can be extracted by this method, this is the primary program that will be used for data analysis. It is designed such that the user can analyze the signal using interactive graphics. This means that the program displays a "menu" of commands on the screen each of which can be executed by simply pointing the light pen at the desired command.

The program runs in two modes: *scanning mode* and *analysis mode*. In scanning mode the user can instruct the program to display any line and if so desired to keep displaying consecutive lines as well as rewind the data tape to the beginning of the data file in order to display previous lines. When the user desires to analyze a particular line he can enter the *analysis mode* by aiming the light pen at the word "analyze" in the menu. This causes the whole menu to be changed to

analysis commands.

In analysis mode the user can identify one particular point in the picture as being a reference point. This is done by aiming the light pen at a point on the graph. As soon as this is done the program will request the temperature, f-stop used and emissivity at that point. From that moment on the temperature an any point on the line scan can be obtained by aiming at it with the light pen and entering the emissivity at that point. The temperature will be displayed on the graphics screen. Analysis mode will also allow the user to quickly find the highest and the lowest temperature in the picture as well as the average temperature of a region between two points identified by the light pen. The average is determined by the program by adding up the voltage values of all points between the left and right limit indicated with the light pen and dividing the sum by the total number of points. This average voltage value is then converted to an average temperature value as discussed on page 41. One can switch back to scanning mode by aiming the light pen at the word "exit".

After a reference point has been identified and the data tape has been rewound to the beginning of the data file the user can use the "auto-scan" feature to determine the temperature of a single point or average value of a fixed region on each scanned line as it varies with each line. After identifying the x coordinate(s) of the point(s) to be examined the program will automatically scan each line, find the temperature of the desired point or region on that line and "dump" that value on another digital cassette mounted on cassette drive zero.

This cassette will later be accessed by program "PLOT" (see page 43) which will plot the values dumped on this cassette as a function of time.

In determining the absolute temperatures within a scanned field the computer makes use of a set of standard calibration curves (See Figures 2-8 and 2-9) that have been supplied by the camera manufacturer. These curves can be mathematically described by the following equation:

$$I = A \times \exp \frac{B}{273 + T}$$

where A and B are constants

I = isotherm level

T = temperature

For each standard f-step setting of the camera there is a specific constant A and B resulting in a unique relationship of I as a function of T.

Before any absolute temperatures can be determined within a field the computer must know the absolute temperature of at least one reference point. This is T_{ra} which has a corresponding digitized voltage level V_{ra} associated with it.

When the temperature of a point within the field is desired, the operator identifies this point with the light pen. The computer finds the voltage level corresponding to that point (V_o) and calculates a corresponding isotherm value for that point using the experimentally

determined relationship (See Chapter II, Section D)

$$I_o = 165.46 \times V_o + 8.4512g \ .$$

Similarly, it calculates the isotherm level I_r of the reference point from its voltage level, and subtracts them to find the difference:

$$\Delta I = I_r - I_o \ .$$

The program then uses the known absolute temperature of the reference point to determine the corresponding absolute isotherm level I_{ra} using the standard calibration curve equation corresponding to the aperture setting of the camera:

$$I_{ra} = A \times \exp \frac{B}{273 + T_{ra}} \ .$$

The absolute isotherm level of the object point can now be found:

$$I_{oa} = I_{ra} - \Delta I$$

which allows the program to calculate the absolute temperature of the *object* point using the inverse calibration curve equation

$$T_{oa} = \frac{B}{\ell n(I_{oa}) - \ell n(A)} - 273 \ .$$

When extension rings are placed between the camera and the lens, the f-stop of the camera is changed to one for which no standard calibration curves are available. However, since the amount of radiation

received by the detector should vary proportionally to the square of the f-stop, it is possible to use the calibration curve of the closest smaller f-stop and correct for the difference in radiation by multiplying the constant A of the calibration curve by a correction factor equal to:

$$C = \left(\frac{f_2}{f_1}\right)^2$$

where

f_2 = f-stop with extention ring

f_1 = closest f-stop less than f_2 for which a calibration curve is available.

From the set of calibration curves, however, it can be seen that, for a constant temperature, the isotherm level does not vary proportionally to the square of the f-stop but rather by a constant factor of approximately 1/1.8.

In order to correct for that, our final correction factor should be

$$C_2 = \left(\frac{f_2}{f_1}\right)^2 \times \frac{\frac{1}{1.8}}{\left(\frac{f_1}{f_3}\right)^2} \quad .$$

where f_3 = closest f-stop greater than f_2 for which a calibration curve is available. The standard isotherm curves are fitted to the following

expression

$$I = A \times \exp \frac{B}{273 + T}$$

where A and B are experimentally determined constants.

Any non-standard aperture curve should also follow this expression and have a unique value for A and B. However, multiplication of a standard isotherm curve by a factor C_2 amounts to correcting only for A. The reason the introduced error is not significant is that the constant B varies less than one percent for all the standard aperture curves and can safely be assumed to be constant.

Program PLOT

This program allows the user to plot the data that were dumped by program MAIN as a function of time. This is particularly useful if one is interested in temperature changes at one point (or region) of an object as they occur over a time period. The user must indicate whether the data were obtained from the camera operating in "field scan mode" (normal operation where both prisms were rotating) or in "single line scan mode" (where the vertical prism was stationary). When in "field scan mode" the program will plot the dumped value of one particular line in each field as a function of that field. However, since each field was scanned in 1/25 of a second the x-axis of the plot is given in increments of 1/25 of a second. In addition to plotting the dumped value of one single line, the program also allows for plotting the *average* of the dumped values of a series of consecutive lines as a function of time. This is of particular value if the dumped values

were average values over a certain part of each line rather than single points. The plot will then represent the average temperature value of a square *region* of the object plotted against time, rather than a single point. Usually this is more significant than plotting the value of single points since the camera has a finite resolution and therefore already averages the signal over a certain finite region.

When operated in "single line scan mode" the program will display the dumped values as a function of line scan number. Besides graphical output on the GT-40 graphics screen the program can also produce a hard copy output in the form of either a plot or a table produced on a printer terminal. A hard copy plot will be a rough copy of the plot on the graphics screen while a table will consist of the printed values of "field #", "temperature", "voltage", "minutes" and "seconds". If the option of a short table is chosen only the values of "temperature" and "seconds" will be printed. In single scan mode the option of a long table is not available and only the values of "temperature" and "scan #" will be printed.

Program QUICK

This program allows the user to take a quick look at the "raw" digitized values and the horizontal and vertical trigger pulse marks as they have been written on tape by the assembly program. This is particularly useful in case there is any doubt that the assembly program has not skipped the right amount of fields or lines. This can quickly be verified by counting the number of HTP and VTP marks as displayed on the screen. The data are displayed in five columns on the screen

until the screen fills up. The next block of data will be displayed by typing any one digit number followed by a carriage return. EOF marks will have a value of 3584B. VTP marks will have a value of 2048B while HTP have a value of 1536B. For easy identification the HTP marks will appear as blinking numbers.

Program ISO

Program ISO plots the digitized data on paper in a two-dimensional matrix while assigning a value of one to 20 to each point depending on what its digitized value was. Values greater than ten were assigned alphabetical characters starting at A = 11. The map thus produced clearly identifies regions of approximately equal temperatures and can be enhanced by drawing lines around each region. Although it is not possible to assign actual temperature values to the isothermal regions because of limited memory space of the computer, the isothermal map can be very useful in locating "hot spots" and steep thermal gradients (See Figure 3-3).

Program MAP

This program will read the digitized data from the cassette in drive #1 and display them on the GT-40 graphics screen in a matrix while assigning different intensities to each data point, based on its digitized value. The result is a rough picture of what one scanned field or part thereof looks like. This program can be helpful in identifying the different objects the camera looked at when the recording was made. No hard copy output is available from this program.

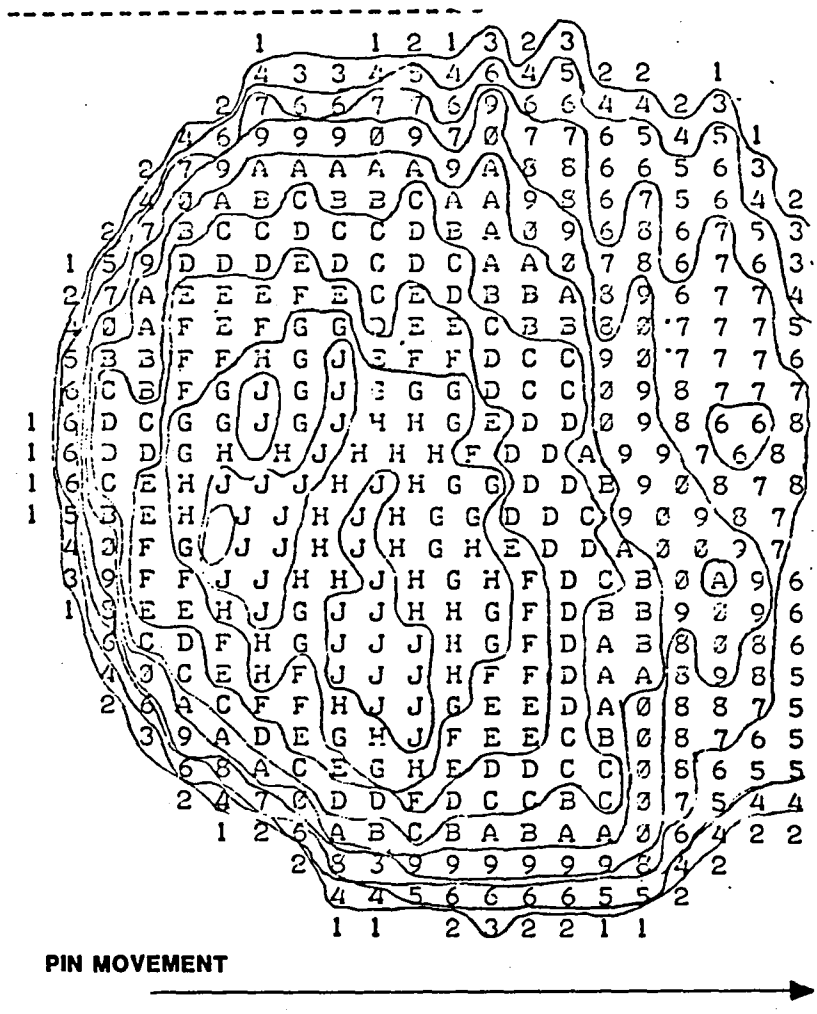

Figure 3-3. Isothermal Map of Rulon on Sapphire Contact Area

CHAPTER IV

TRIBOLOGICAL EXPERIMENTAL APPARATUS AND PROCEDURE

This chapter discusses four tribo-experiments that were used to test the infrared radiation analysis system.

A. Rulon Pin on Sapphire Disk

A device was built by Mr. Scott Bair that would allow a pin of 5.1 mm diameter made out of "Rulon E" (a filled teflon) to be loaded against a reciprocating sapphire disk by air pressure (see Figure 4-1) The AGA 750 camera looked through the sapphire disk at the circular contact area between the pin and the sapphire. The sapphire disk was connected to a dc motor turning at 113 rpm by a mechanical link which caused the disk to reciprocate. The maximum sliding velocity was 11 cm/sec. A load of 44N was applied to the pin and a recording was made of the signal produced by the infrared camera as it scanned the contact area of the pin (see Figure 4-2). The system infrared emission was recorded for seven seconds from start-up.

B. Rulon Pin on Steel Plate

This was the first of three experiments conducted at Mechanical Technology, Incorporated (MTI) in Schenectady, New York. A 0.476 cm diameter Rulon pin was pressed against a reciprocating Nitrolloy (low alloy steel) plate. The pin was mounted stationary relative to the camera while the plate was forced back and forth in a reciprocating

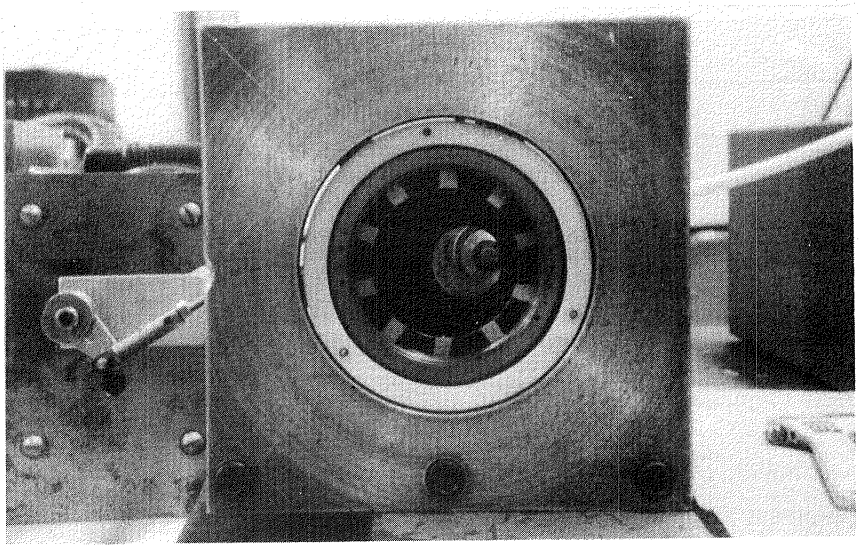

Figure 4-1. Rulon Pin on Sapphire Disk Experiment

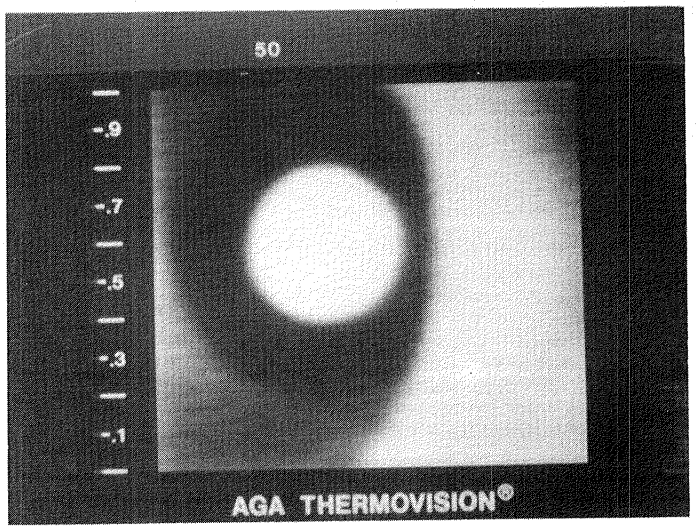

Figure 4-2. Thermogram of Rulon Pin on Sapphire Disk

motion by a DC motor (See Figure 4-3). The stroke length was 40 mm. A surface micro-thermocouple had been inserted in the metal surface in an attempt to measure the surface temperature to compare it with the IR measurement. The thermocouple is shown schematically in Figure 4-4. The camera was located to observe the steel surface as it emerged from under the pin.

In this experiment the camera was switched to single line scanning and the vertical scanning prism was positioned such that the camera would scan one single line parallel to the motion of the plate and through the center of the track of the pin on the plate. Recordings were made of steady periodic operation using three speeds: 500 rpm, 1000 rpm, 1500 rpm and three loads: 1.18 kg, 2.18 kg, 4.18 kg at each speed. A small strip of black non-glossy paper having an emissivity of 0.9 was placed on the right side of the scanned line in order to provide a reference source of known emissivity and ambient temperature. The ambient temperature of 26C was assumed to be that of the reference source on the plate. A special triggering device designed by Mr. Gene Clopton was used to *externally* trigger the vertical camera trigger pulse (normally produced by the camera itself). It was set up such that it would produce a vertical trigger pulse each time the sliding plate was in its left-most position.

This triggering device as shown in Figure 2-2 produces a small infrared beam at a 30 degree angle that will be reflected back into a receiver by a reflecting strip of paper attached to the reciprocating device. As soon as the amount of radiation received goes from high to low it causes a vertical trigger pulse to be produced.

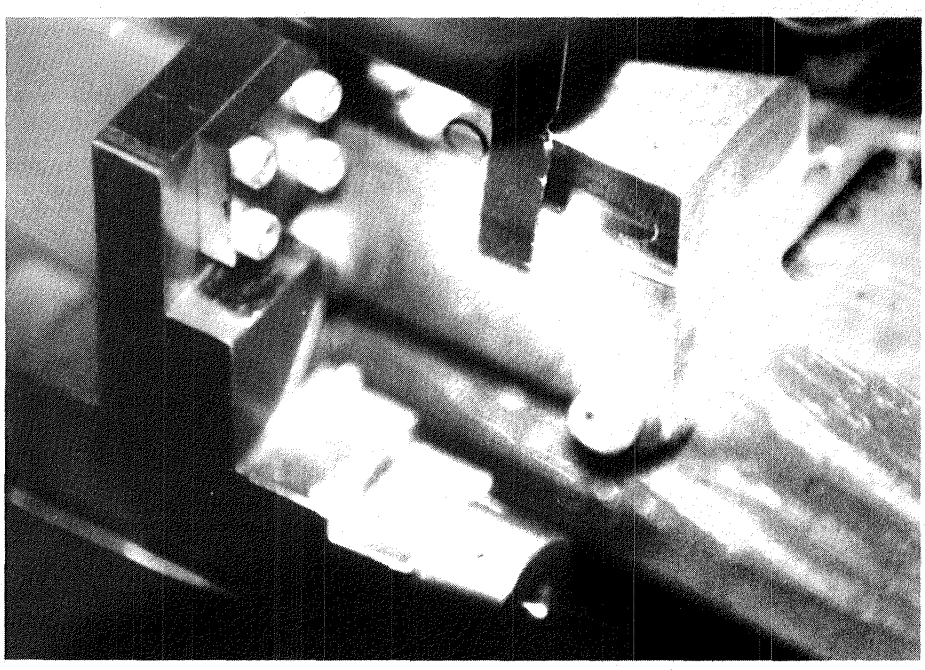

Figure 4-3. Rulon Pin on Steel Plate Experiment

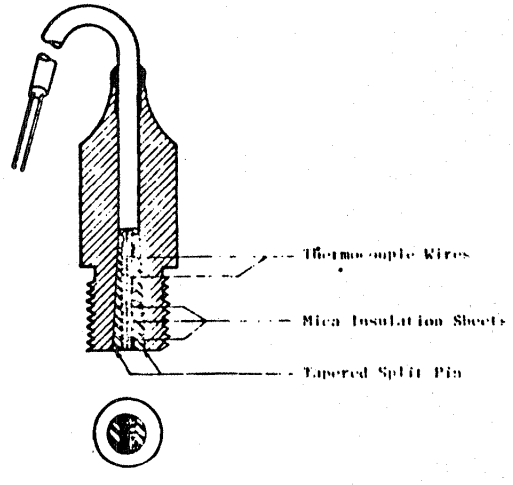

Figure 4-4. The Thermocouple

C. Rulon Pin on Sapphire Plate

This experiment was the second experiment conducted at MTI and a modification of the experiment described in Section 4B. (See Figure 4-5). The 0.476 cm Rulon pin was caused to slide against a stationary sapphire plate and loaded with 1.18 kg, 2.18 kg and 4.18 kg at three velocities; 500 rpm, 1000 rpm and 1500 rpm at a stroke of 40 mm. Again the camera was set up to scan a single line parallel to the sliding motion of the pin and through the center of the pin. The vertical trigger mechanism was coupled to the DC motor such that it would cause a vertical trigger pulse at the point that the pin would attain its maximum velocity moving to the right. Only the right one-half of the cycle was being scanned because the use of the 66 mm extension ring limited the field of view of the camera to approximately half the stroke. The strip of black reference paper was not attached on the left of the pin and moved with the pin.

D. Stirling Engine Seal Simulator

This was the third experiment conducted at MTI. A Nitrolloy low alloy steel circular rod was reciprocating in and out of a circular Rulon seal. The stroke length was about 50 mm (See Figure 4-6). Recordings were made at four speeds: 300 rpm, 600 rpm, 900 rpm and 1100 rpm and five seal pressures: 0 psi, 225 psi, 450 psi, 600 psi and 900 psi. The seal was loaded around the rod by means of air pressure. The camera was aimed such that it would scan a single line

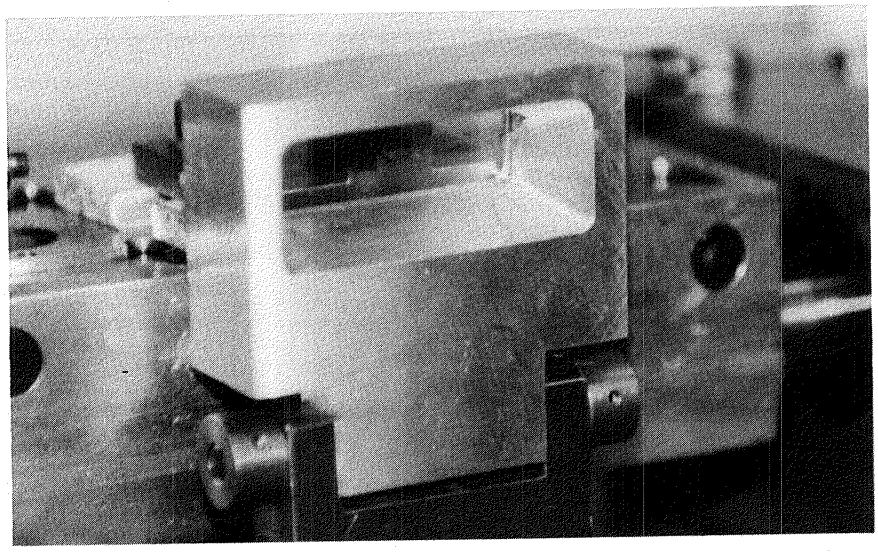

Figure 4-5. Rulon Pin on Sapphire Plate

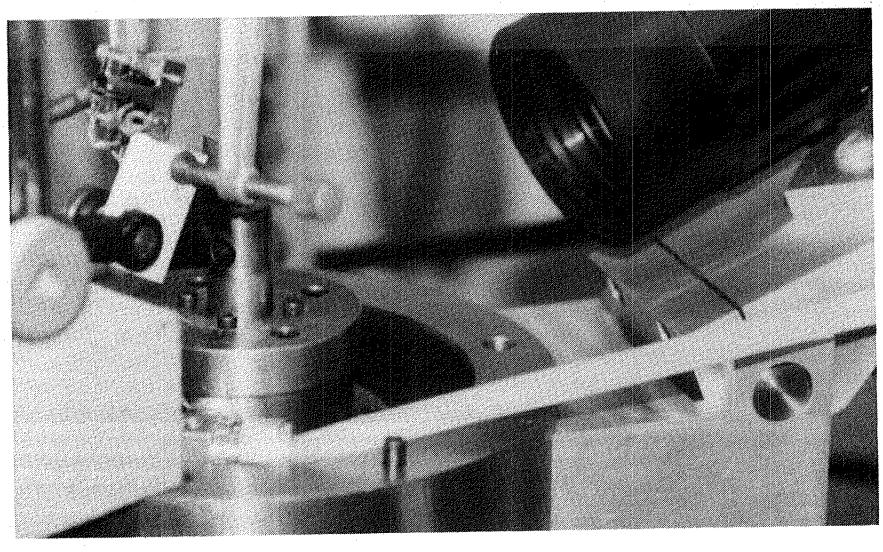

Figure 4-6. Stirling Engine Seal Simulator

perpendicular to the motion of the rod at the point immediately above the seal. A thermocouple was attached to a hex-nut that appeared on the left side of the picture and which would serve as a reference object of known emissivity and temperature. The emissivity of the nut was determined to be 0.98. The vertical trigger pulses were triggered as the rod was in its uppermost position and starting to move downward.

CHAPTER V

PRESENTATION OF THE RESULTS

This chapter presents the results of the computer analysis of the infrared radiation data recorded during the experiments described in Chapter IV.

A. Rulon Pin on Sapphire Disk

The first analysis done on these data was a transient average temperature analysis of one line scanned through the center of the pin. It was found that the average temperature of the chosen line oscillated in a range of approximately two degrees C with a frequency of approximately 0.26 seconds. The maximum observed temperature during an observation period of seven seconds rose from 21C to 32C and was still slightly increasing at the end of the seven seconds of recovery. A plot of temperature versus time can be found in Figure 5-1.

The oscillating frequency of the temperature corresponds to twice the rotational frequency of the DC motor (which ran at 113 RPM) and shows that the pin cools off by approximately two degrees twice during the cycle, and identifies the instance where the relative sliding velocity was zero (the reciprocating points). From Figure 5-1 it can be seen that the temperature profile is different for the upward motion of the disk as compared to its downward motion. We attribute this to uneven loading combined with the fact that the shaft on which the

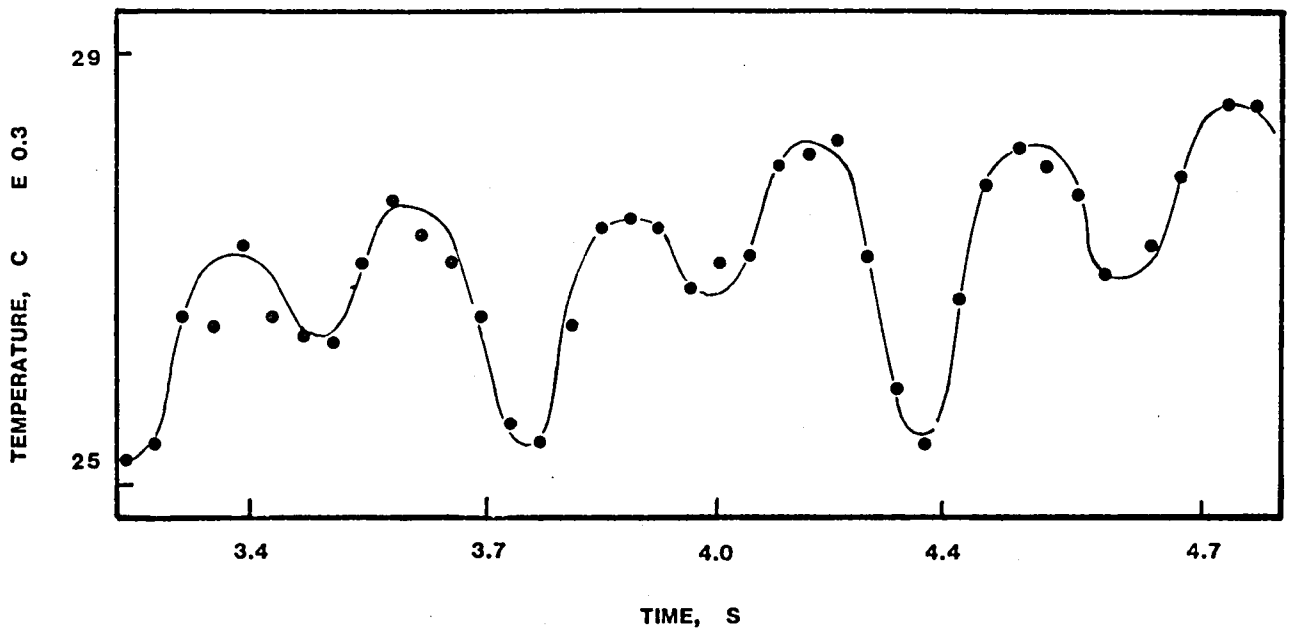

Figure 5-1. Rulon Pin on Sapphire Disk center Line Temperature

Rulon pin was mounted was flexible and caused the pin to be moved upward and downward relative to the examined line. Since the temperature distribution over the pin is not uniform due to uneven loading. The camera would not see the same temperatures on the downward stroke as compared to the upward stroke.

The maximum temperature of 32C is based on an emissivity of 0.3 for the Rulon pin and may be considered an upper limit because the emissivity of the Rulon was later recalibrated and found to be approximately 0.9, which will lower the maximum temperature by several degrees. The ambient temperature was 21C.

The second analysis concerned the plotting of an isothermal map of the contact using program ISO. The results are shown in Figure 3-3. The motion of the sapphire plate was vertical and downward. A hot spot on the contact can be found below the center of the contact and also a steep thermal slope can be observed on the trailing edge of the contact.

B. Rulon Pin on Steel Plate

An attempt was made to trace the temperature of a fixed point on the steel plate during part of the stroke in the 1500 rpm and 4.18 kg load. Since the thermocouple could be clearly identified during each scan displayed by the computer during analysis, three points were chosen relative to the thermocouple (see Figure 5-2). Their temperatures were recorded as a function of position on the screen during each scan where they were visible and the results were plotted. (See Figure 5-3).

It was found that the surface temperature of the thermocouple was consistently higher than the temperature of the surrounding surface

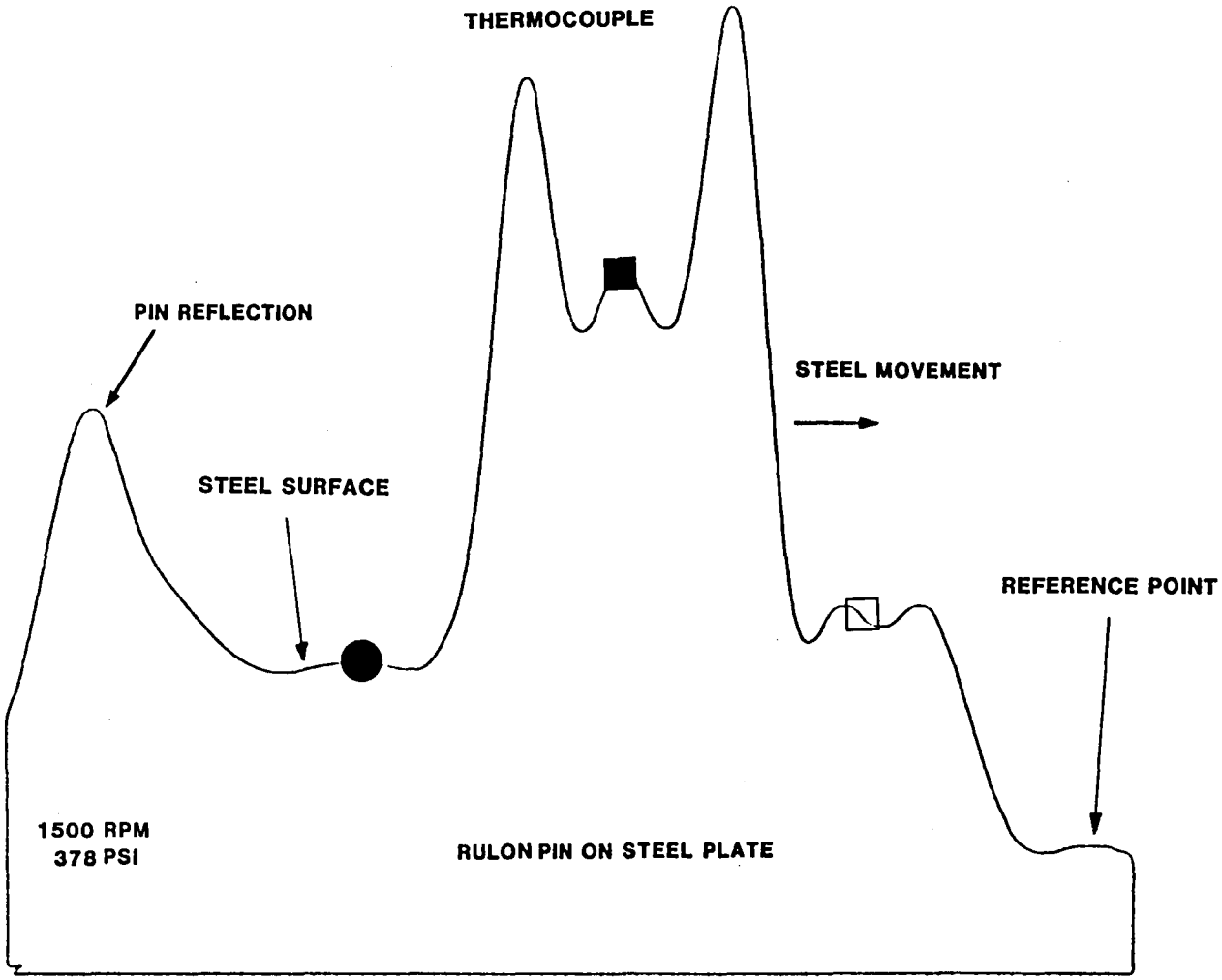

Figure 5-2. Rulon Pin on Steel Plate Center Line Scan

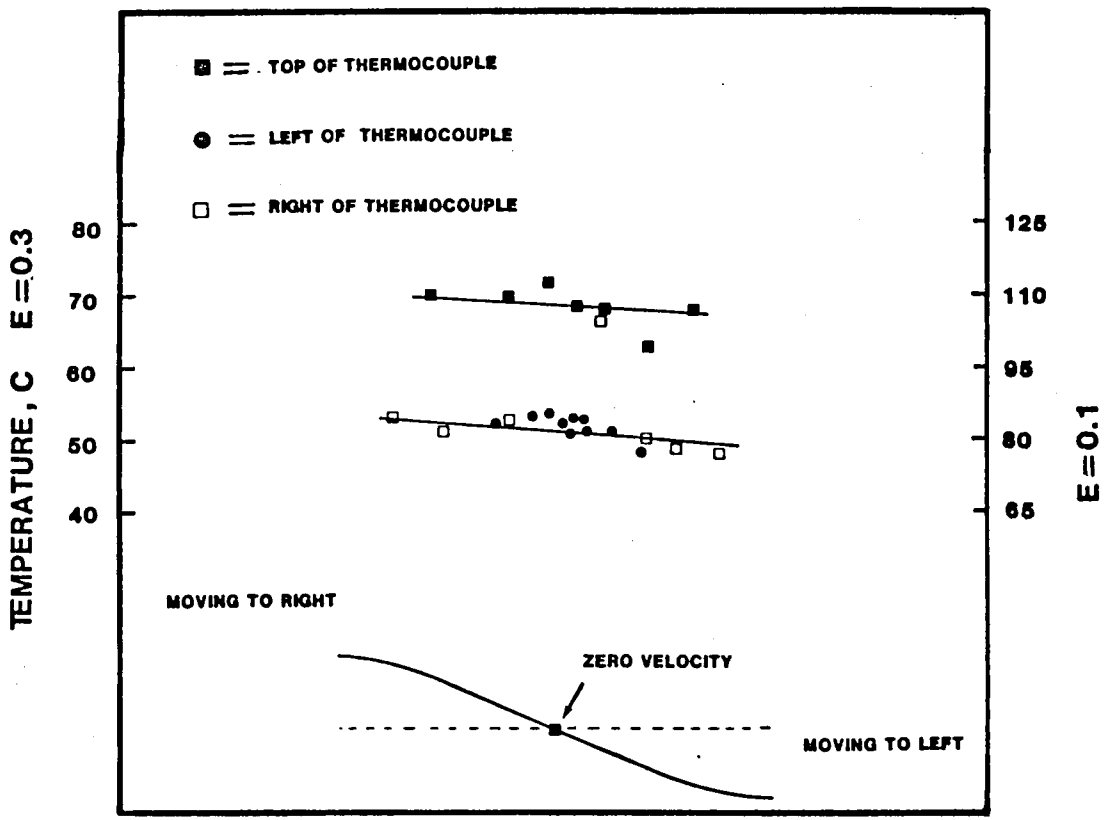

Figure 5-3. Rulon Pin on Steel Plate.
Plate Temperature as a Function of Stroke

apparently because the thermocouple changed the local thermal resistance of the surface. However both the temperatures of the points to the left and right of the thermocouple as well as the thermocouple itself decayed slightly during the period in which they were observed. This was to be expected since the only energy input into the plate took place just before and after the observed period and thus only cooling could take place. The cooling rate was very small however as can be seen in Figure 5-3 which is consistent with our findings in Section D of this chapter.

In addition the temperature of the plate was recorded at a point fixed to the right of the Rulon pin as the plate was sliding by. A plot of plate temperature at this point versus cycle position is presented in Figure 5-4. The data points that are off the scale represent the thermocouple passing through the point being examined and form convenient reference points as to what instant in the cycle is being observed. From this graph the following information can be derived. As the plate moves to the right friction between the pin and the plate causes it to be heated as it emerges from under the pin. Since there is very little cooling taking place, the temperature seen at the right of the pin remains high even after the plate has started to move to the left again. It isn't until the plate has reached its leftmost position that the rightmost part of the plate slides under the point being observed. This part of the plate remains relatively cool since it never encounters the pin itself. The temperature seen at this point therefore is a low point in the graph. As soon as the plate starts to move to the right again. Parts of the plate that have been exposed

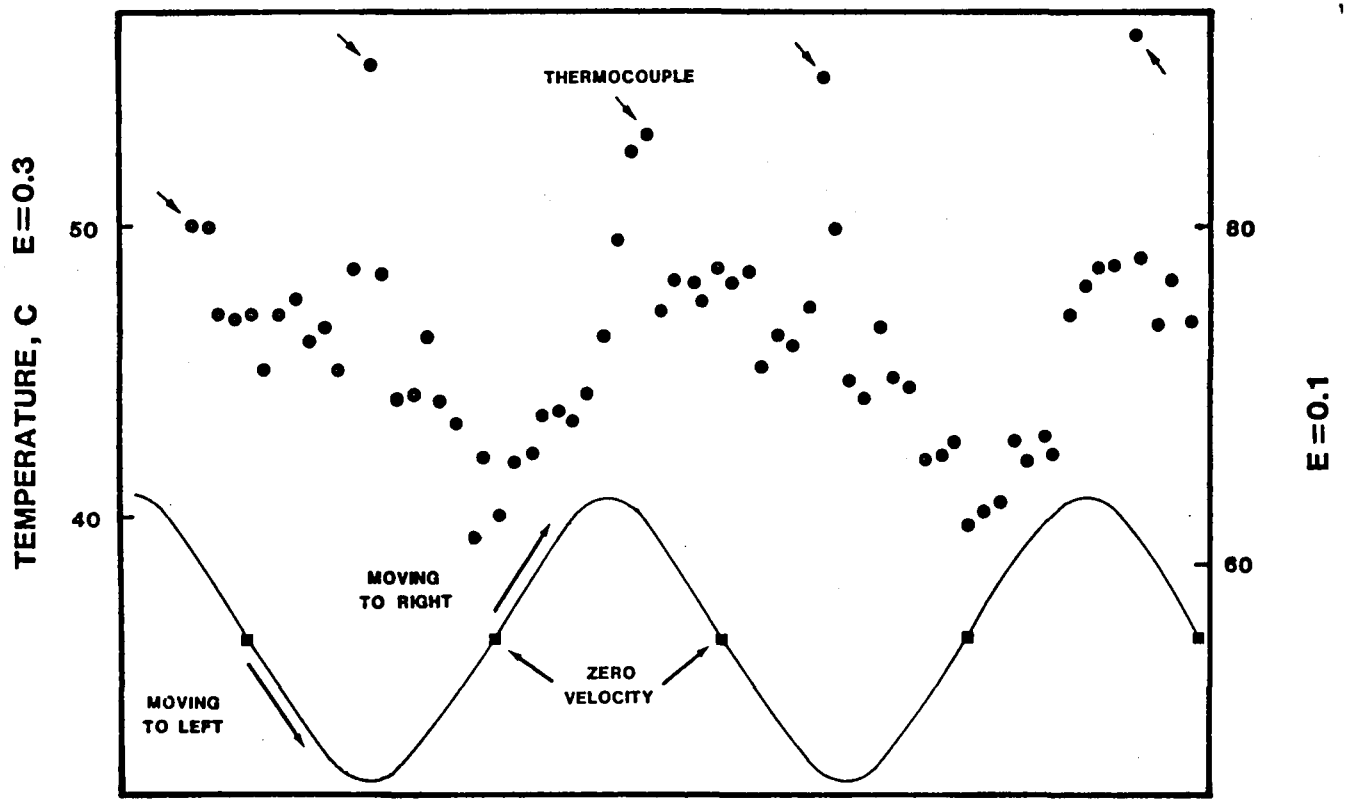

Figure 5-4. Rulon Pin on Steel Plate.
Plate Temperature at a fixed point relative to the AGA 750.

to increasing pin sliding velocities appear under the observed point and the temperature rises again to a maximum. If any significant cooling had taken place during the cycle the temperature should have dropped after the plate had reversed its direction from right to left. Since this is not the case we may conclude that an essentially constant temperature profile exists across the plate during the cycle where the middle of the plate which is subjected to highest pin velocities is hottest while the ends are coolest.

The apparent scatter in the data is most likely caused by small DC voltage variations within the camera as well as the fact that the friction coefficient and emissivity are not constant during the cycle. Also the presence of the thermocouple causes a severe scatter of some of the data points.

Since the temperature profiles are similar for all speeds and loads, a table was made recording the maximum and minimum temperatures found during each cycle of different rpm and loads taken at a point slightly to the right of the pin. (See Table 5-1)

Even though the emissivity of the surface was calibrated with the camera and found to be approximately 0.05 we believe that it was higher because of the development of a Rulon transfer layer rubbed off on the steel. Therefore the data was analyzed at both an emissivity of 0.1 and 0.3 to give an upper and lower bound for the plate temperature. All temperatures were found to be decreasing with decreasing load and speed although the decrease from 100 kg to 50 kg load at each speed appeared to be smaller than expected.

Table 5-1. Rulon Pin on Steel Plate
(Plate Temperatures)

RPM	Load kg	E = 0.1 highest temperature	E = 0.1 lowest temperature	E = 0.3 highest temperature	E = 0.3 lowest temperature
1500	4.18	84	64	52	38
	2.18	79	64	48	39
	1.18	78	65	48	39
1000	4.18	68	59	43	39
	2.18	62	46	40	32
	1.18	59	46	38	31
500	4.18	56	44	38	29
	2.18	53	39	35	30
	1.18	53	38	36	29

C. Rulon Pin on Sapphire Plate

The data from this experiment were examined for contact temperatures at the point of maximum velocity during the stroke as well as at the reciprocating point as the pin was in its rightmost position. The field of view of the camera was limited to the right half of the stroke and the temperature values at the very leftmost part of the screen are less reliable because of lens edge distortion. Therefore the temperatures for maximum velocity (being on the left hand side of the screen) were recorded as the pin was moving to the left as well as when it reappeared on the screen going to the right. These temperatures are based on an emissivity value for Rulon of 0.9 which was measured.

The difference between the minimum and maximum temperatures during one stroke never exceeded 10C as can be seen in Table 5-2, and the maximum temperature observed was 66C at 1500 rpm and 4.18 kg. The high point was consistently found at the left hand side of the screen which corresponded to a higher velocity while the low point in the cycle was always found during the point of zero velocity at the right hand side of the screen. This was to be expected since the highest energy input into the pin occurs at highest velocities. From Table 5-2 it can also be seen that the temperatures decrease with loading as well as with velocity, although the decrease is very slight when comparing the results for 2.18 kg loading and 1.18 kg loading.

A temperature profile of the pin as scanned by the camera can be found in Figure 5-5. This plot was produced with the EXPLORER III

Table 5-2. Rulon on Sapphire (pin temperatures)

RPM	Load kg	Maximum Temperature °C E = 0.9	x position on screen	Minimum Temperature °C E = 0.9	x position on screen
1500	4.18	- 66	296	58	820
		65	389		
	2.18	- 57	279	52	802
		58	177		
	1.18	- 53	338	47	761
		50	380		
1000	4.18	- 64	211	49	812
		57	270		
	2.18	51	338	46	812
		55	228		
	1.18	- 49	245	43	718
		51	126		
500	4.18	- 58	287	48	803
		60	126		
	2.18	55	110	47	803
	1.18	- 55	177	47	786
		56	177		

Note: A negative value indicates the pin was moving to the left.

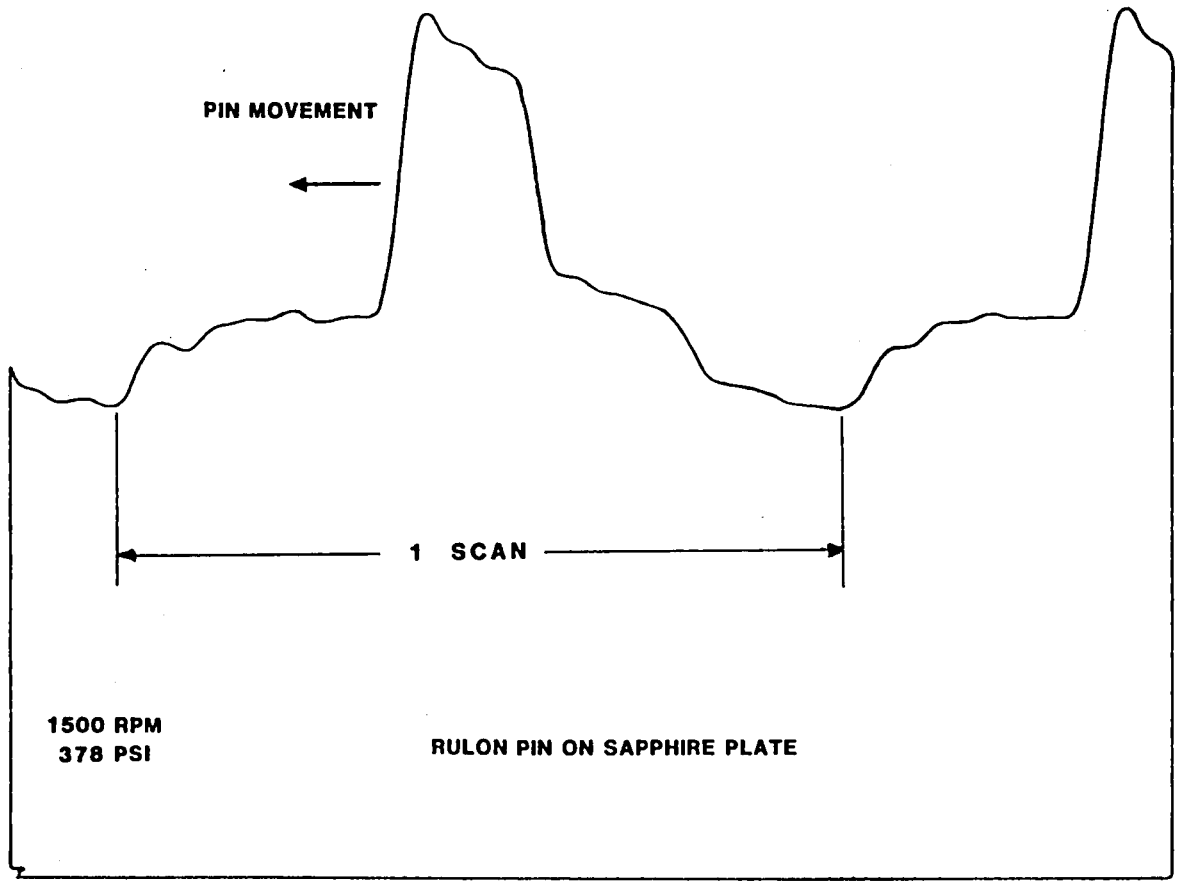

Figure 5-5. Rulon on sapphire single Line Scan

digital oscilloscope. This figure presents the pin as it is moving to the left at 1500 rpm, at 4.18 kg loading. Similar plots have been made at different speeds and it was found consistently that at high loads the left side of the pin was hotter than the right side, regardless of the direction in which the pin was moving. We believe this was due to uneven loading during the movement of the pin. This is a reasonable explanation since we found that while we were making the first test runs with this apparatus the camera indicated that the bottom half of the pin was considerably hotter than the top half even though we thought initially that the pin and the sapphire were properly aligned. A new alignment corrected the problem but this clearly indicated the effect of even the slightest uneven loading.

D. Stirling Engine Seal Simulator

The data taken from this experiment were analyzed to find the highest and lowest temperatures during one cycle of steady state operation at each speed and seal pressure. These values can be found in Table 5-3. These temperatures were based on an emissivity for the steel of 0.05, which was based on measurements done with the camera at MTI. We feel however that these temperatures represent an *upper limit* in light of the fact that the surface of the rod was not as smooth as the sample we used for emissivity calibration and a slight oil film was present on the rod. This may have changed the emissivity to as high as 0.3, thus lowering the maximum observed temperature from 195C at 1100 rpm and 900 psi to 97C.

Table 5-3. Stirling Engine Seal Simulator Rod Temperature

RPM	Pressure (psi)	Highest Temperature (°C) E = 0.05	Lowest Temperature (°C) E = 0.05
1100	900	195	153
	675	180	141
	450	159	123
	225	136	115
	0	123	104
900	900	122	108
	675	122	109
	450	120	114
	225	115	105
	0	123	108
600	900	142	119
	675	136	112
	450	124	106
	225	116	105
	0	114	106
300	900	110	101
	675	111	104
	450	113	104
	225	115	104
	0	110	94

In general the temperatures observed decreased with pressure and velocity the only notable exception being the 900 rpm case where temperatures seemed to be fairly constant. We have no firm explanation for this phenomenon other than the fact that the 900 rpm runs were made as a last minute decision immediately after all other runs had been done, the previous one being the 1100 rpm run. Since the recordings at 900 rpm were made in order of increasing pressure it is conceivable that the rod had not had a chance of cool off adequately from the 1100 rpm run and thus caused the low pressure case temperature readings at 900 rpm to be too high. This explanation seems particularly likely since further analysis of our data as presented in this section indicates that the cooling rate of the rod was considerably longer than its heating rate.

A plot was made of the temperature at the center of the rod as a function of time for the 600 rpm, 900 psi case. The results are found in Figure 5-6. Originally we had expected the temperature to be *high* as the rod would come up out of the seal and *low* due to air cooling as it would move downward into the seal. However it was found that the temperature profile was essentially symmetrical with respect to the lower reciprocating point in the stroke, i.e., the rod's temperature profile was nearly identical for the downward part of the stroke and the upward part. This indicates that during steady state operation the cooling rate of the rod is slow compared to the mechanical cycle time which controls the heating. Therefore the thermal mass causes the temperature profile over the rod to remain essentially unchanged during the downward part of the stroke. Since the bottom and top of the rod always

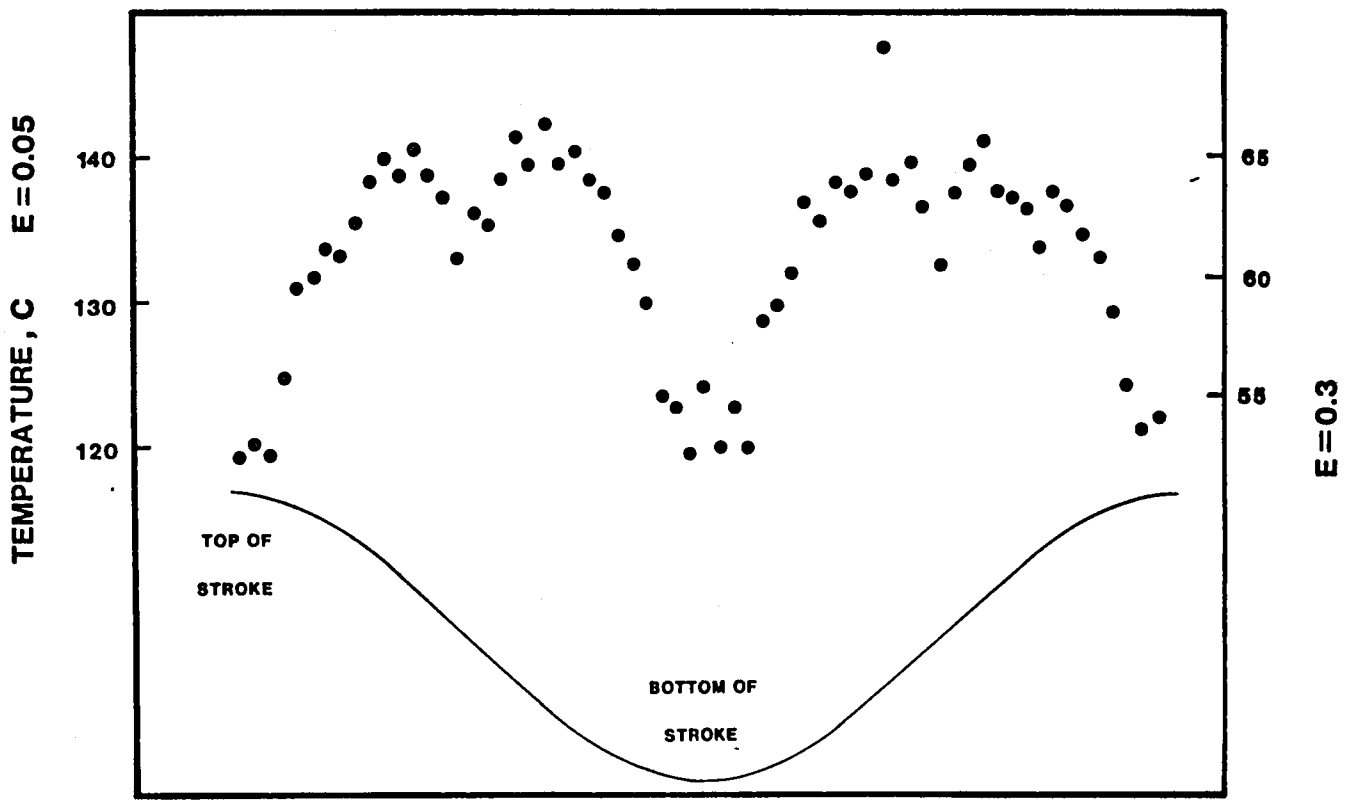

Figure 5-6. Stirling Engine Seal Simulator Rod Temperature

enter the seal at low velocities the temperature remains low at these points while the middle of the rod remains hottest because it always enters and leaves the seal at highest velocity.

Another interesting aspect of Figure 5-6 is that the temperature *decreases* slightly at the point of highest velocity in the stroke and thus causes a "dip" in the graph at both peaks. We think that this is caused by an oil film being developed at the high velocities. (A thin layer of oil was present on the rod.) Frictional energy is in part a product of velocity and load. As the velocity increases the friction may decrease if an oil film forms between the two rubbing surfaces. If the decrease in friction offsets the increase in velocity, the temperature will decrease locally.

The apparent scatter of the data points in Figure 5-6 is due to an interfering signal picked up during the recording, a slight fluctuation in the DC level of the camera, and friction coefficient variations during the stroke.

A radiation profile was plotted using the EXPLORER III digital oscilloscope and can be found in Figure 5-7. This figure represents one scanned line across the rod as it emerges from the seal at 300 rpm and 900 psi.

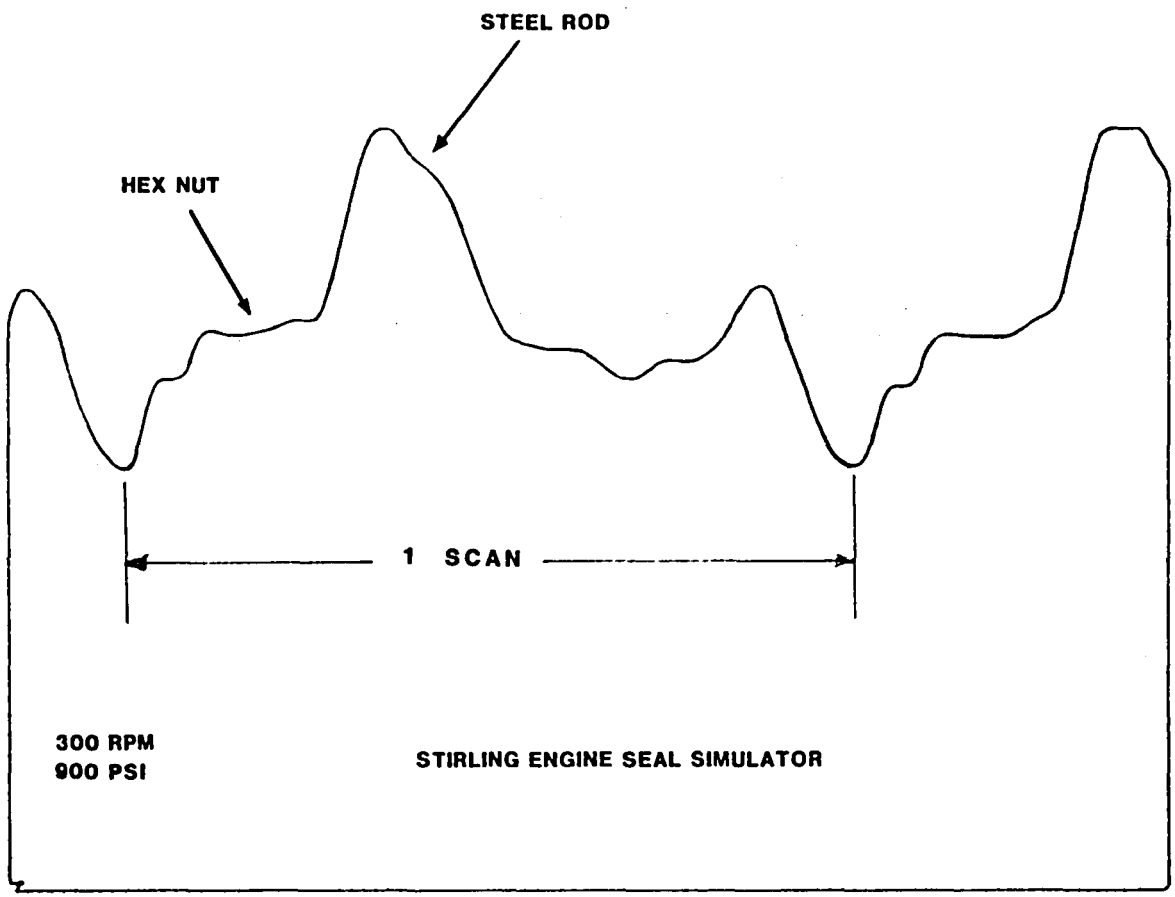

Figure 5-7. Stirling Engine Seal Simulator single Line Scan

CHAPTER VI

CONCLUSIONS AND RECOMMENDATIONS

From the analysis of the four friction experiments we conclude that the system can calculate surface temperatures and display surface temperature profiles on scanned lines. The single line scanning modification proved to be very useful for temperature observations in high velocity situations. The external triggering device performed well in starting each scanned line at approximately the same point in the cycle although reference points on the object itself as seen by the camera proved more useful for easy cycle position identification.

A. The Computer-aided IR System

One of the main limitations of the AGA 750 is its spotsize over which radiation is integrated. With the extension rings and lens employed to give a flat field the diameter of this spotsize is somewhat less than one-tenth of the scan width. If the area from which the radiation is received is known, then temperatures on an area whose diameter is 0.13 mm could be measured. Another limitation is the necessity of having a calibrated reference object with known emissivity and temperature in the field of view in order to be able to calculate absolute temperatures. The main limitations of the computer analysis aspect of the system were:

1. memory size
2. computing speed
3. data transfer speed and reliability
4. limited hard copy output

Possible sources of error introduced by the system are:

1. integration of temperatures over a finite region due to finite resolution,
2. uncertainty in reference temperature and emissivity,
3. uncertainty in object emissivity which may vary with temperature,
4. varying DC level of the camera,
5. amplifier instability during signal amplification,
6. inaccuracies in the calibration curve used by the computer, especially in calculating temperatures less than 60C which requires extrapolation.

In view of these limitations the following recommendations for future use of the system can be made:

1. Fresnel lenses can be used to pre-magnify the object.
2. Screens with known emissivity and a known hole size smaller than the spotwise of the camera may be used to find temperatures at small spots.
3. The calibration curve mentioned on page 41 can be recalibrated for temperatures less than 60C.
4. Use of a computer with more core memory and a BASIC *Compiler* rather than a BASIC *interpreter* will greatly speed up the data processing.
5. Use of high-speed mass storage like floppy disks rather than cassette tapes will cut the data transfer time by a factor of 100.

6. A matrix printer terminal rather than a teletype terminal will greatly speed up and improve the quality of hard copy output.

B. The Friction Experiments

Both in the Rulon-on-steel and the stirling engine seal experiments it was found that the surface cooling time was long in comparison with the cycle time of the device. As a result a temperature pattern was created on the surface that remained during the cycle. Radiation profiles of the steel plate in the Rulon-on-steel experiment showed that the presence of the thermocouple changed the thermal characteristics of the surface due to a changed thermal resistance. From the Rulon-on-sapphire experiments we learned that alignment of the specimen had a major influence on the temperature distribution across the contact surface of the pin.

DISTRIBUTION LIST FOR NASA CR-165479

Recipient	No. Of Copies
NASA Lewis Research Center 21000 Brookpark Road Cleveland, OH 44135	
Attn: W. A. Tomazic, MS 500-215	3 + reproducible
R. E. Cunningham, MS 6-1	3
D. M. Thomas, MS 501-11	1
N. T.Musial, MS 500-311	1
Report Control Office, MS 5-5	1
Library , MS 60-3	2
Technology Utilization Office, MS 7-3	1
D. G. Beremand, MS 500-215	1
J. G. Slaby, MS 500-215	1
F. J. Kutina, MS 500-215	1
W. K. Tabata, MS 500-215	1
NASA Scientific & Technical Information Facility P. O. Box 8757 Balt./Wash. International Airport Maryland 21240 Attn: Accessioning Department	25
NASA Langley Research Center Langley Station Hampton, VA 23365 Attn: Library	1
NASA Ames Research Center Moffet Field, CA 94035 Attn: Library	1
NASA Hugh L. Dryden Research Center P. O. Box 273 Edwards, CA 93523 Attn: Library	1
NASA Goddard Space Flight Center Greenbelt, MD Attn: Library	1
Jet Propulsion Laboratory 4800 Oak Grove Drive Pasadena, CA 91103 Attn: Library	1

The Following recipients require one copy:

NASA Jet Propulsion Laboratory
4800 Oak Grove Drive
Pasadena, CA 91103
Attn: H. Cotrill, Mgr.
Automotive Research Projects, MS 138-208

NASA Headquarters
Washington, DC 20546
Attn: RF-14/J. Anderson
Program Manager, OEP

NASA Headquarters
Washington, DC 20546
Attn: REC-1/J. F. Slomski

Winfred N. Crim
Division of Coal Utilization
Department of Energy
GTN E-178
Washington, DC 20545

Dr. Robert J. Gottschall
ER 151
Department of Energy
GTN J-309
Washington, DC 20545

E. Lister
Division of Coal Utilization
Department of Energy
GTN E-178
Washington, DC 20545

Paul V. Lombardi
Department of Energy
MS 5H-039
Forrestal Building
Washington, DC 20585

Robert B. Morrow
Department of Energy
GTN B-107
Washington, DC 20545

John W. Neal
Division of Coal Utilization
Department of Energy
GTN E-178
Washington, DC 20545

Patrick L. Sutton
Department of Energy
MS 5H-039
Forrestal Building
Washington, DC 20585

Henry A. Themak
Department of Energy
MS 5H-039
Forrestal Building
Washington, DC 20585

AFAPL/DO
Attn: E. E. Bailey
Wright Patterson AFB
OH 45433

AFWAL-MLBT
Attn: William E. Berner
Wright Patterson AFB
OH 45433

Argonne National Laboratory
Attn: Dr. Alex Davis, P.E.
Building 17-EES
Argonne, IL 60439

Argonne National Laboratory
Attn: R. E. Holz
9700 South Cass Avenue, Bldg. H330
Argonne, Il 60493

Argonne National Laboratory
Attn: Dr. Kenneth Uherka
Components Tech. Div., Bldg. 330
9700 South Cass Avenue
Argonne, Il 60439

Kenneth Bradford
P. O. Box 99909
Cleveland, OH 44199

Department of Transportation
Attn: H. Miller
Trans. Systems Center, Code TSC-404
Kendall Square
Cambridge, MA 02142

House of Representatives
Attn: Honorable Mary Rose Oakar
107 Cannon House Office Building
Washington, DC 20515

NUWES
Attn: Charles R. Gundersen
Code 7022
Keyport, WA 98345

Oak Ridge National Laboratory
Attn: F. A. Creswick
P. O. Box Y
Oak Ridge, TN 37830

Oak Ridge National Laboratory
Attn: Beverly Wilkes
P. O. Box X
4500 N, Room I-205K
Oak Ridge, TN 37830

SERI
Attn: Henry Kelley
1536 Cole Boulevard
Golden, CO 80401

Solar Energy Research Institute
Attn: Joseph Finegold
1617 Cole Boulevard
Golden, CO 80401

U. S. Army Materials &
Mechanics Research Center
Attn: Dr. R. Nathan Katz, Chief
Ceramics Division
Watertown, MA 02171

U. S. Army Mobility Equipment
R & D Command
Attn: Paul Arnold
DRDME-EM
Fort Belvoir, VA 22060

U.S. Army Mobility Equipment
R & D Command
Attn: Richard Belt
DRDME-EC
Fort Belvoir, VA 22060

Bucknell University
Attn: Dr. Barry Maxwell
Mechanical Engineering Depart.
Lewisburgh, PA 17837

California Polytechnic State Univ.
Attn: Raymond G. Gordon
Mechanical Engineering Dept.
San Luis Obispo, CA 93407

California Polytechnic State Univ.
Attn: Professor C. R. Russell
Mechanical Engineering Dept.
San Luis Obispo, CA 93407

Cambridge University
Attn: Allan J. Organ
University Engineering Dept.
Trumpington Street
Cambridge, CB2 1PZ
GREAT BRITAIN

Case Western Reserve University
Attn: Prof. A. Dybbs
Dept. of Mechanical &
Aerospace Engineering
Cleveland, OH 44106

Carnegie-Mellon University
Attn: Prof. William F. Hughes
Dept. of Mechanical Engineering
Pittsburgh, PA 15213

Harwell Laboratories
Attn: E. H. Cooke Yarborough
Electronics & Applied Physics Div.
Bldg. 347.3 AERE-Harwell
Oxfordshire OX11 ORA
UNITED KINGDOM

Massachusetts Institute of Technology
Attn: Prof. Joseph L. Smith, Jr.
Mechanical Engineering Dept.
Room 41-204
Cambridge, MA 02139

Rensselaer Polytechnic Institute
Attn: Prof. Fred Ling
Depart. of Mechanical Engineering
Troy, NY 12181

Lieutenant G. T. Reader, R.N.
Royal Naval Engineering College
Manadon, Plymouth PL 5.3AQ
UNITED KINGDOM

University of Calgary
Attn: Dr. G. Walker, Professor
Dept. of Mechanical Engineering
Calgary, Alberta T2N 1N4
CANADA

University of Reading
Attn: Professor Graham Rice
Dept. of Engineering & Cybernetics
Reading, England
UNITED KINGDOM

University of Tokyo
Attn: Yoshihiro Ishizaki
Faculty of Engineering
Department of Nuclear Engineering
Bunkyo-ku, TOKYO
JAPAN

University of Tokyo
Attn: Professor Susumu Kotake
Institute of Space &
Aeronautical Science
Komaba, Meguro-Ku, TOKYO
JAPAN

University of Washington
Attn: R. P. Johnston
Joint Center for Graduate Study
100 Sprout Road
Richland, W 99352

University of Wisconsin - R.F.
Attn: Dr. J. R. Senft
River Falls, WI 54022

University of Witwatersrand
Johannesburg
Attn: Dr. C. J. Rallis
School of Mechanical Engineering
1 Jan Smuts Avenue
Johannesburg, 2001
SOUTH AFRICA

Weizman Institute of Science
Attn: S. Shrtikman
Professor of Applied Physics
REHOUOT, ISRAEL

Ford Aerospace & Communications Corp.
Attn: Robert L. Pons
Aeronutronic Division
Newport Beach, CA 92663

M.A.N.
Attn: Werner Uhl
6905 Hutcheson Street
Falls Church, VA 22043

Maschinenfabrik
Augsburg-Nurnberg AG, MAN
Attn: Dipl. Inq. H. Schaaf
Postfach 10 00 80
D 8900 Augsburg 1
WEST GERMANY

Motoren-Werke Manheim Ag
Attn: Dr. Ing. F. A. Zacharias
Postfach 1563
D 6800 Manheim 1
WEST GERMANY

N. V. Philips Gloeilampenfabrieken
Attn: M. L. Hermans
Philips Research Laboratories
Eindhoven
THE NETHERLANDS

Philips Laboratories
Attn: Alex Daniels
345 Scarborough Road
Briarcliff Manor, NY 10510

Stirling Thermal Motors, Inc.
Attn: Dr. R. J. Meijer
2841 Boardwalk
Ann Arbor, MI 48104

United Stirling
Attn: Bengt Hallare
211 The Strand
Alexandria, VA 22314

United Stirling
Attn: Worth Percival
211 The Strand
Alexandria, VA 22314

United Stirling Research Laboratories
Attn: Kaj Rosenqvist
Box 856
S-201 80 Malmo
SWEDEN

Advanced Energy Programs
Attn: B. J. Tharpe
General Manager Dept.
P. O. Box 8661
Philadelphia, PA 19101

Advanced Mechanical Technology, Inc.
Attn: Dr. Walter D. Syniuta, Pres.
141 California Street
Newton, MA 02158

Aerojet Energy Conversion Company
Attn: Mark I. Rudnicki
P. O. Box 13222
Sacramento, CA 95813

Aerojet Liquid Rocket Company
Attn: Lawrence C. Hoffman
Dept. 9860, Bldg. 2001
P. O. Box 13222
Sacramento, CA 95813

Aerospace Corporation
Attn: Wolfgang Roessler
2350 Eawt EL Segundo Blvd.
El Segundo, CA 90245

AGA Innovation
Attn: Sigvard Thulin
P. O. B 2007
S-183 02 TABY
SWEDEN

Arthur D. Little, Inc.
Attn: Prafulla C. Mahata
Acorn Park
Cambridge, MA 02140

Dynasim Company
Attn: Richard P. Heintz
428 W. South
Kalamazoo, MI 49007

Eaton Corporation
Attn: Dr. Lamont Eltinge
Director of Research
P. O. Box 766
Southfield, MI 48037

EMAX Incorporated
Attn: K. N. Singh
720 Granview Avenue
Columbus, OH 43215

Energy Research & Generation, Inc.
Attn: Dr. Glen Benson
Director of R, D. & E
Lowell & 57 Street
Oakland, CA 94608

Fairchild Space & Electronic Company
Attn: A. Schock
Germantown, MD 20767

Flow Energy Division
Attn: Randall C. Fowler
201 San Antonio Circle, Suite 145
Mountain View, CA 94040

Flow Industries, Inc.
Attn: Dr. John H. Olsen
P. O. Box 5040
21414-68th Avenue, South
Kent, WA 98031

Ford Motor Company
Attn: Ernest Kitzner
Rm. S-2100 Scientific Research Lab.
P. O. Box 2053
Dearborn, MI 48121

Foster-Miller Associates
Attn: Dr. William M. Toscano
350 2nd Avenue
Waltham, MA 02154

General Electric Company
Attn: William Auxer
Space Division
P. O. Box 8661
Philadelphia, PA 19101

General Motors Research Laboratory
Attn: F. Earl Heffner
Engine Research Department
Warren, MI 48090

Grumman Aerospace Corporation
Attn: Clifford A. Hoelzer
Head, Propulsion Systems
M.S. C32-05
Bethpage, NY 11714

IIT Research Institute
Attn: Vernon L. Hill
10 West 35 Street
Chicago, IL 60616

International Harvester
Attn: Paul N. Blumberg
Science & Technology Laboratory
16 W. 260 83rd Street
Hinsdale, IL 60521

International Trade &
Industry, Ministry of
Attn: Takao Tomings
Director, Automotive Division
Kasumigaseki, TOKYO 100
JAPAN

Japan Automobile Research Inst., Inc.
Attn: Atsushi Watari, President
Yatable-cho, Tsukuba-gun
Ibaraki-ken 305
JAPAN

Martini Engineering
Attn: Dr. W. R. Martini
2303 Harris
Richland, WA 99352

Mechanical Technology Inc.
Attn: Merton Allen
968 Albany-Shaker Road
Latham, NY 12110

Mechanical Technology Inc.
Attn: Bruce Goldwater
968 Albany-Shaker Road
Latham, NY 12110

Mechanical Technology Inc.
Attn: Dr. Gene Mannella
968 Albany-Shaker Road
Latham, NY 12110

Mechanical Technology Inc.
Attn: Dr. B. Sternlicht
968 Albany-Shaker Road
Latham, NY 12110

Mechanical Technology Inc.
Attn: Dr. D. F. Wilcock
968 Albany-Shaker Road
Latham, NY 12110

Motor Vehicle Man. Assn.
of the United States, Inc.
Attn: Christian Van Schayk
300 New Center Bldg.
Detroit, MI 48202

Ormat Turbines, Ltd.
Attn: Israel Urieli
Szydlowski Road
YAVNE, ISRAEL

Rasor Associates, Inc.
Attn: Dr. Edward J. Britt
Direct Energy Conversion Dept.
253 Humboldt Court
Sunnyvale, CA 94086

Sigma Research Incorporated
Attn: E. D. Waters
2950 George Washington Way
Richland, WA 99352

Space Conditioning Research
Institute of Gas Technology
Attn: Jaroslav Wurn
3424 South State Street
Chicago, IL 60616

Stirling Power Systems Corporation
Attn: William Houtman
7101 Jackson Road
Ann Arbor, MI 48103

Sunpower, Inc.
Attn: W. Beale
6 Byard Street
Athens, OH 45701

TCA Stirling Engine
Research & Development Corp.
Attn: Dr. Ted Finkelstein
P. O. Box 643
Beverly Hills, CA 90213

Teledyne Continental Motors
Attn: T. Schwallie
General Products Division
76 Getty Street
Muskegon, MI 49442

Teledyne Energy Systems
Attn: G. Linkous
110 W. Timonium Road
Timonium, MD 21093

Thermal Electron Corporation
Attn: Parinal S. Patel
R & D Center
101 First Avenue
Waltham, MA 02154

United Aircraft Products, Inc.
Attn: John F. Unger
Manager, Advanced Technology
Box 1335
Dayton, OH 45401

Valley Forge Space Center
Attn: Rolf Laessig
G. E. Space Division, Room 12236
P. O. Box 8661
Philadelphia, PA 19101

Varian Associates
Attn: Chris Flegal
MS G-028
611 Hansen Way
Palo Alto, C 94303

Wasson Associates
P. O. Box 1180
Aptos, CA 95003

Westinghouse Electric Corporation
Attn: Library/R. Holman
Advanced Energy Systems Div.
P. O. Box 10864
Pittsburgh, PA 15236

1. Report No.	2. Government Accession No.	3. Recipient's Catalog No.
NASA CR-165479		

4. Title and Subtitle	5. Report Date
Final Report: Preliminary Study of Temperature Measurement Techniques for Stirling Engine Reciprocating Seals	August 1981
	6. Performing Organization Code
7. Author(s) Donald F. Wilcock Leo Hoogenboom	8. Performing Organization Report No. 82TR4
	10. Work Unit No.
9. Performing Organization Name and Address Mechanical Technology Incorporated 968 Albany-Shaker Road Latham, New York 12110	11. Contract or Grant No. DEN3-227
	13. Type of Report and Period Covered Contractor Report
12. Sponsoring Agency Name and Address U.S. Department of Energy Division of Transportation Energy Conservation Washington, D.C. 20545	14. Sponsoring Agency Code DOE/NASA/0227-1

15. Supplementary Notes

Final Report, prepared under Interagency Agreement DE-A101-77CS51040
NASA-Lewis Research Center Project Manager: R.E. Cunningham
Cleveland, Ohio 44135

16. Abstract

Direct infra-red measurement of surface temperatures of a rod exiting a loaded cap seal or simulated seal are compared with surface thermocouple measurements. Significant cooling of the surface requires several milliseconds so that exit temperatures may be considered representative of internal contract temperatures.

17. Key Words (Suggested by Author(s))	18. Distribution Statement
Seals Stirling Engines Rod Seals PTFE Compounds Temperature Measurements Infra-Red Pyrometry Fast-Response Thermocouples	Unclassified - Unlimited

19. Security Classif. (of this report)	20. Security Classif. (of this page)	21. No. of Pages	22. Price*
Unclassified	Unclassified	135	

* For sale by the National Technical Information Service, Springfield, Virginia 22151

End of Document